

Today:

A wee bit of EMG and then....

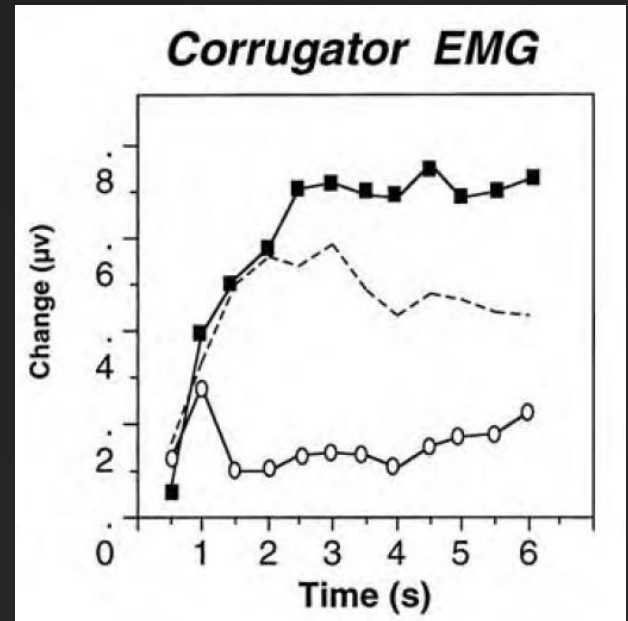
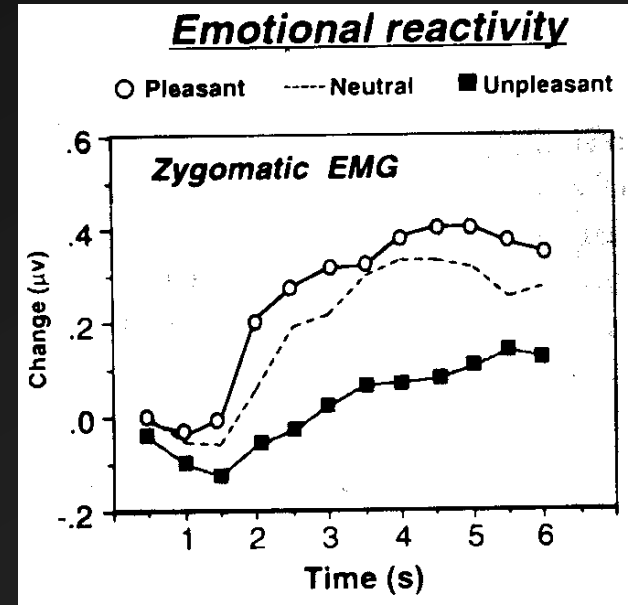
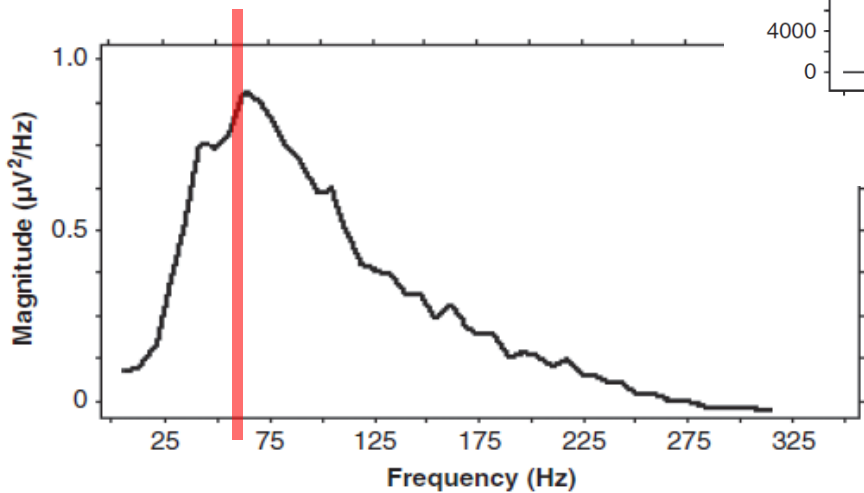
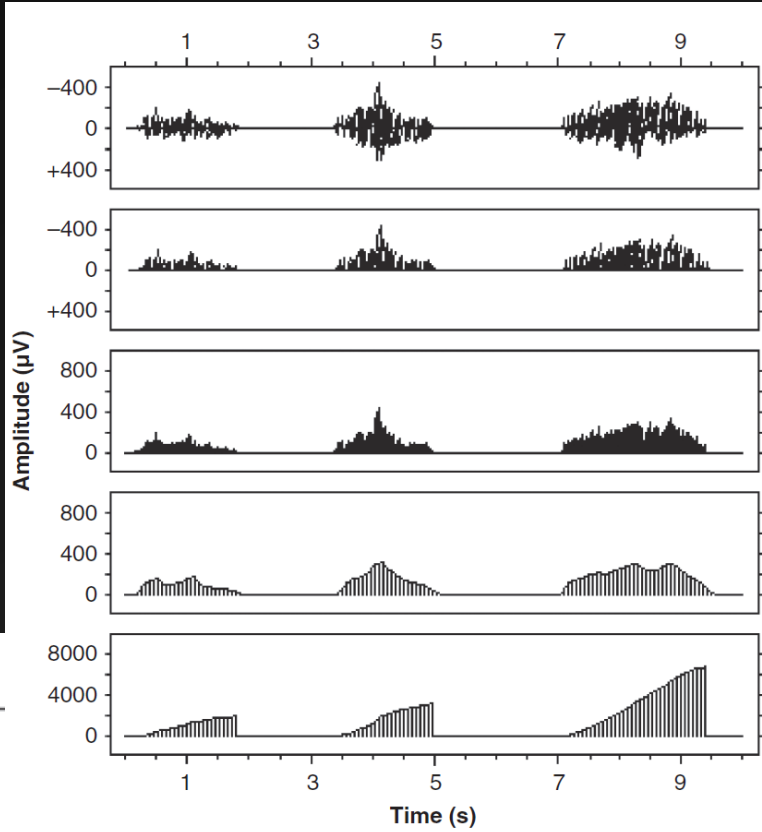
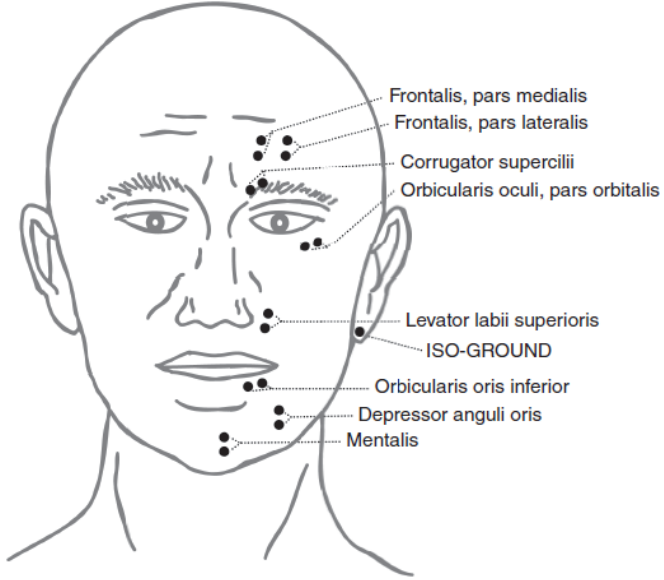
The Electroencephalogram

Announcements 3/24/25

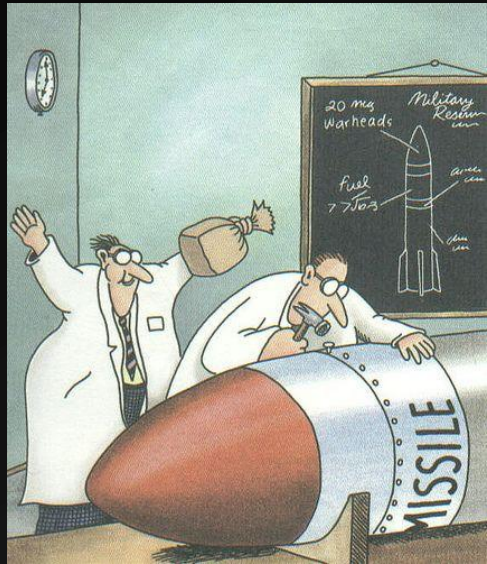
- Paper/Proposal [Guidelines](#) available
 - On course webpage
 - Link in D2L
- Paper/Proposal two paragraph prospectus due via D2L no later than Monday April 21
- Student Course Surveys – complete by last day of class (May 5)
- 501B Lab Section
 - Complete data collection by Wed Mar 26
 - Complete data reduction (EKG and EMG) by April 1

Questions and Feedback

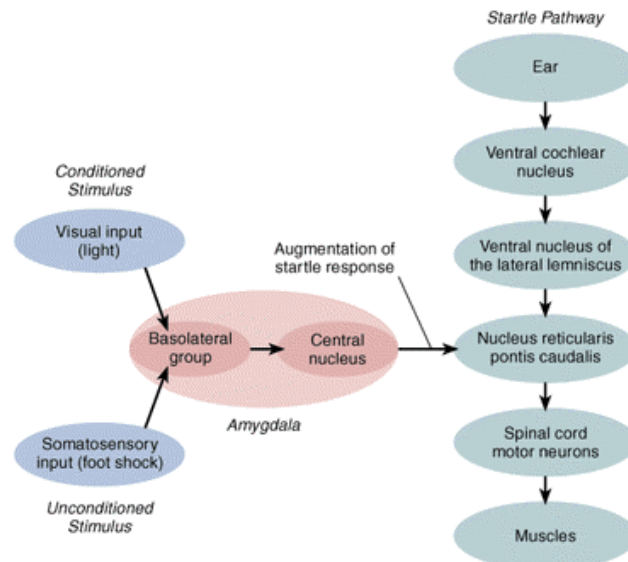
Brief Review



Brief Review – Emotion Modulated Startle

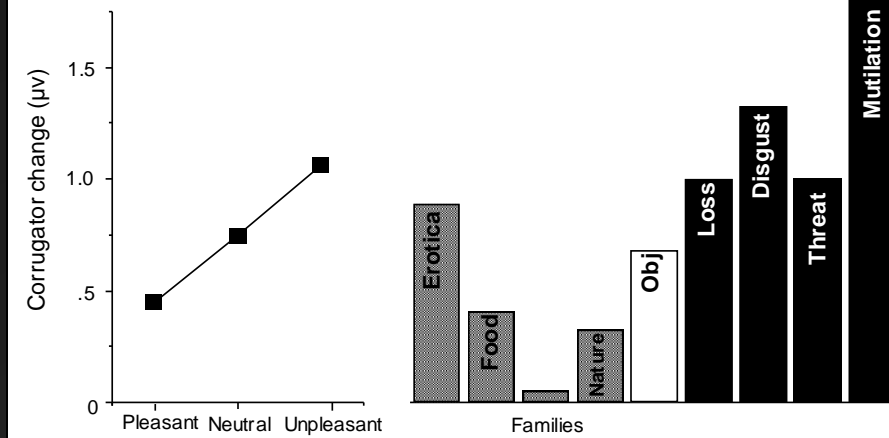


► Neural Circuits Responsible for an Auditory Startle Response and for Its Augmentation by Conditioned Aversive Stimuli

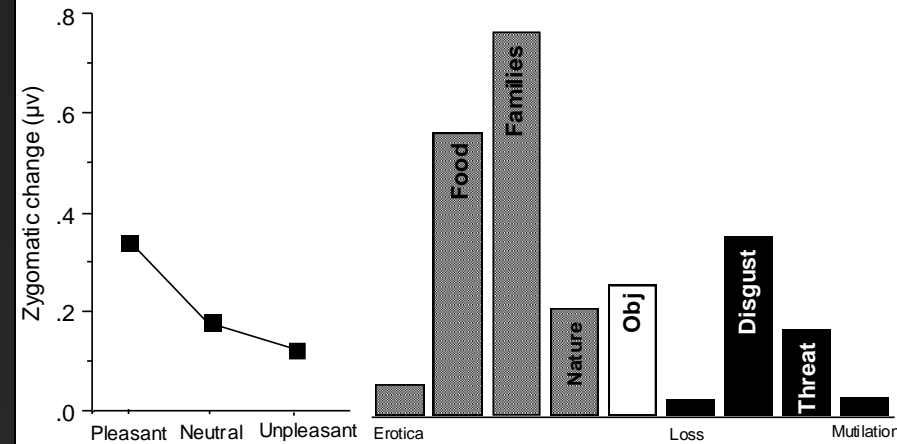


Source: Adapted from Davis, M., *Trends in Pharmacological Sciences*, 1992, 13, 35–41.

Corrugator EMG



Zygomatic EMG



A few Applications

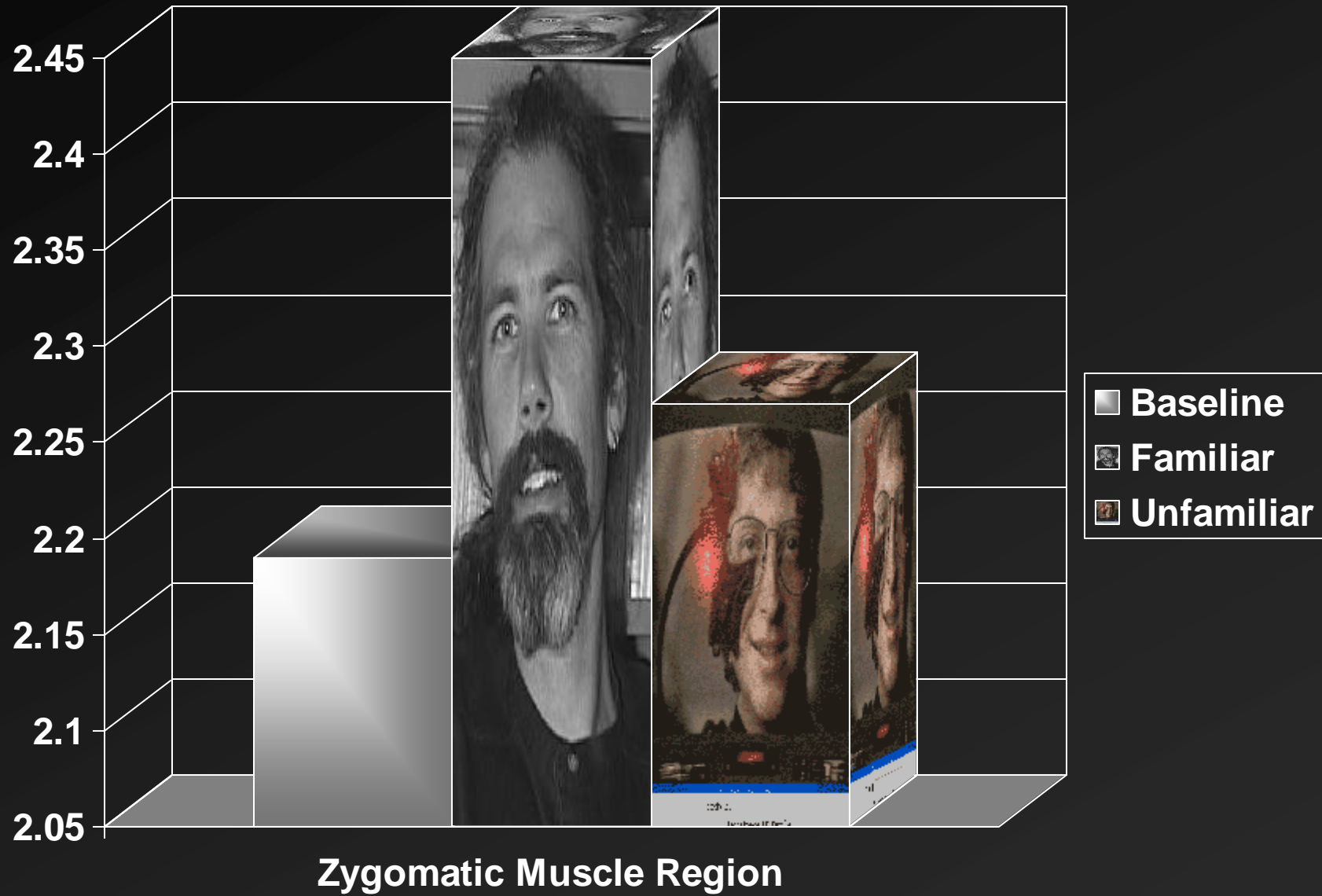
- Startle Probe
- Subtle affect
 - Mere Exposure
 - Subliminal effects
 - Mortality Salience
 - Biofeedback of EEG -- outcome measure
 - Emotion Regulation – outcome measure
 - Empathy – individual difference measure

The Phenomenon:

- People prefer stimuli to which they have been previously exposed to unfamiliar stimuli
- In absence of any reinforcement (“mere” exposure)
- Examples:
 - People we see incidentally in our routines
 - Songs
 - Scientific journal preferences
- Effect size $r=.26$ (Meta-analysis, Bornstein, 1989)

The logic:

- Evolutionary account Bornstein (1989)
 - it may be adaptive to prefer the familiar over the novel
 - novel objects could present a potential threat
 - organisms that had a fear of the strange and unfamiliar were more likely to survive, reproduce, and pass on genetic material
 - Preferring the familiar may thus be an adaptive trait that has evolved in humans and nonhumans
- Prediction:
 - unfamiliar as compared with familiar stimuli may be associated with more negative attitudes because of the unfamiliar stimuli's association with potential danger
 - Thus may see greater corrugator activity to novel than to familiar
 - No prediction for positive affect (Zygomaticus activity)



Loosely translated from Harmon-Jones & Allen, 2001

A few Applications

- Startle Probe
- Subtle affect
 - Mere Exposure
 - Subliminal effects
 - Mortality Salience
 - Biofeedback of EEG -- outcome measure
 - Emotion Regulation – outcome measure
 - Empathy – individual difference measure



30 ms



5 ms



Unconscious Facial Reactions

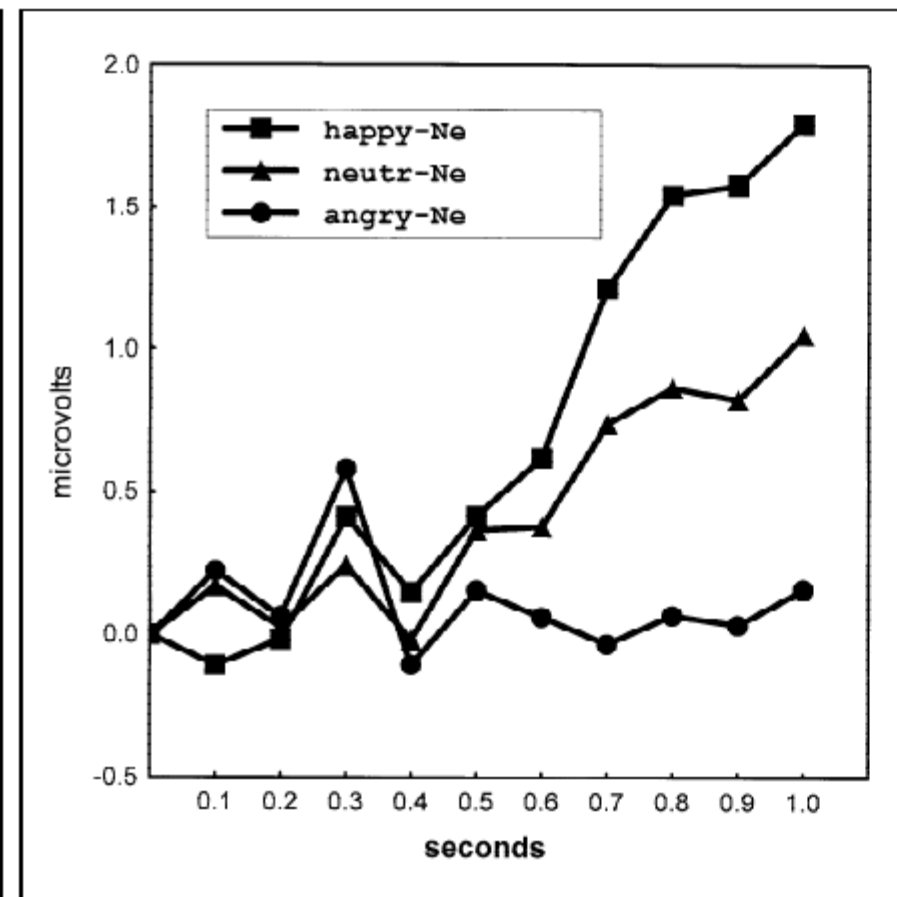


Fig. 1. Mean facial electromyographic response for the *zygomatic major* muscle, plotted in intervals of 100 ms during the first second of exposure. Three different groups of participants were exposed to identical neutral faces ("Ne"), preceded by unconscious exposure of happy, neutral ("neutr"), or angry target faces, respectively.

A few Applications

- Startle Probe
- Subtle affect
 - Mere Exposure
 - Subliminal effects
 - Mortality Salience
 - Biofeedback of EEG -- outcome measure
 - Emotion Regulation – outcome measure
 - Empathy – individual difference measure

Word Relatedness Task

Sneaker

Sub-threshold word

Fajita

<response>

Rock

Sub-threshold word

Boulder

<response>

Sub-threshold words:

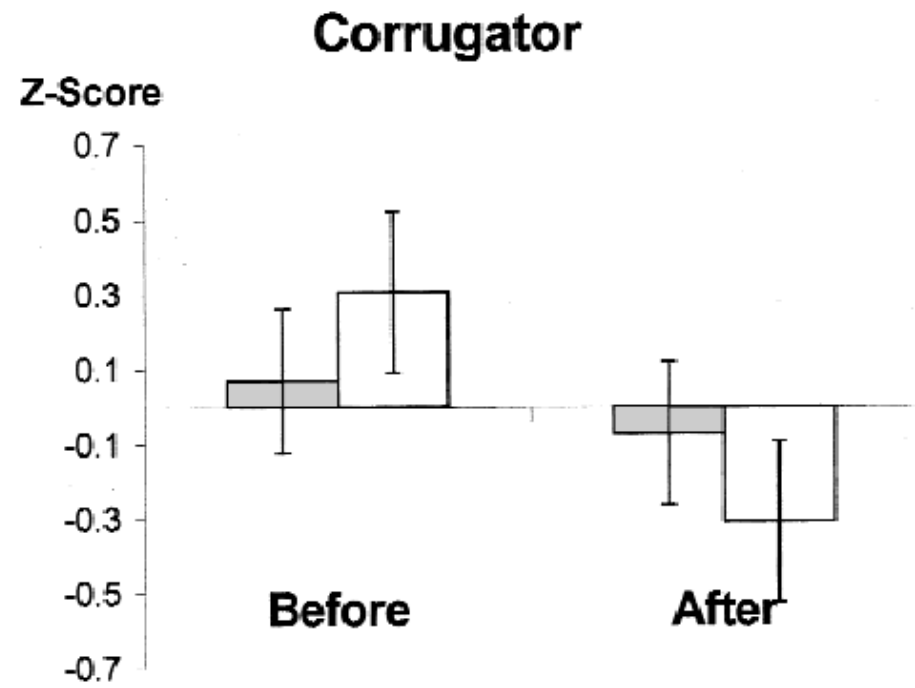
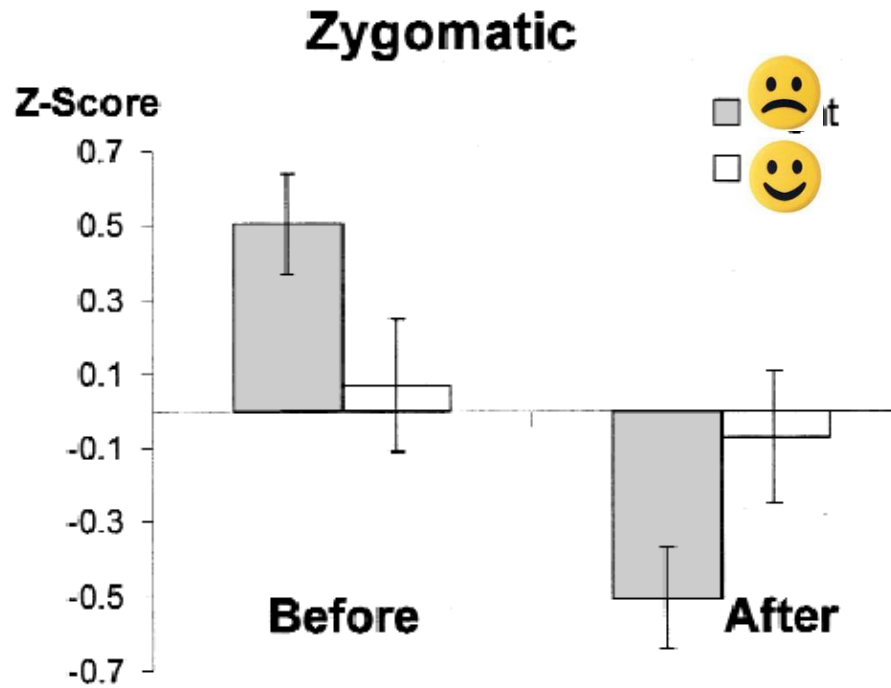
Dead

Pain

Another loose translation: Arndt, J., Allen, J.J.B., & Greenberg, J. (2001). Traces of terror: Subliminal death primes and facial electromyographic indices of affect. *Motivation and Emotion*, 25, 253-277.

A few Applications

- Startle Probe
- Subtle affect
 - Mere Exposure
 - Subliminal effects
 - Mortality Salience
 - Biofeedback of EEG -- outcome measure
 - Emotion Regulation – outcome measure
 - Empathy – individual difference measure



A few Applications

- Startle Probe
- Subtle affect
 - Mere Exposure
 - Subliminal effects
 - Mortality Salience
 - Biofeedback of EEG -- outcome measure
 - Emotion Regulation – outcome measure
 - Empathy – individual difference measure

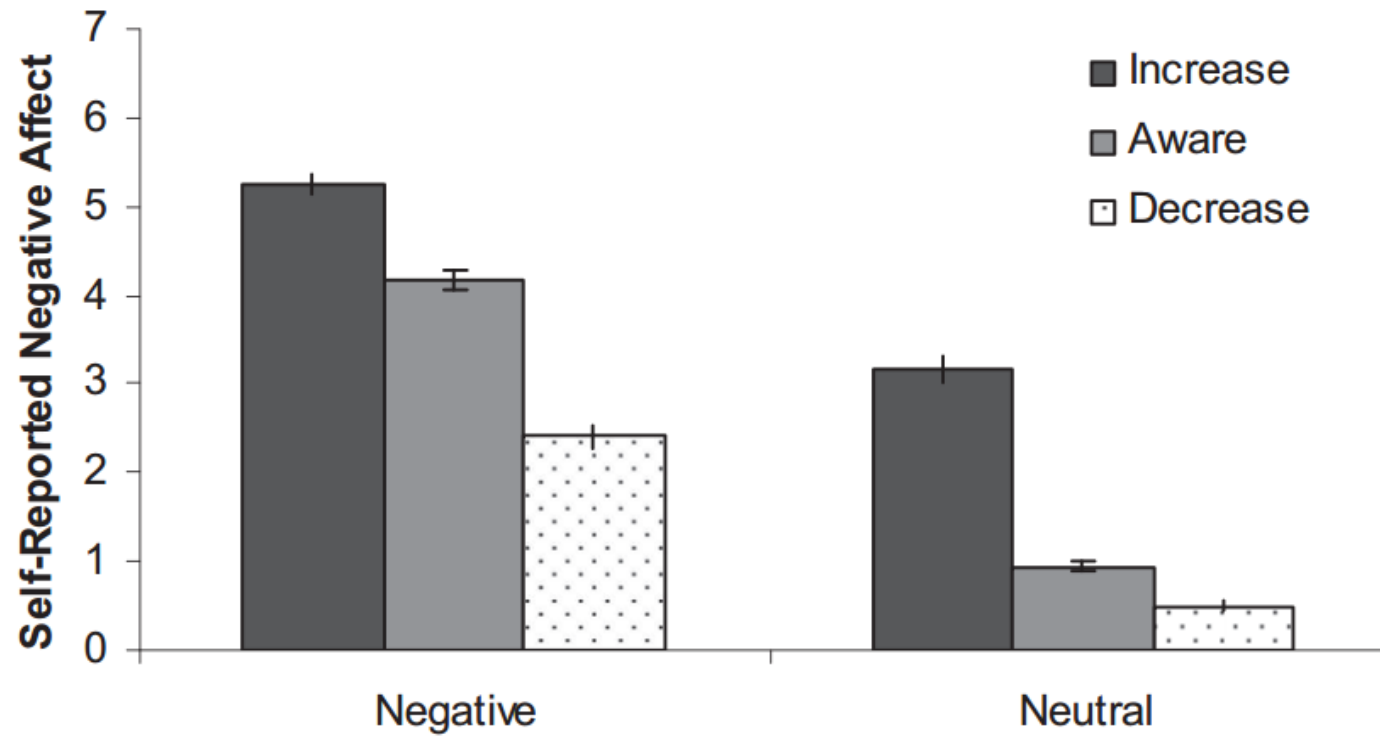


Figure 1. Self-reported negative affect on a 7-point Likert scale, where 0 = “not negative at all” and “7” = “strongly negative.”

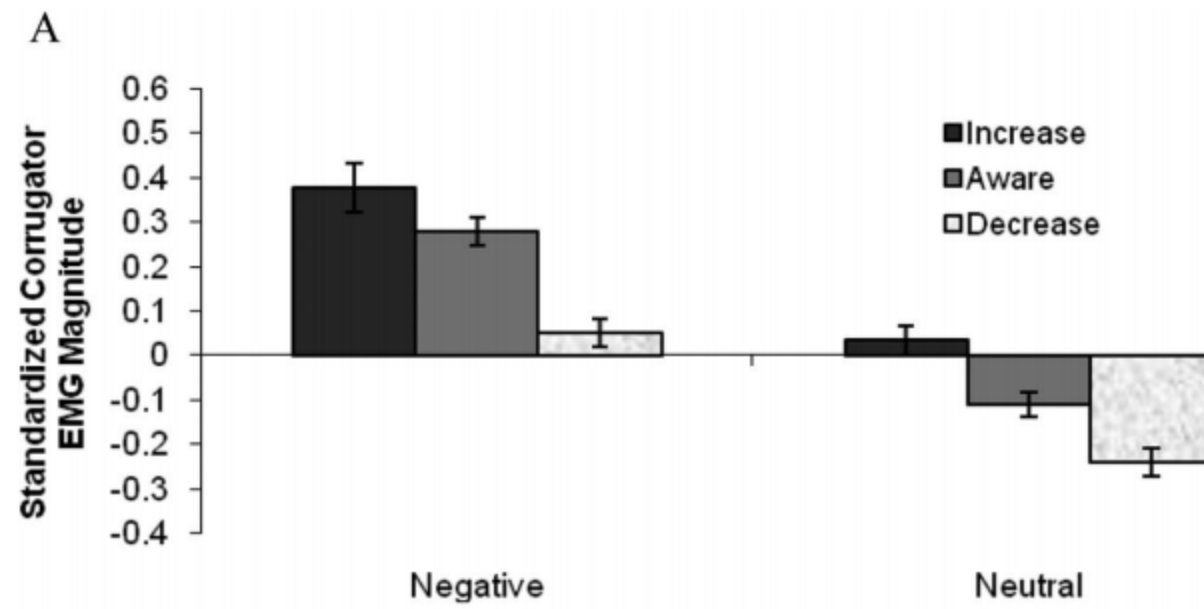
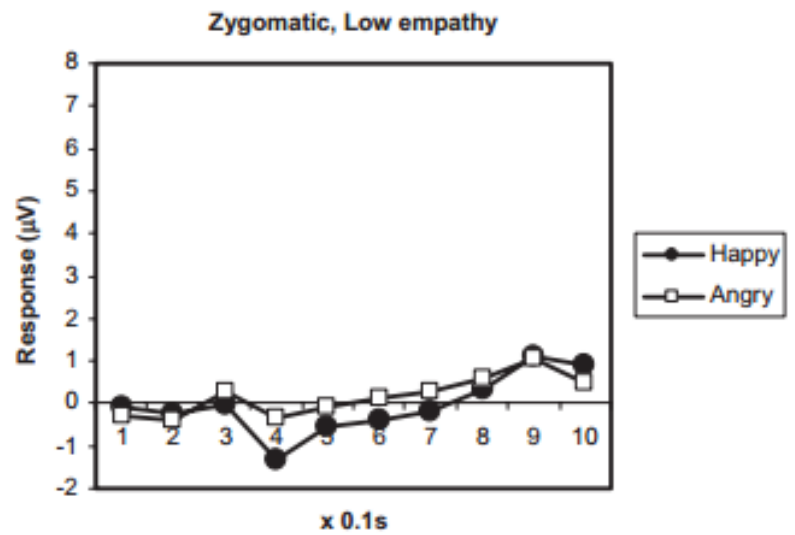
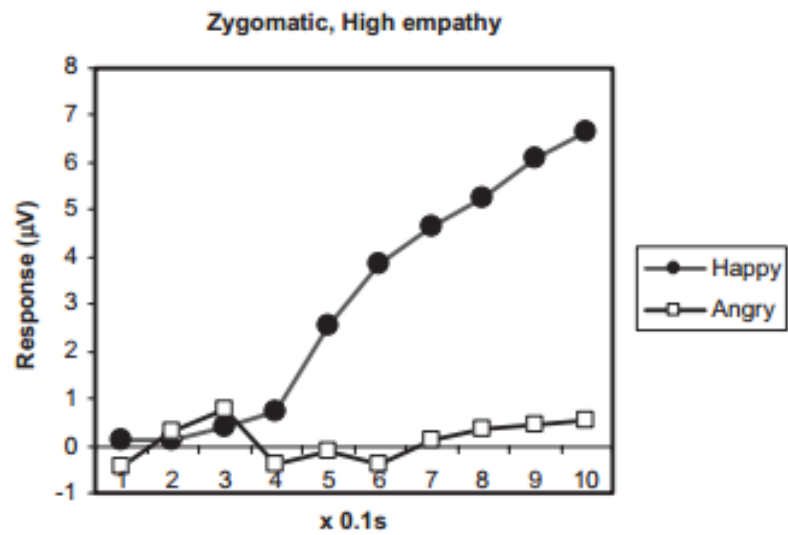


Figure 2. Standardized (A) corrugator EMG and (B) startle magnitude (averaged over Times 1 and 2).

A few Applications

- Startle Probe
- Subtle affect
 - Mere Exposure
 - Subliminal effects
 - Mortality Salience
 - Biofeedback of EEG -- outcome measure
 - Emotion Regulation – outcome measure
 - Empathy – individual difference measure



Faces

Figure 1. The *zygomaticus major* muscle response to pictures of happy and angry facial expressions for the High and Low empathy groups, plotted as a function of 100-ms intervals during the first second after stimulus onset.

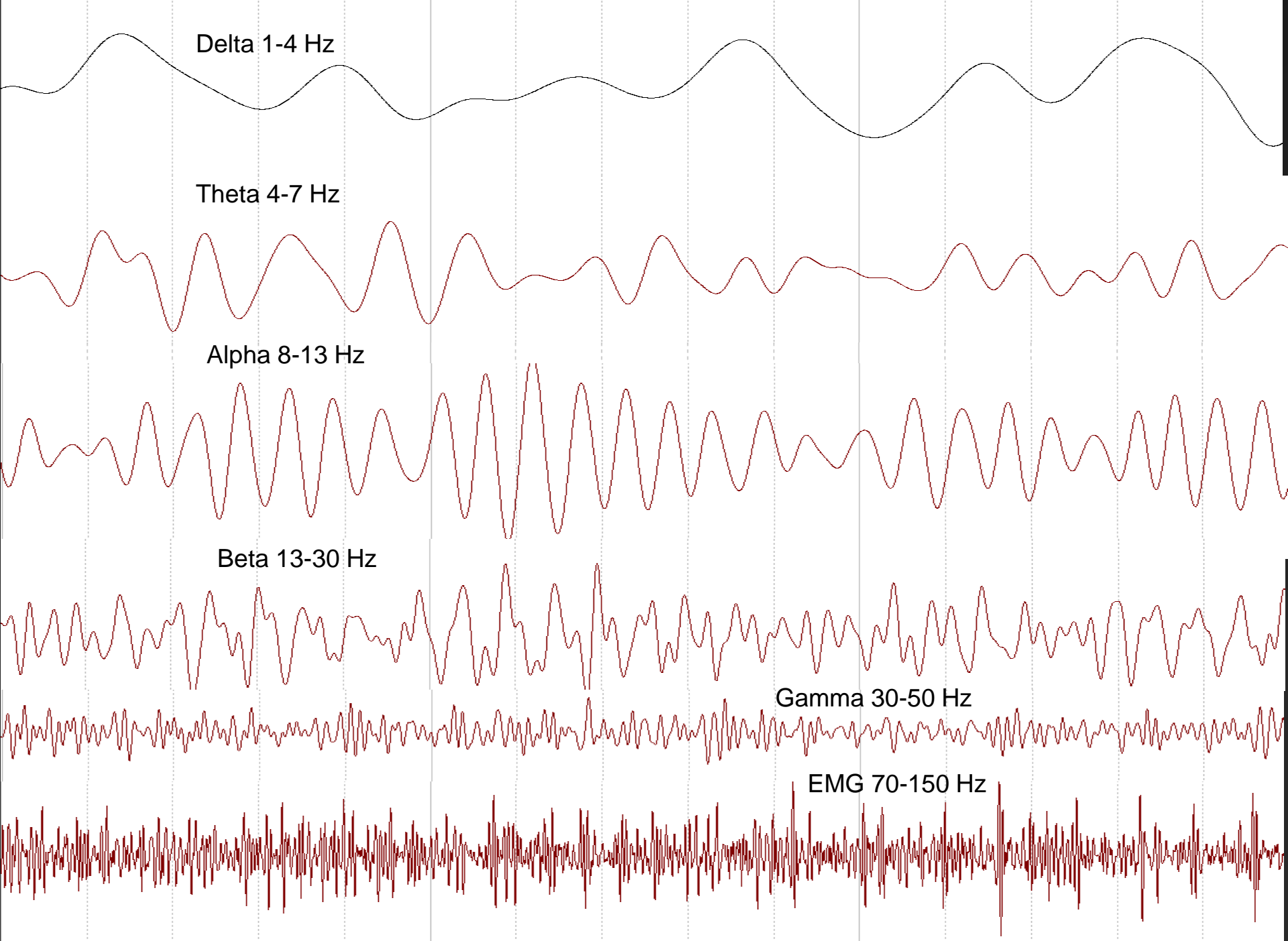
The Electroencephalogram

Basics in Recording EEG, Frequency Domain
Analysis and its Applications



Electroencephalogram (EEG)

- The EEG--an oscillating voltage recorded on scalp surface
 - Reflects Large # Neurons
 - Is small voltage
- Bands of activity and behavioral correlates
 - Gamma 30-50 Hz
 - Beta 13-30 Hz
 - Alpha 8-13 Hz
 - Theta 4-8 Hz
 - Delta 0.5-4 Hz
- Event-related activity (voltage: ERP; time-frequency)

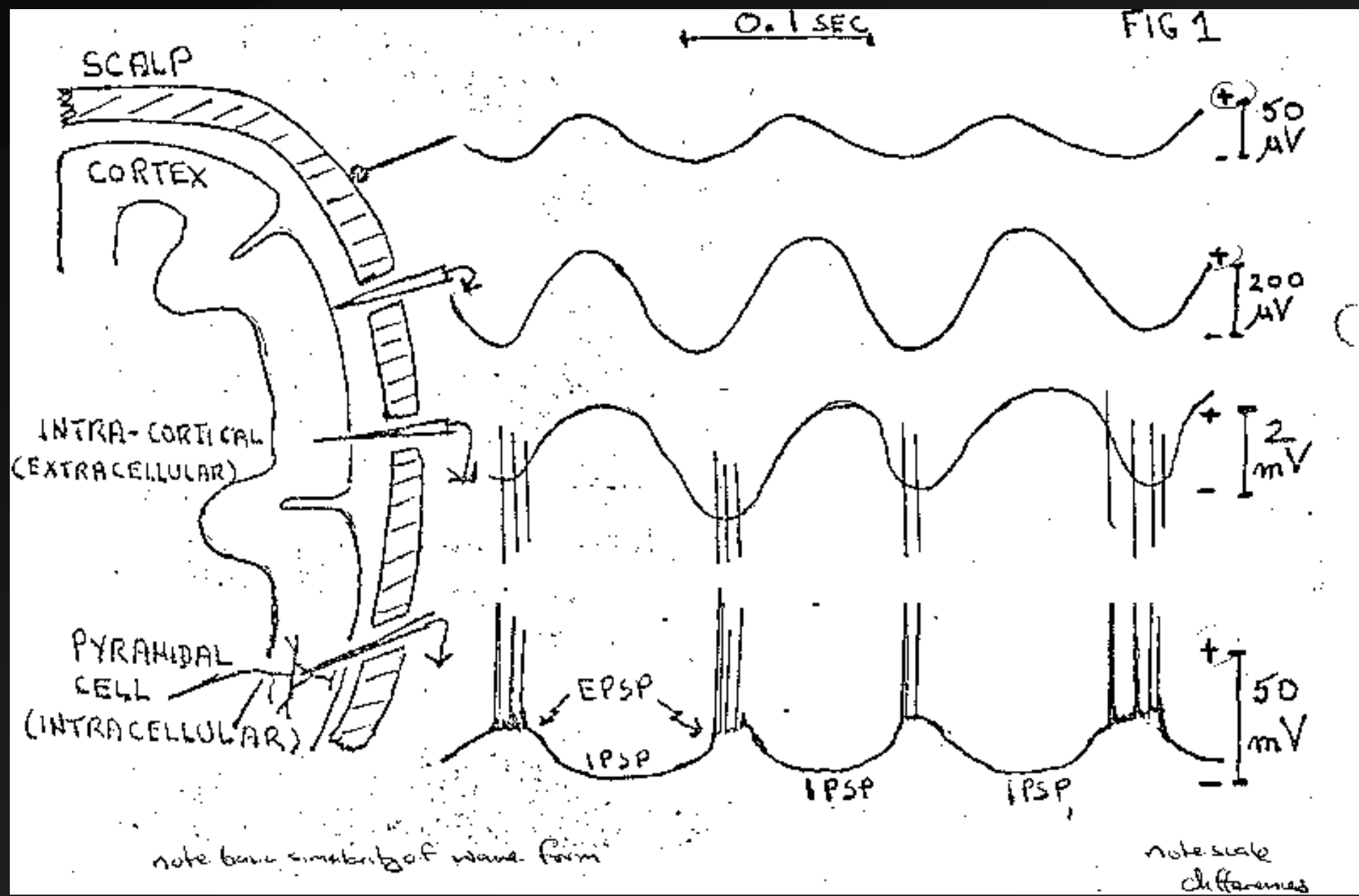


Utility of EEG

- *Relatively noninvasive*
- Excellent time resolution

Sources of scalp potentials

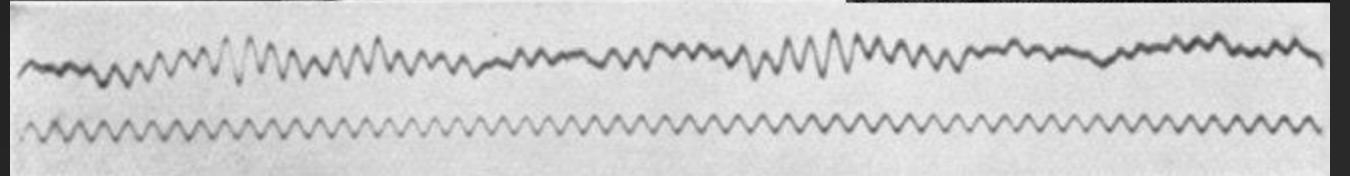
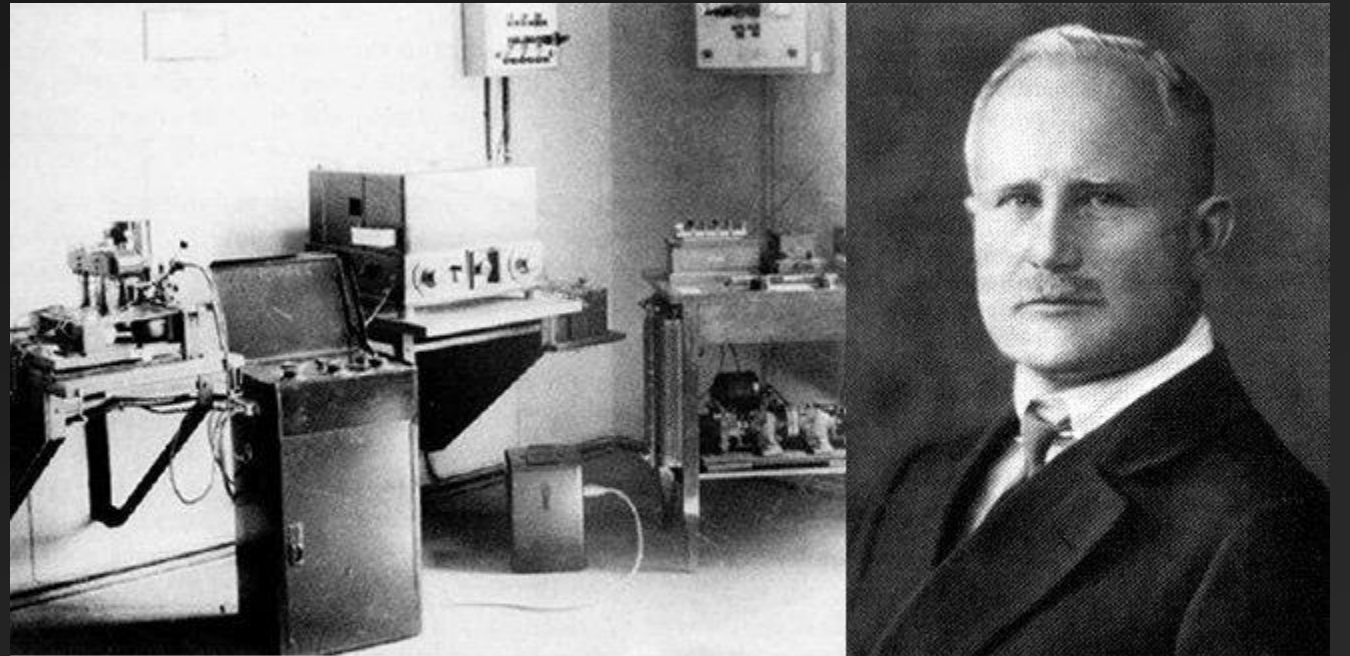
- Glial Cells – minimal, some DC steady potentials
- Neurons
 - Action Potentials – NO, brain tissue has strong capacitance effects, acting as Low Pass filter
 - Slow waves
 - Synaptic potentials – YES, both IPSPs and EPSPs from functional synaptic units are major contributors
 - Afterpotentials – May contribute to a lesser extent



Brief history of EEG

➤ Hans Berger, 1929

Siemens galvanometer





Prof. Dr. Hans Berger
1873 - 1941

Brief history of EEG

- Hans Berger, 1929
- 1930s Signal processing: capture on chart paper and analyze by visual inspection
- Alpha waves were first identified and anything higher was called beta!
 - Then frequencies described in the 1930s
 - Hoagland, Rubin, & Cameron (1936) delta waves
 - Jasper & Andrews (1936) claimed to have seen frequencies higher than 30 Hz and called them gamma waves but this was met with skepticism initially

➤ Mechanic

➤ William

➤ Oscillat

filters

➤ First model (1935) had four frequencies

➤ By 1944, 10 frequencies!

➤ Not till 1960s, with mainframe computers were computational approaches tractable

➤ Cooley & Tukey (1965): Fast Fourier Transform (FFT)

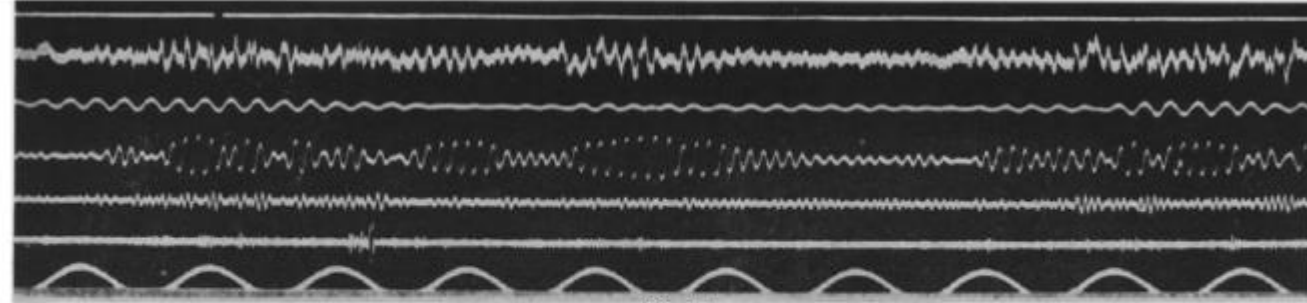


Fig. 1

Results of analysis of EEG by band-pass filters.

A. Oscillogram (from top to bottom): non-analyzed EEG, parietal-occipital leads. Outputs of filters: θ - rhythm (3,5-7 c/sec.), α - rhythm (8-12 c/sec.), β - rhythm (13-25 c/sec.), γ - rhythm (26-70 c/sec.); time mark 1 sec.



An Algorithm for the Machine Calculation of Complex Fourier Series

By James W. Cooley and John W. Tukey

An efficient method for the calculation of the interactions of a 2^m factorial experiment was introduced by Yates and is widely known by his name. The generalization to 3^m was given by Box et al. [1]. Good [2] generalized these methods and gave elegant algorithms for which one class of applications is the calculation of Fourier series. In their full generality, Good's methods are applicable to certain problems in which one must multiply an N -vector by an $N \times N$ matrix which can be factored into m sparse matrices, where m is proportional to $\log N$. This results in a procedure requiring a number of operations proportional to $N \log N$ rather than N^2 . These methods are applied here to the calculation of complex Fourier series. They are useful in situations where the number of data points k , or can be chosen to be, a highly composite number. The algorithm is here derived and presented in a rather different form. Attention is given to the choice of N . It is also shown how special advantage can be obtained in the use of a binary computer with $N = 2^m$ and how the entire calculation can be performed within the array of N data storage locations used for the given Fourier coefficients.

Consider the problem of calculating the complex Fourier series

$$(1) \quad X(j) = \sum_{k=0}^{N-1} A(k) \cdot W^{jk}, \quad j = 0, 1, \dots, N-1,$$

where the given Fourier coefficients $A(k)$ are complex and W is the principal N th root of unity,

$$(2) \quad W = e^{2\pi i/N}.$$

A straightforward calculation using (1) would require N^2 operations where "operation" means, as it will throughout this note, a complex multiplication followed by a complex addition.

The algorithm described here iterates on the array of given complex Fourier amplitudes and yields the result in less than $2N \log_2 N$ operations without requiring more data storage than is required for the given array A . To derive the algorithm, suppose N is a composite, i.e., $N = r_1 r_2 \dots r_m$. Then let the indices in (1) be expressed

$$(3) \quad j = j_1 r_2 + j_2, \quad j_1 = 0, 1, \dots, r_1 - 1, \quad j_2 = 0, 1, \dots, r_2 - 1, \\ k = k_1 r_2 + k_2, \quad k_1 = 0, 1, \dots, r_1 - 1, \quad k_2 = 0, 1, \dots, r_2 - 1.$$

Then, one can write

$$(4) \quad X(j_1, j_2) = \sum_{k_1=0}^{r_1-1} \sum_{k_2=0}^{r_2-1} A(k_1, k_2) \cdot W^{(j_1 r_2 + j_2)(k_1 r_2 + k_2)}.$$

Received August 17, 1964. Research in part at Princeton University under the sponsorship of the Army Research Office (Durham). The authors wish to thank Richard Garwin for his essential role in communication and encouragement.

297

License or copyright restrictions may apply to redistribution; see <https://www.ama-assn.org/journal-terms-of-use>

Since

$$(5) \quad W^{r_2 k_2} = W^{(j_1 r_2 + j_2) k_2},$$

the inner sum, over k_2 , depends only on j_2 and k_2 and can be defined as a new array,

$$(6) \quad A_1(j_2, k_2) = \sum_{k_1=0}^{r_1-1} A(k_1, k_2) \cdot W^{j_1 r_2 k_1 k_2}.$$

The result can then be written

$$(7) \quad X(j_1, j_2) = \sum_{k_1=0}^{r_1-1} A_1(j_2, k_2) \cdot W^{(j_1 r_2 + j_2) k_1 r_2}.$$

There are N elements in the array A_1 , each requiring r_1 operations, giving a total of $N r_1$ operations to obtain A_1 . Similarly, it takes $N r_2$ operations to calculate X from A_1 . Therefore, this two-step algorithm, given by (6) and (7), requires a total of

$$(8) \quad T = N(r_1 + r_2)$$

operations.

It is easy to see how successive applications of the above procedure, starting with its application to (6), give an m -step algorithm requiring

$$(9) \quad T = N(r_1 + r_2 + \dots + r_m)$$

operations, where

$$(10) \quad N = r_1 r_2 \dots r_m.$$

If $r_j = s_j t_j$ with $s_j, t_j > 1$, then $s_j + t_j < r_j$ unless $s_j = t_j = 2$, when $s_j + t_j = r_j$. In general, then, using as many factors as possible provides a minimum to (9), but factors of 2 can be combined in pairs without loss. If we are able to choose N to be highly composite, we may make very real gains. If all r_j are equal to r , then, from (10) we have

$$(11) \quad m = \log_r N$$

and the total number of operations is

$$(12) \quad T(r) = rN \log_r N.$$

If $N = r^m$, then we find that

$$(13) \quad \frac{T}{N} = m \cdot r + n \cdot s + p \cdot l + \dots,$$

$$\log_r N = m \cdot \log_r r + n \cdot \log_r s + p \cdot \log_r l + \dots,$$

so that

$$\frac{T}{N \log_r N}$$

is a weighted mean of the quantities

$$\frac{r}{\log_r r}, \frac{s}{\log_r s}, \frac{l}{\log_r l}, \dots,$$

License or copyright restrictions may apply to redistribution; see <https://www.ama-assn.org/journal-terms-of-use>

whose values run as follows

r	$\frac{r}{\log_r r}$
2	2.00
3	1.88
4	2.00
5	2.15
6	2.31
7	2.49
8	2.67
9	2.82
10	3.01

The use of $r_j = 3$ is formally most efficient, but the gain is only about 6% over the use of 2 or 4, which have other advantages. If necessary, the use of r_j up to 10 can increase the number of computations by no more than 50%. Accordingly, we can find "highly composite" values of N within a few percent of any given large number.

Whenever possible, the use of $N = 2^m$ with $r = 2$ or 4 offers important advantages for computers with binary arithmetic, both in addressing and in multiplication economy.

The algorithm with $r = 2$ is derived by expressing the indices in the form

$$(14) \quad j = j_{m-1} 2^{m-1} + \dots + j_1 2 + j_0, \\ k = k_{m-1} 2^{m-1} + \dots + k_1 2 + k_0,$$

where j_i and k_i are equal to 0 or 1 and are the contents of the respective bit positions in the binary representation of j and k . All arrays will now be written as functions of the bits of their indices. With this convention (1) is written

$$(15) \quad X(j_{m-1}, \dots, j_0) = \sum_{k_0=0}^{1} \dots \sum_{k_{m-1}=0}^{1} A(k_{m-1}, \dots, k_0) \cdot W^{(j_{m-1} 2^{m-1} + \dots + j_0)(k_{m-1} 2^{m-1} + \dots + k_0)},$$

where the sums are over $k_i = 0, 1$. Since

$$(16) \quad W^{(j_{m-1} 2^{m-1} + \dots + j_0) k_{m-1} 2^{m-1}},$$

the innermost sum of (15), over k_{m-1} , depends only on j_{m-1} , k_{m-2}, \dots, k_0 and can be written

$$(17) \quad A_1(j_{m-1}, k_{m-2}, \dots, k_0) = \sum_{k_{m-1}=0}^1 A(k_{m-1}, \dots, k_0) \cdot W^{(j_{m-1} 2^{m-1} + \dots + j_0) k_{m-1} 2^{m-1}}.$$

Proceeding to the next innermost sum, over k_{m-2} , and so on, and using

$$(18) \quad W^{(j_{m-1} 2^{m-1} + \dots + j_0) k_{m-2} 2^{m-2}},$$

one obtains successive arrays,

$$(19) \quad A_l(j_{m-1}, \dots, j_{l-1}, k_{m-1}, \dots, k_l) = \sum_{k_{l-1}=0}^1 \dots \sum_{k_{m-1}=0}^1 A(k_{m-1}, \dots, k_l) \cdot W^{(j_{m-1} 2^{m-1} + \dots + j_l) k_{m-1} 2^{m-1} + \dots + j_l k_l 2^l}$$

for $l = 1, 2, \dots, m$.

License or copyright restrictions may apply to redistribution; see <https://www.ama-assn.org/journal-terms-of-use>

a	b	c	No. Pts.	Time (minutes)
4	4	3	2^{11}	.02
11	0	0	2^{11}	.02
4	4	4	2^{11}	.04
12	0	0	2^{11}	.07
5	4	4	2^{10}	.10
5	5	3	2^{10}	.12
13	0	0	2^{10}	.15

IBM Watson Research Center
Yorktown Heights, New York
Bell Telephone Laboratories,
Murray Hill, New Jersey
Princeton University
Princeton, New Jersey

J. G. E. P. Box, L. R. Connor, W. R. Collins, O. L. Davies (Ed.), F. R. Hinesworth & G. F. Smith, *The Design and Analysis of Industrial Experiments*, Oliver & Boyd, Edinburgh, 1964.

J. I. Good, "The interaction algorithm and practical Fourier series," *J. Roy. Statist. Soc. Ser. B*, v. 20, 1958, p. 361-372; Addendum, v. 22, 1960, p. 372-375. MR 21 #1674; MR 23 #A621.

Writing out the sum this appears as

$$(20) \quad A(j_0, \dots, j_{l-1}, k_{m-l-1}, \dots, k_0) \\ = A_l(j_0, \dots, j_{l-1}, 0, k_{m-l-1}, \dots, k_0) \\ + (-1)^{j_{l-1} 2^{l-1}} A_l(j_0, \dots, j_{l-1}, 1, k_{m-l-1}, \dots, k_0) \\ \dots \\ + W^{(j_{l-1} 2^{l-1} + \dots + j_0) k_{m-l-1} 2^{m-l-1}} A_l(j_0, \dots, j_{l-1}, 0, 1, k_{m-l-1}, \dots, k_0).$$

According to the indexing convention, this is stored in a location whose index is

$$(21) \quad j_0 2^{m-1} + \dots + j_{l-1} 2^{m-l} + k_{m-l-1} 2^{m-l-1} + \dots + k_0.$$

It can be seen in (20) that only the two storage locations with indices having 0 and 1 in the 2^{m-l} bit position are involved in the computation. Parallel computation is permitted since the operation described by (20) can be carried out with all values of j_0, \dots, j_{l-1} , and k_0, \dots, k_{m-l-1} simultaneously. In some applications¹ it is convenient to use (20) to express A_l in terms of A_{l-1} , giving what is equivalent to an algorithm with $r = 4$.

The last array calculated gives the desired Fourier sums,

$$(22) \quad X(j_{m-1}, \dots, j_0) = A_m(j_0, \dots, j_{m-1})$$

in such an order that the index of an X must have its binary bits put in reverse order to yield its index in the array A_m .

In some applications, where Fourier sums are to be evaluated twice, the above procedure could be programmed so that no bit-inversion is necessary. For example, consider the solution of the difference equation,

$$(23) \quad aX(j+1) + bX(j) + cX(j-1) = F(j).$$

The present method could be first applied to calculate the Fourier amplitudes of $F(j)$ from the formula

$$(24) \quad B(k) = \frac{1}{N} \sum_j F(j) W^{-kj}.$$

The Fourier amplitudes of the solution are, then,

$$(25) \quad A(k) = \frac{B(k)}{aW^k + b + cW^{-k}}.$$

The $B(k)$ and $A(k)$ arrays are in bit-inverted order, but with an obvious modification of (20), $A(k)$ can be used to yield the solution with correct indexing.

A computer program for the IBM 7094 has been written which calculates three-dimensional Fourier sums by the above method. The computing time taken for computing three-dimensional $2^2 \times 2^2 \times 2^2$ arrays of data points was as follows:

¹ A multiple-processing circuit using this algorithm was designed by R. E. Miller and S. Wingard of the IBM Watson Research Center. In this case $r = 4$ was found to be most practical.

License or copyright restrictions may apply to redistribution; see <https://www.ama-assn.org/journal-terms-of-use>

Over 12,400 citations

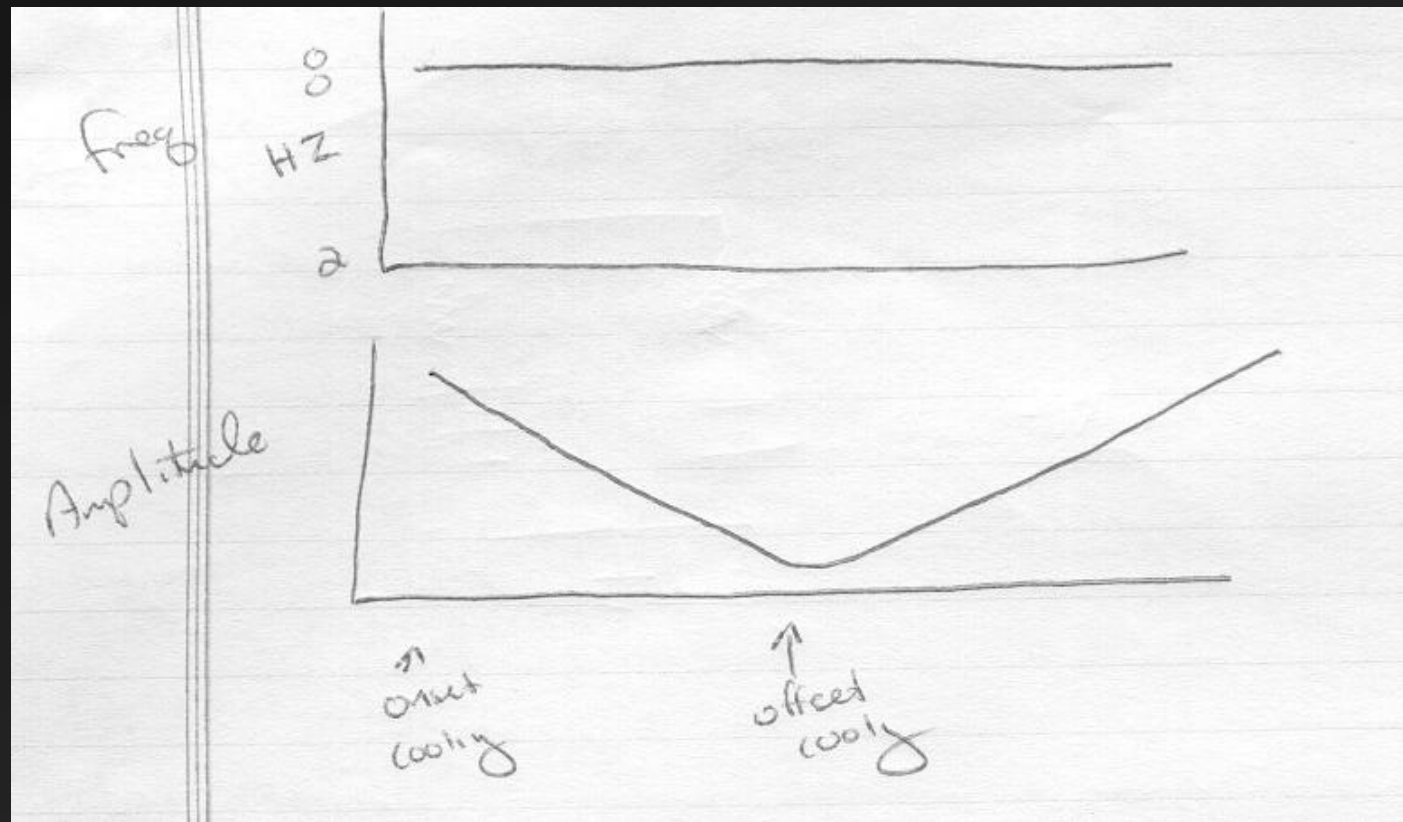
Alpha and Synchronization

- Why Alpha?
 - It is obvious and hard to miss!
 - Accounts for ~70% of EEG activity in adult human brain
- From where, Alpha?
 - Historically, thought to be thalamocortical looping
 - Adrian (1935) demolished that theory
 - Recorded EEG simultaneously in cortex and thalamus
 - Damage to cortex did not disrupt thalamic alpha rhythmicity
 - Damage to thalamus DID disrupt cortical alpha rhythmicity
 - Thalamic rhythmicity remains even in decorticate preparations (Adrian, 1941)
 - Removal of 1/2 thalamus results in ipsilateral loss of cortical alpha



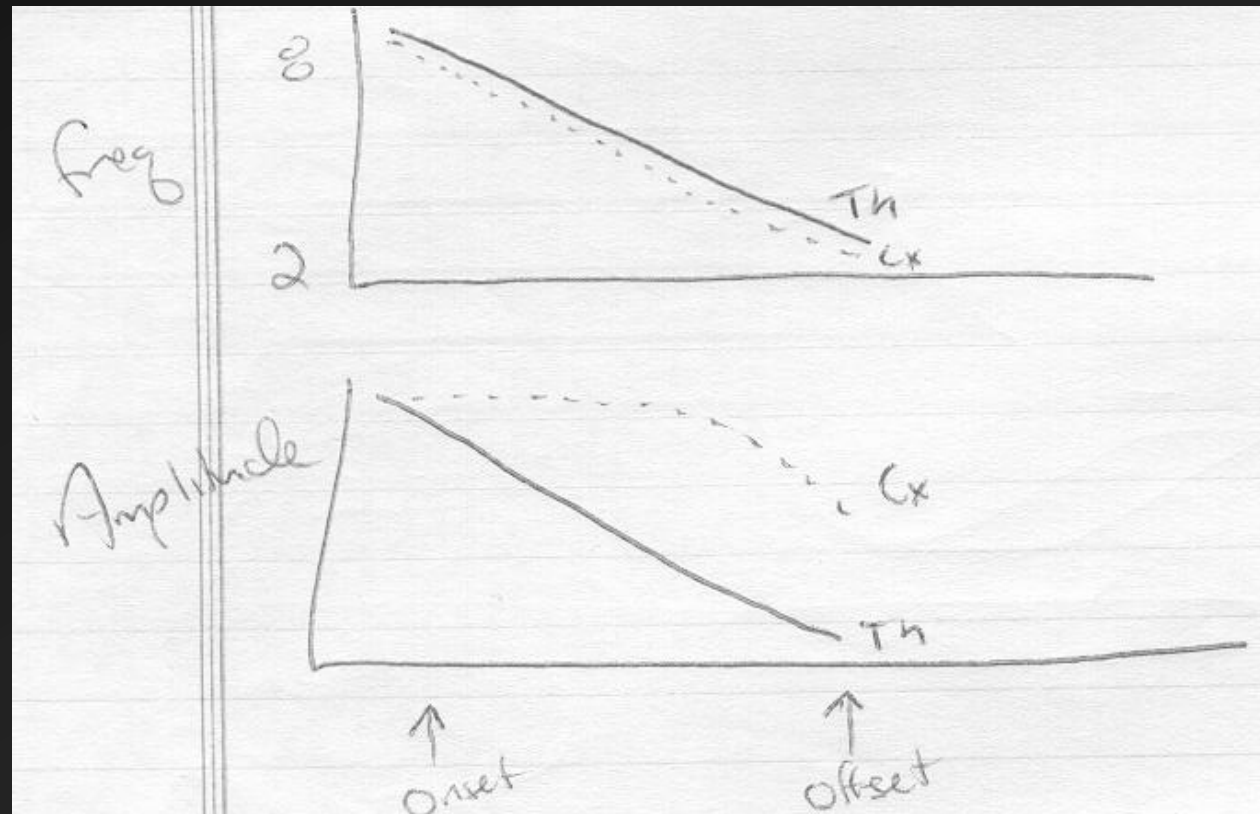
Alpha and Synchronization

- Andersen and Andersen (1968)
 - Cooling of Cortex resulted in change in amplitude but not frequency of Alpha



Alpha and Synchronization

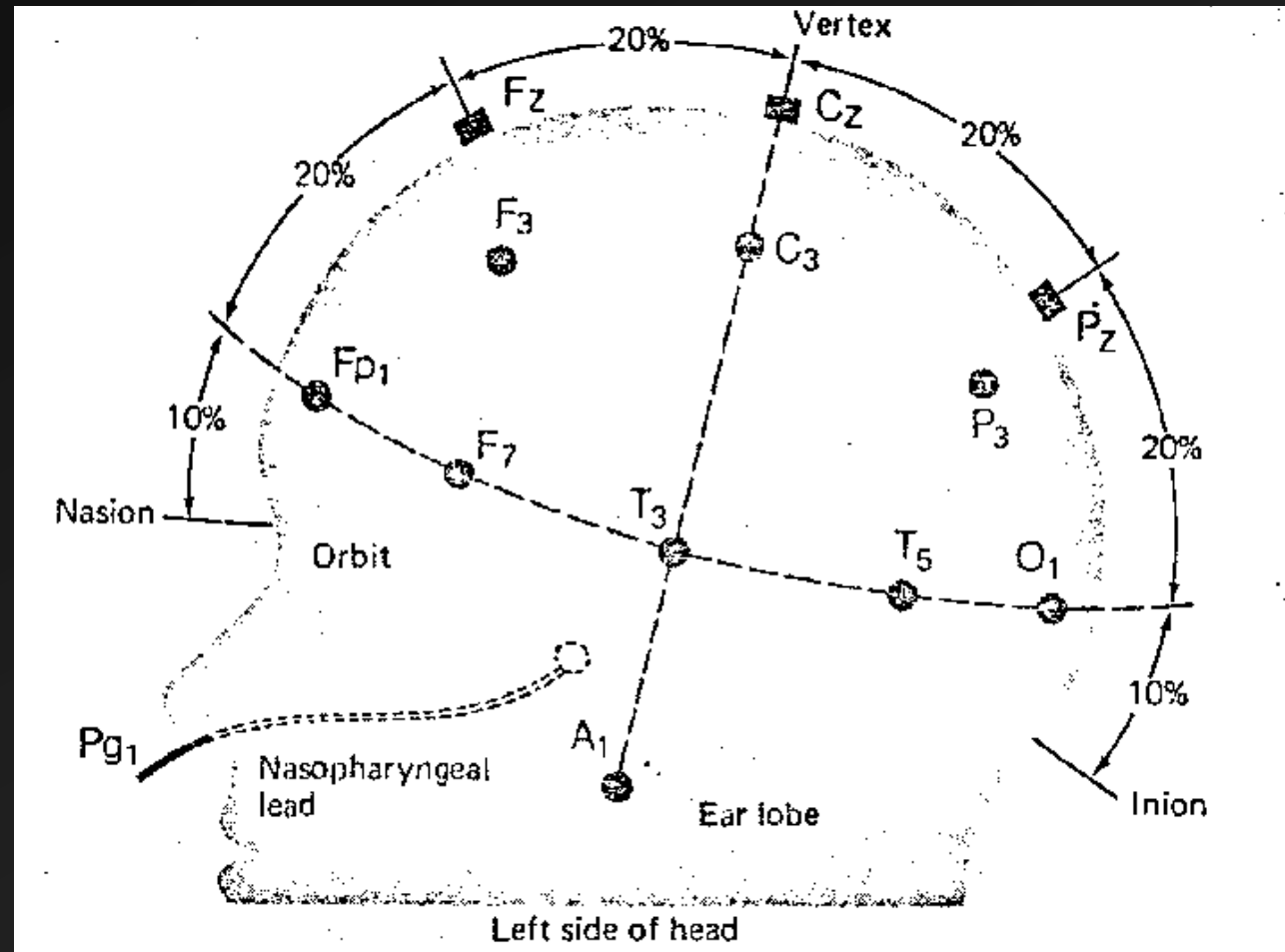
- Andersen and Andersen (1968)
 - Cooling of Thalamus resulted in change in amplitude and frequency of Alpha at both thalamus and cortex



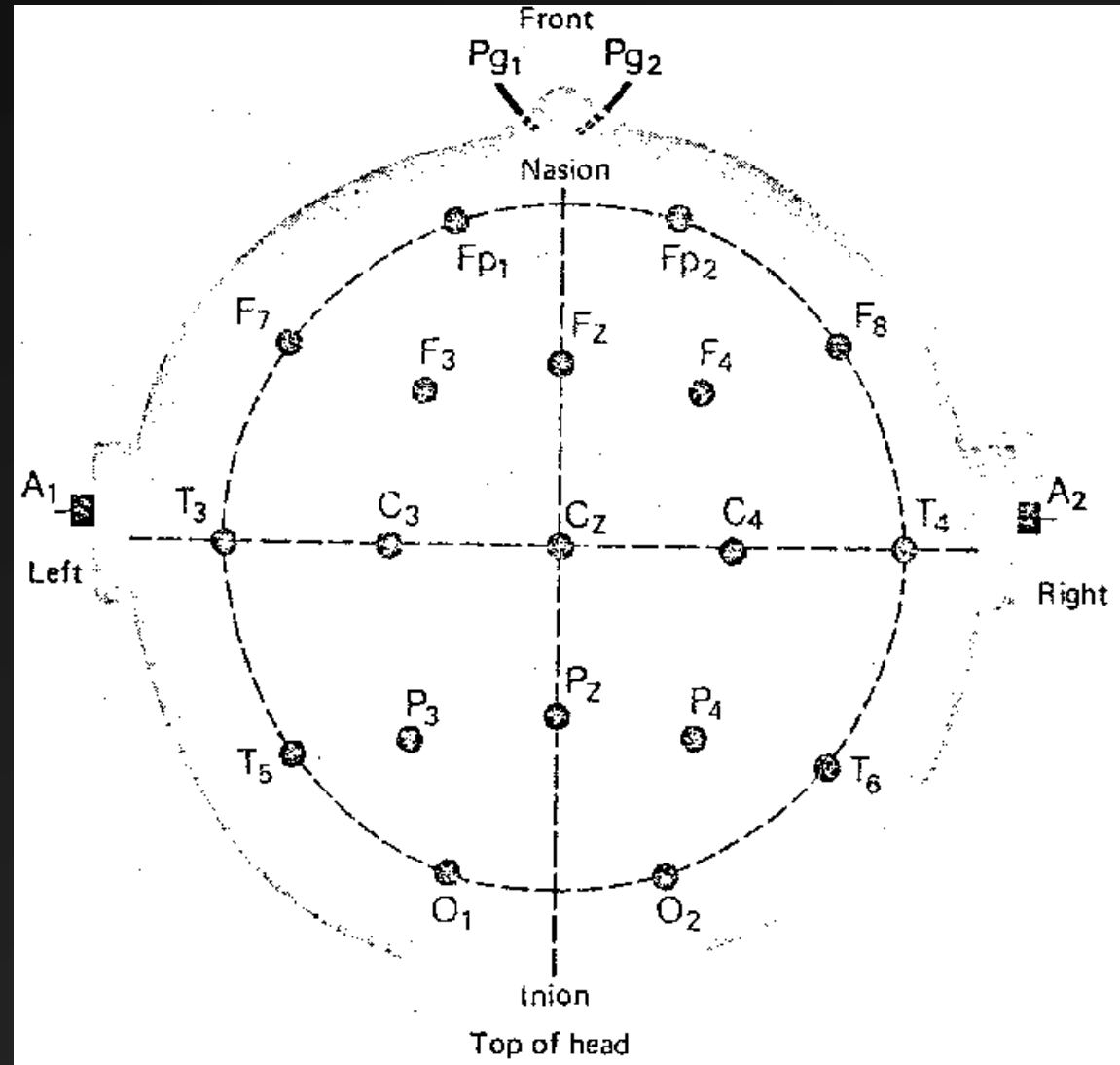
Alpha and Synchronization

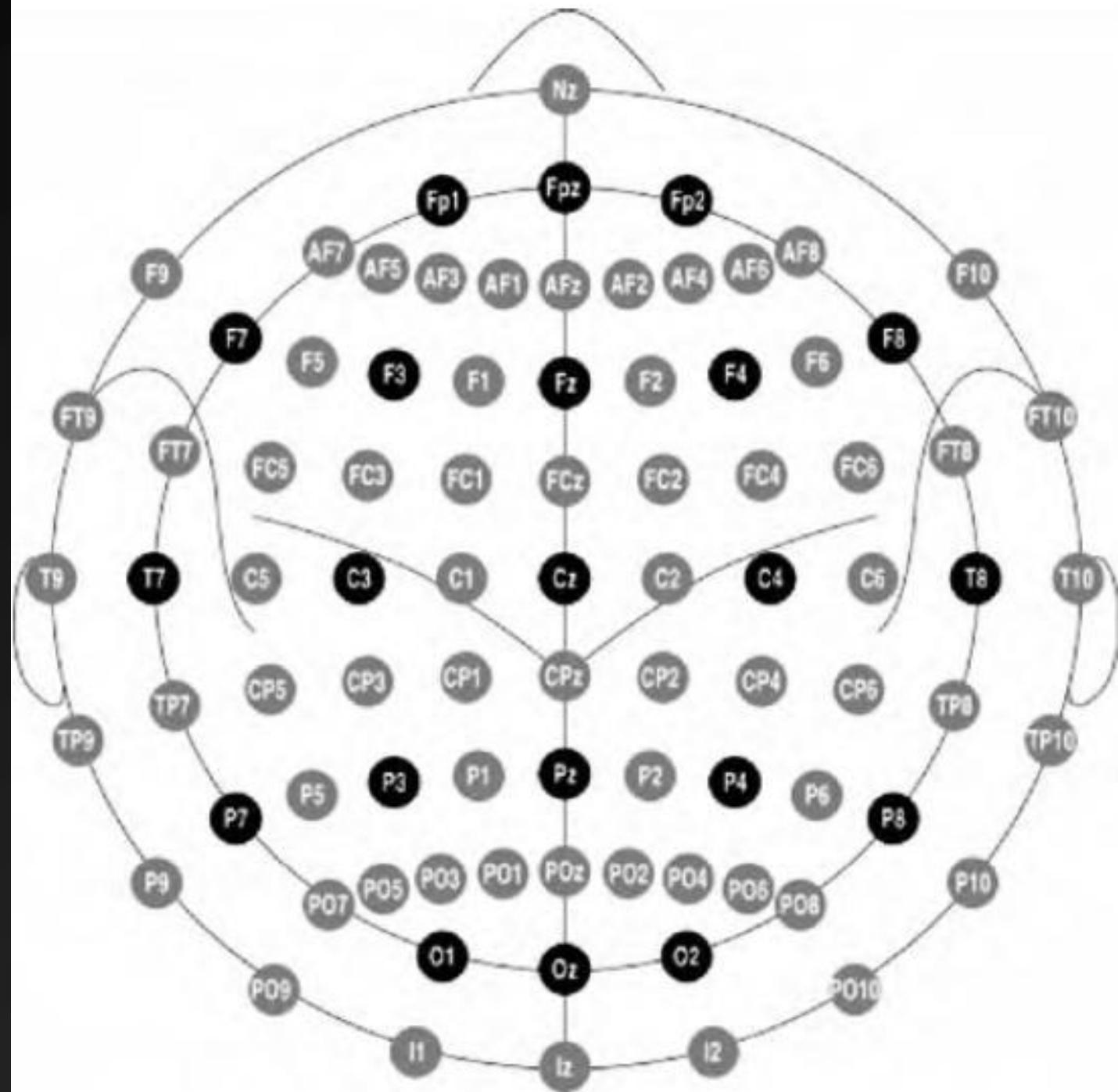
- In sum, Thalamus drives the alpha rhythmicity of the EEG
 - Cortex certainly does feedback to thalamus, but thalamus is responsible for driving the EEG
 - Particularly the Reticularis nucleus (Steriade et al. 1985)
- What causes change from rhythmicity to desynchronization?
 - Afferent input to thalamic relay nuclei
 - Mode-specific enhancement observed

Recording EEG



Recording EEG





Systems are surface-based, not anatomically-based

NeuroImage 46 (2009) 64–72

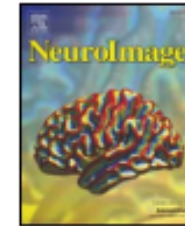


ELSEVIER

Contents lists available at [ScienceDirect](#)

NeuroImage

journal homepage: www.elsevier.com/locate/ynimg



Automated cortical projection of EEG sensors: Anatomical correlation via the international 10–10 system

L. Koessler^{a,b}, L. Maillard^b, A. Benhadid^a, J.P. Vignal^b, J. Felblinger^a, H. Vespignani^b, M. Braun^{a,c,d,*}

^a INSERM U947, Nancy University, France

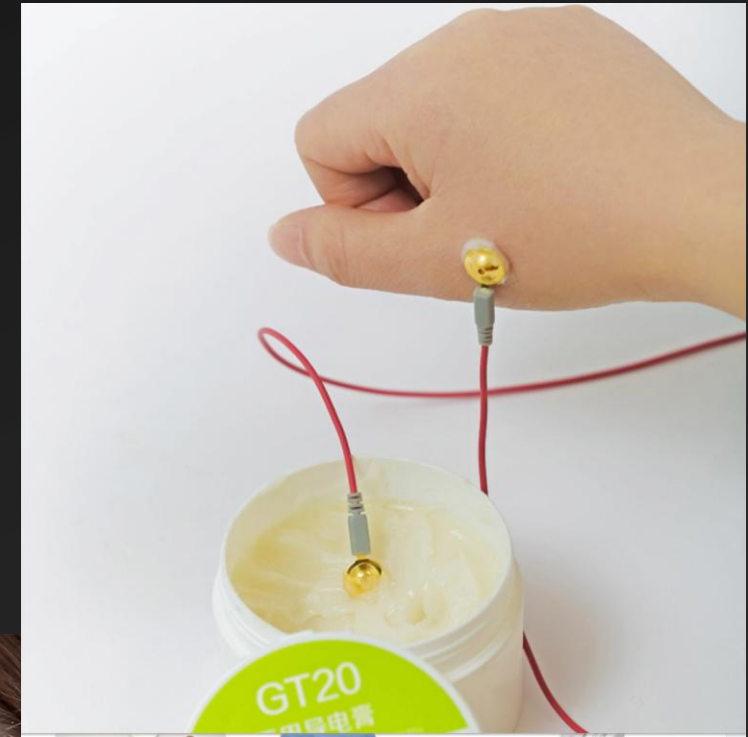
^b Neurology Department, University Hospital, Nancy, France

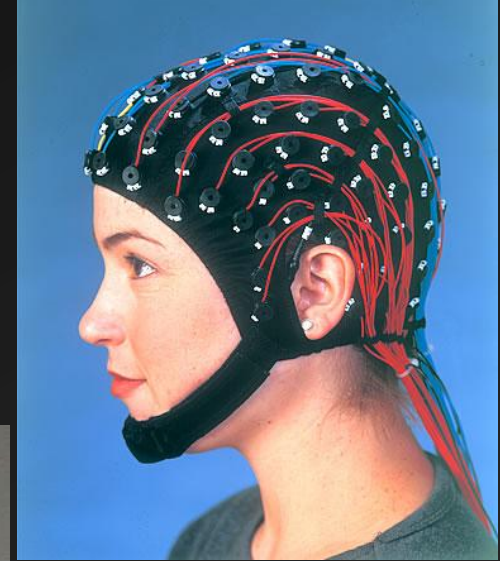
^c Neuroradiology Department, University Hospital, Nancy, France

^d Anatomy Department, Nancy University, France

Electrodes, Electrolyte, Preparation

- Ag-AgCl preferred, Gold OK if slowest frequencies not of interest
 - Polarizing electrodes act as capacitors in series with signal
- Electrolyte: ionic, conductive
- Affixing
 - Subcutaneous needle electrodes (OUCH)
 - Collodion (YUCK)
 - Adhesive conductive paste
 - Electrocap





Recording References

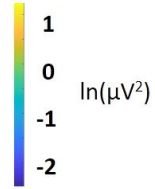
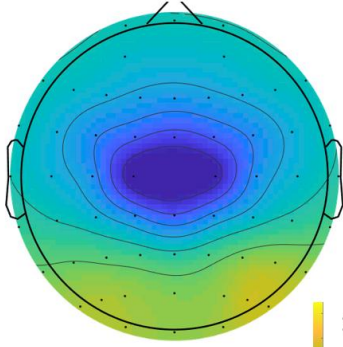
- Measure voltage potential differences
 - Difference between what and what else?
- “Monopolar” versus Bipolar
 - No truly inactive site, so monopolar is a relative term
 - Relatively monopolar options
 - Body – BAD IDEA
 - Head
 - Linked Ears or Mastoids
 - Tip of Nose
- Reference choice nontrivial as it will change your ability to observe certain signals

Recording References

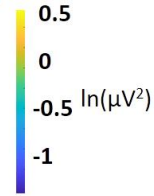
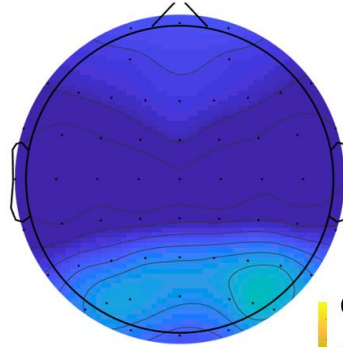
- Bipolar recording
 - Multiple active sites
 - Sensitive to differences between electrodes
 - With proper array, sensitive to local fluctuations (e.g. spike localization)
- Off-line derivations
 - Averaged Mastoids
 - Average Reference (of EEG Leads)
 - With sufficient # electrodes and surface coverage, approximates inactive site (signals cancel out)
 - Artifacts “average in”
 - Current Source Density (more in advanced topics)

Open

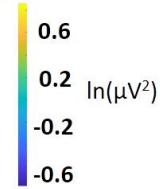
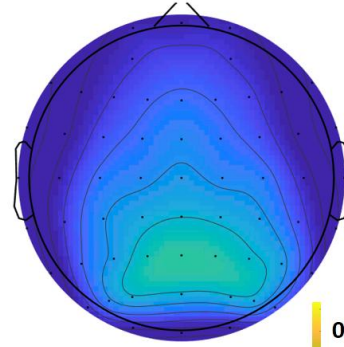
Cz



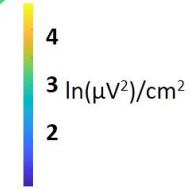
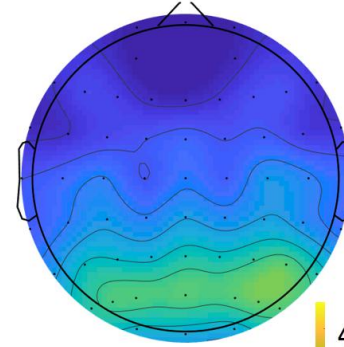
AR



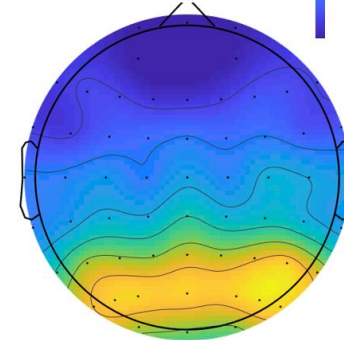
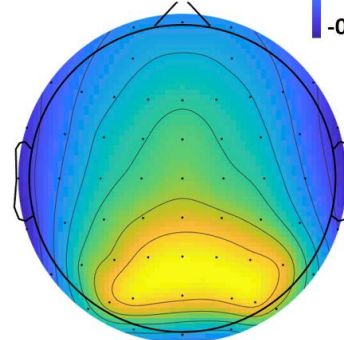
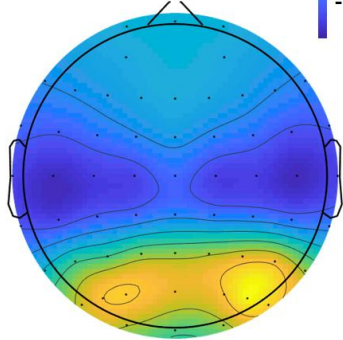
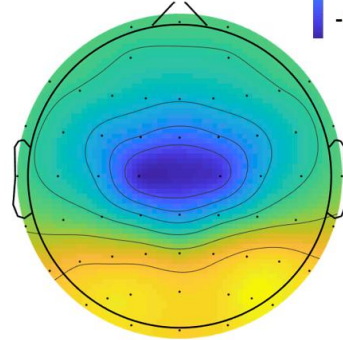
LM



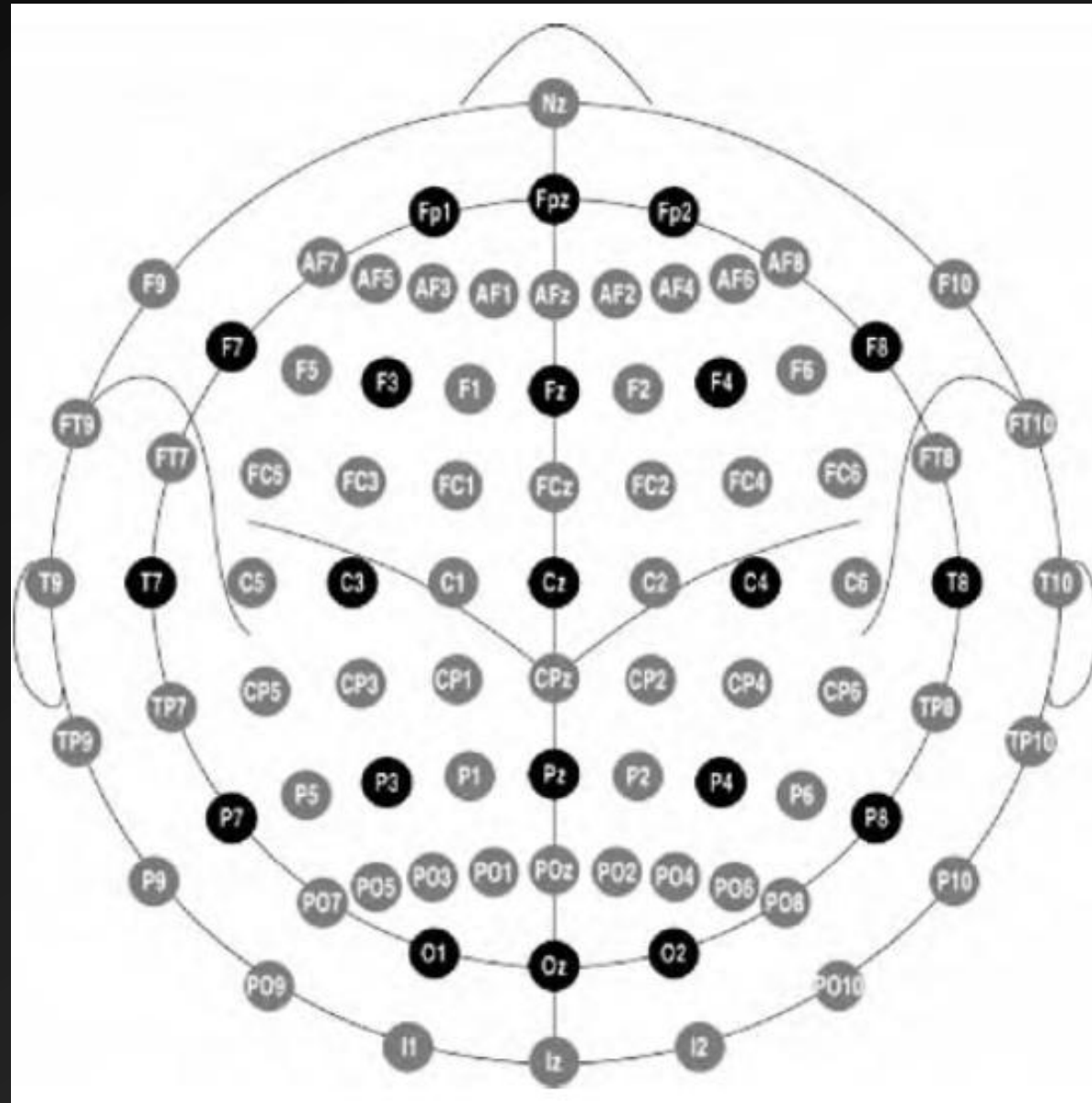
CSD



Closed



Electrode Placement

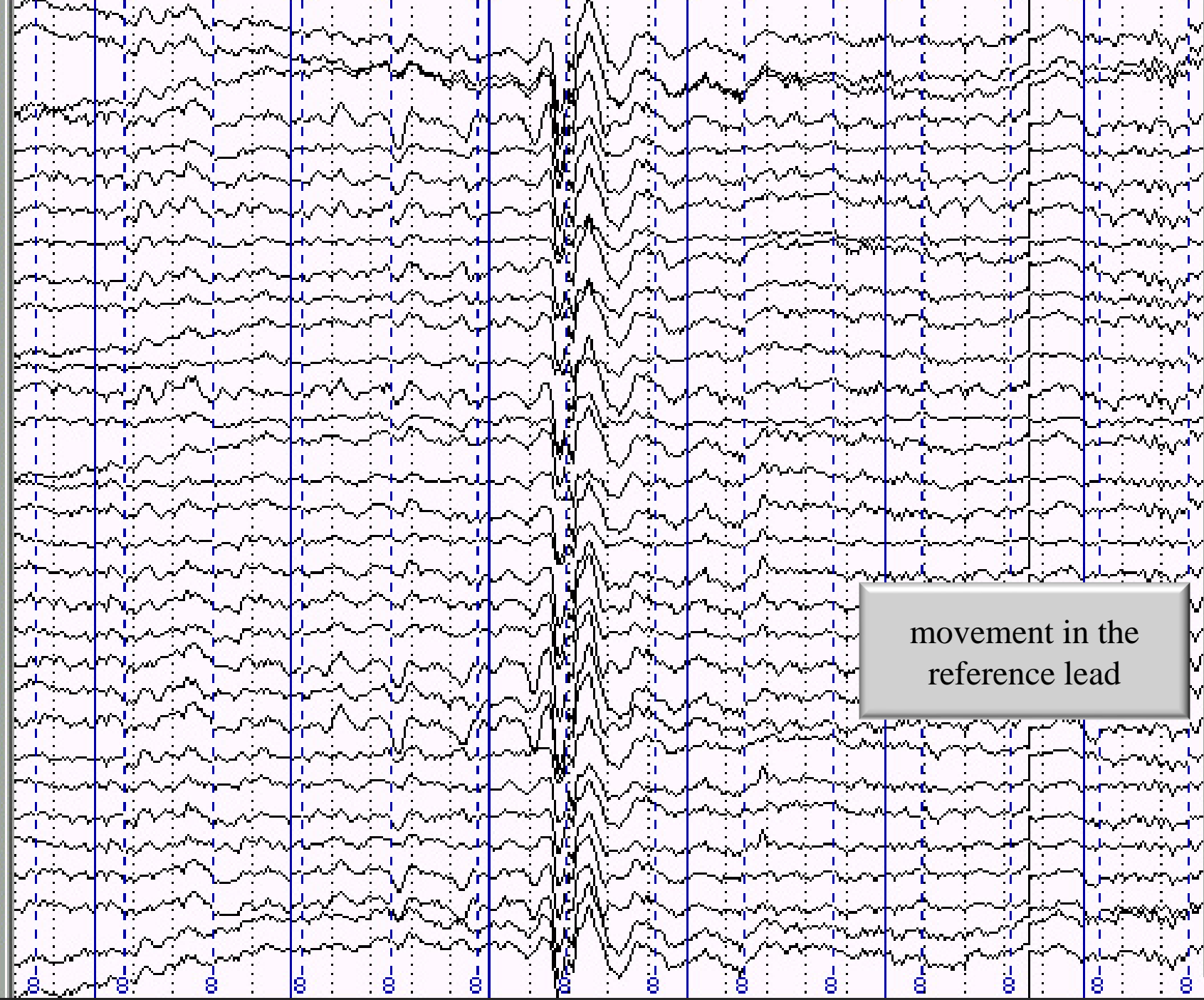


Dreaded Artifacts

- Three sources
 - 60-cycle noise
 - Ground subject
 - 60 Hz Notch filter
 - Muscle artifact
 - No gum!
 - Use headrest
 - Measure EMG and reject/correct for influence
 - Eye Movements
 - Eyes are dipoles
 - Reject ocular deflections including blinks
 - Use correction procedure (more in advanced lecture)

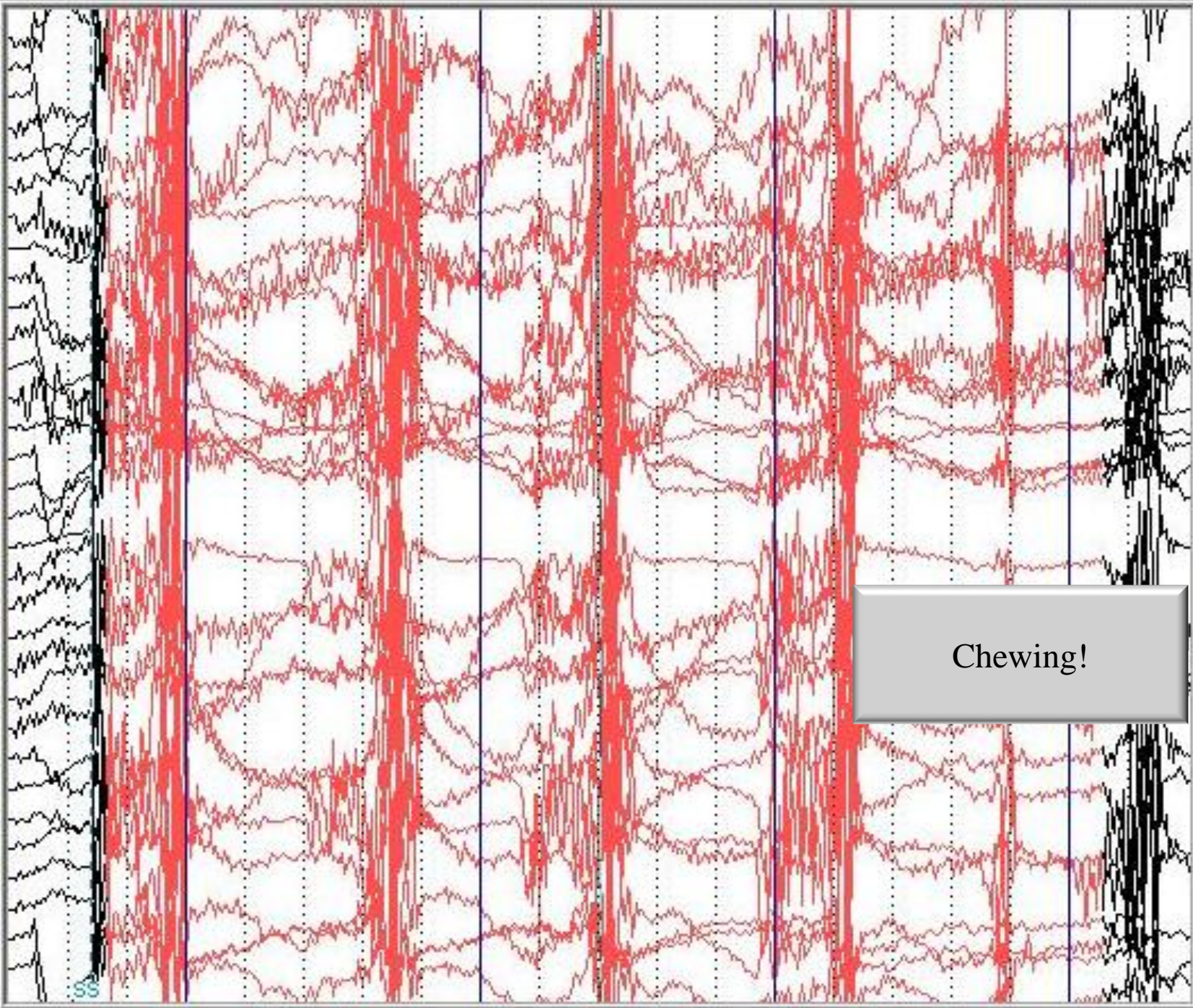
*Name
That
Artifact!*

LVEOG
RVEOG
NASION
O1
P3
T5
T3
C3
F7
F3
FP1
FZ
A1
PZ
FP2
F4
F8
C4
T4
T6
P4
O2
A2
OZ
FTC1
FTC2
TCP1
TCP2
PO1
PO2
LEMG
REMG

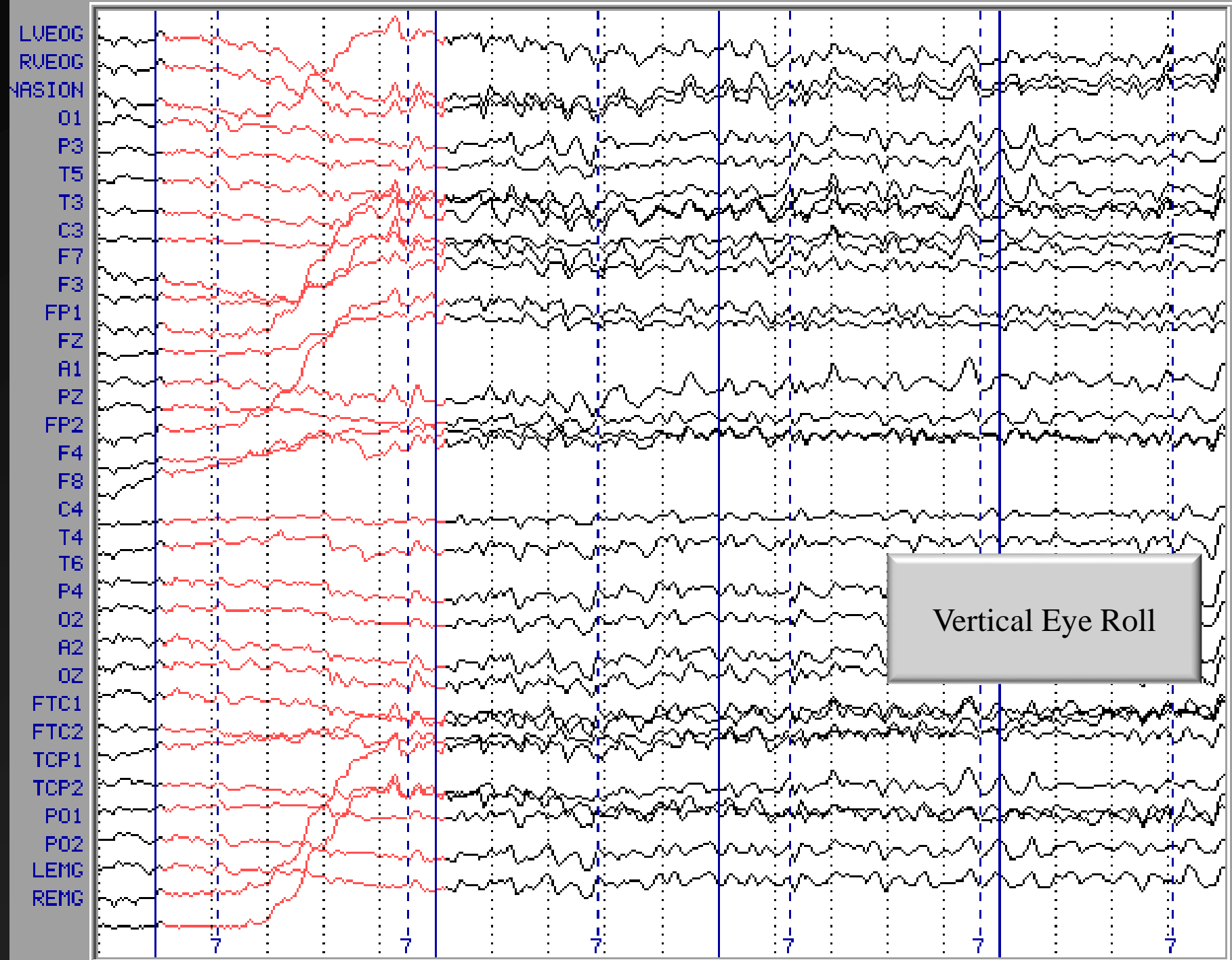


movement in the
reference lead

LVEOG
RVEOG
NASION
O1
P3
T5
T3
C3
F7
F3
FP1
FZ
A1
PZ
FP2
F4
F8
C4
T4
T6
P4
O2
A2
OZ
FTC1
FTC2
TCP1
TCP2
P01
P02
LEMG
REMG

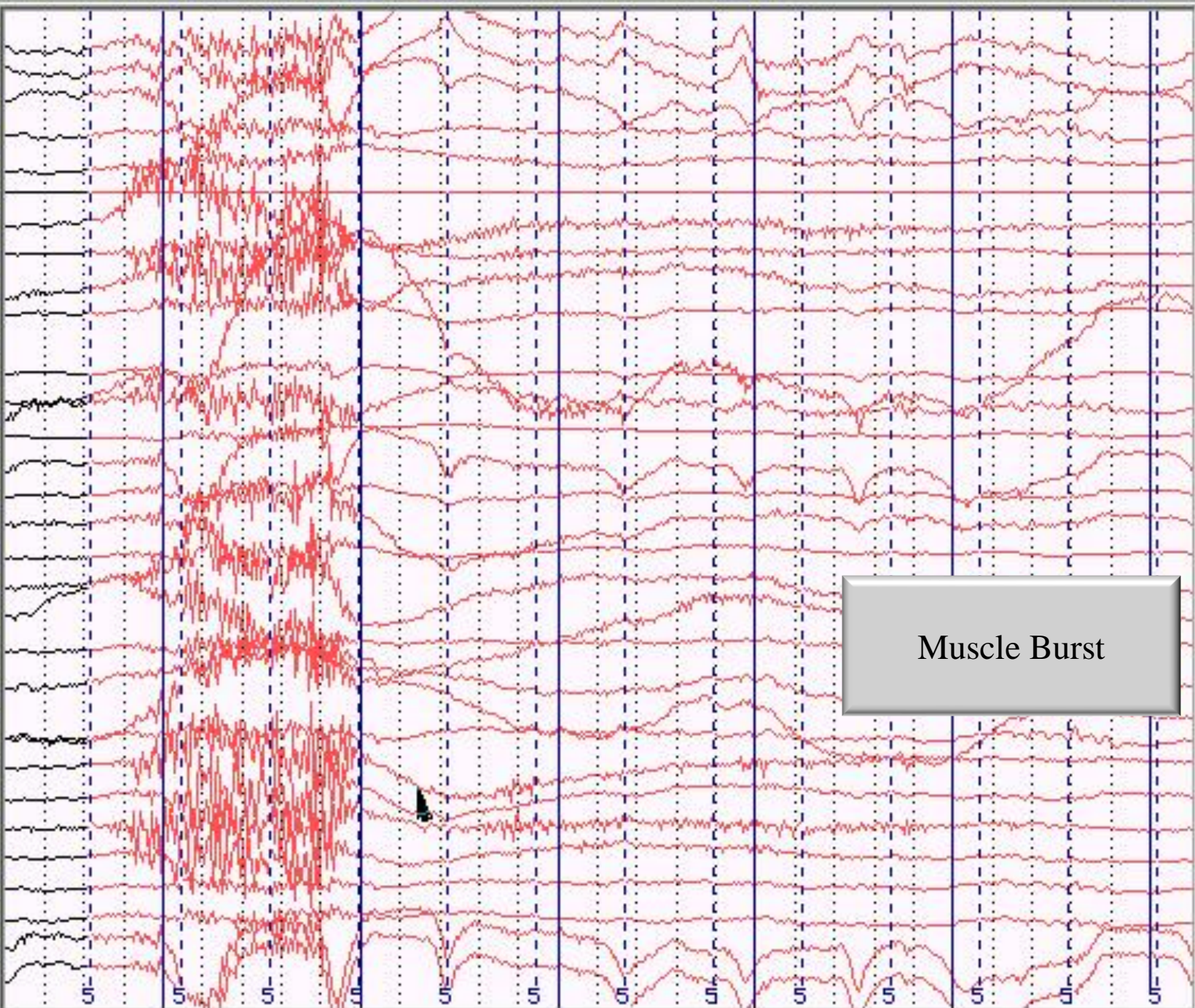


Chewing!

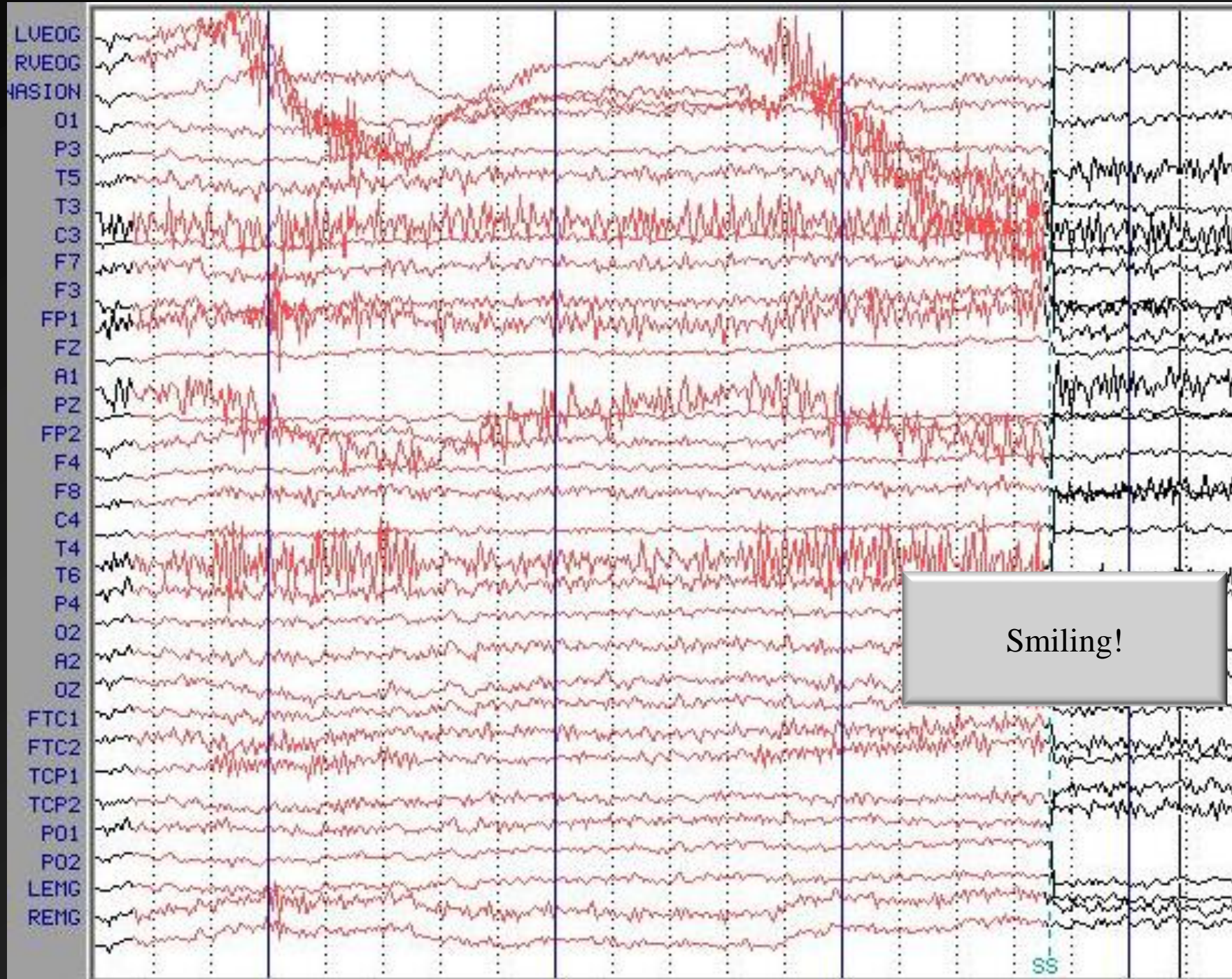


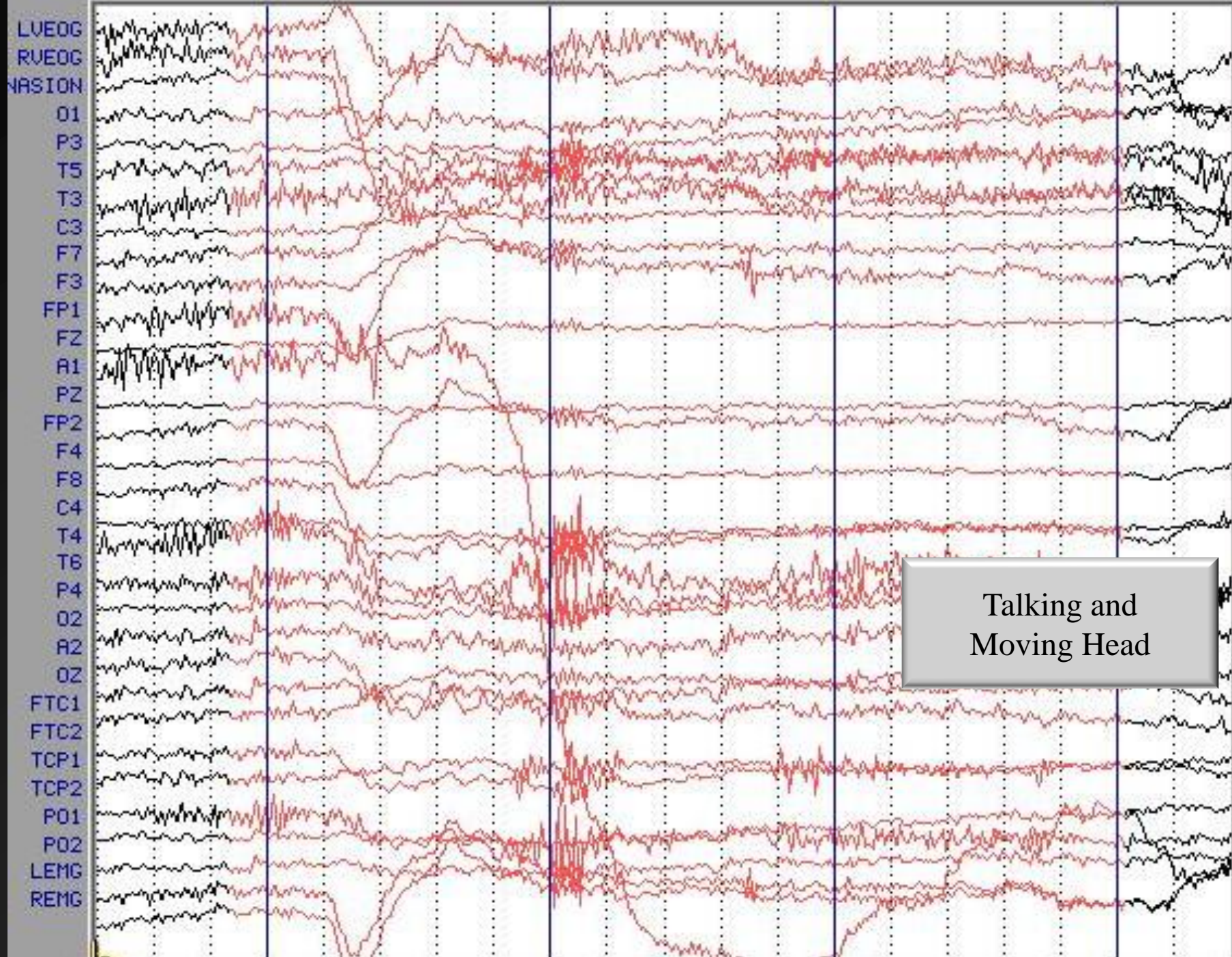
Vertical Eye Roll

LUEOG
RUEOG
NASION
O1
P3
T5
T3
C3
F7
F3
FP1
FZ
A1
PZ
FP2
F4
F8
C4
T4
T6
P4
O2
A2
OZ
FTC1
FTC2
TCP1
TCP2
P01
P02
LEMG
REMG

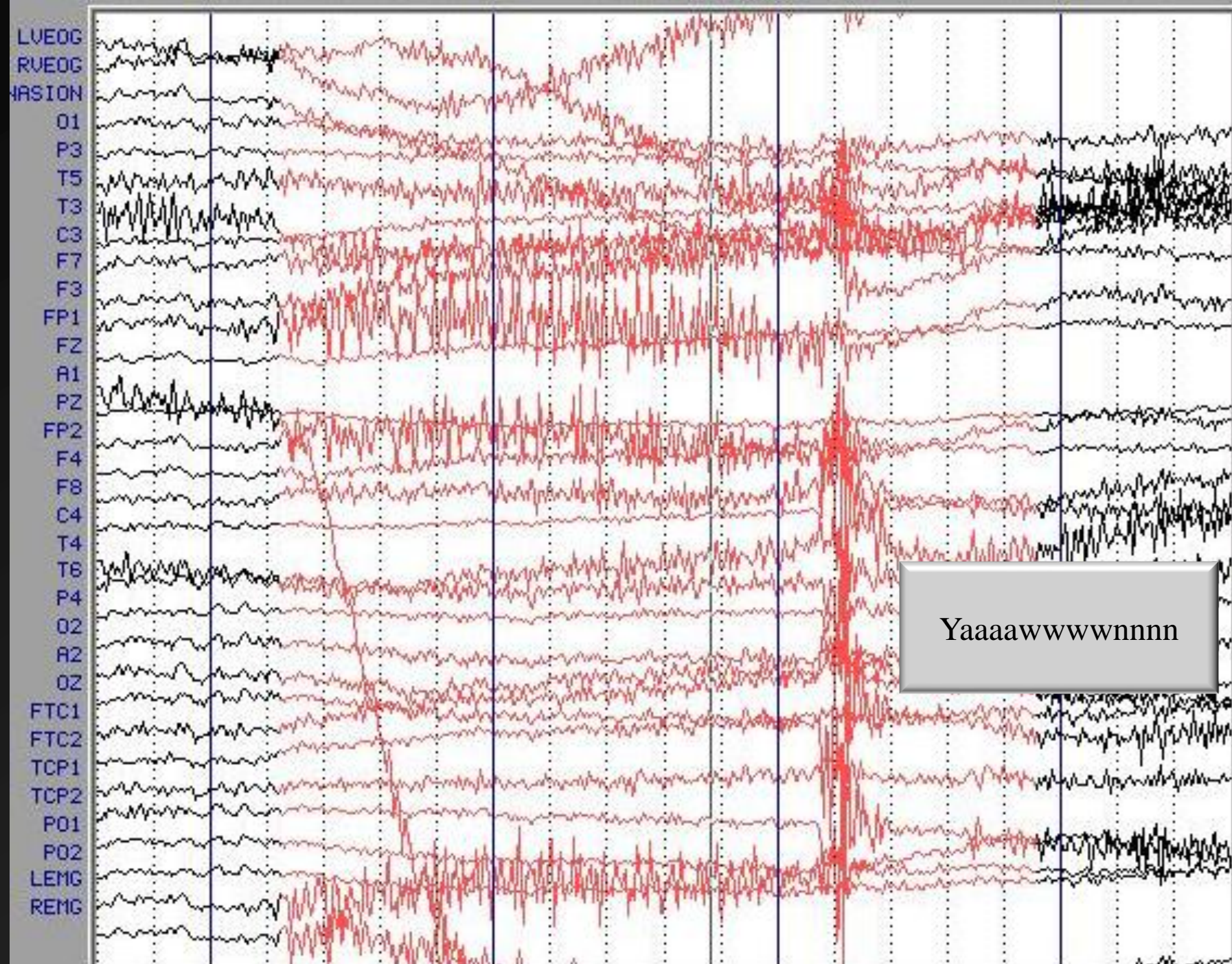


Muscle Burst

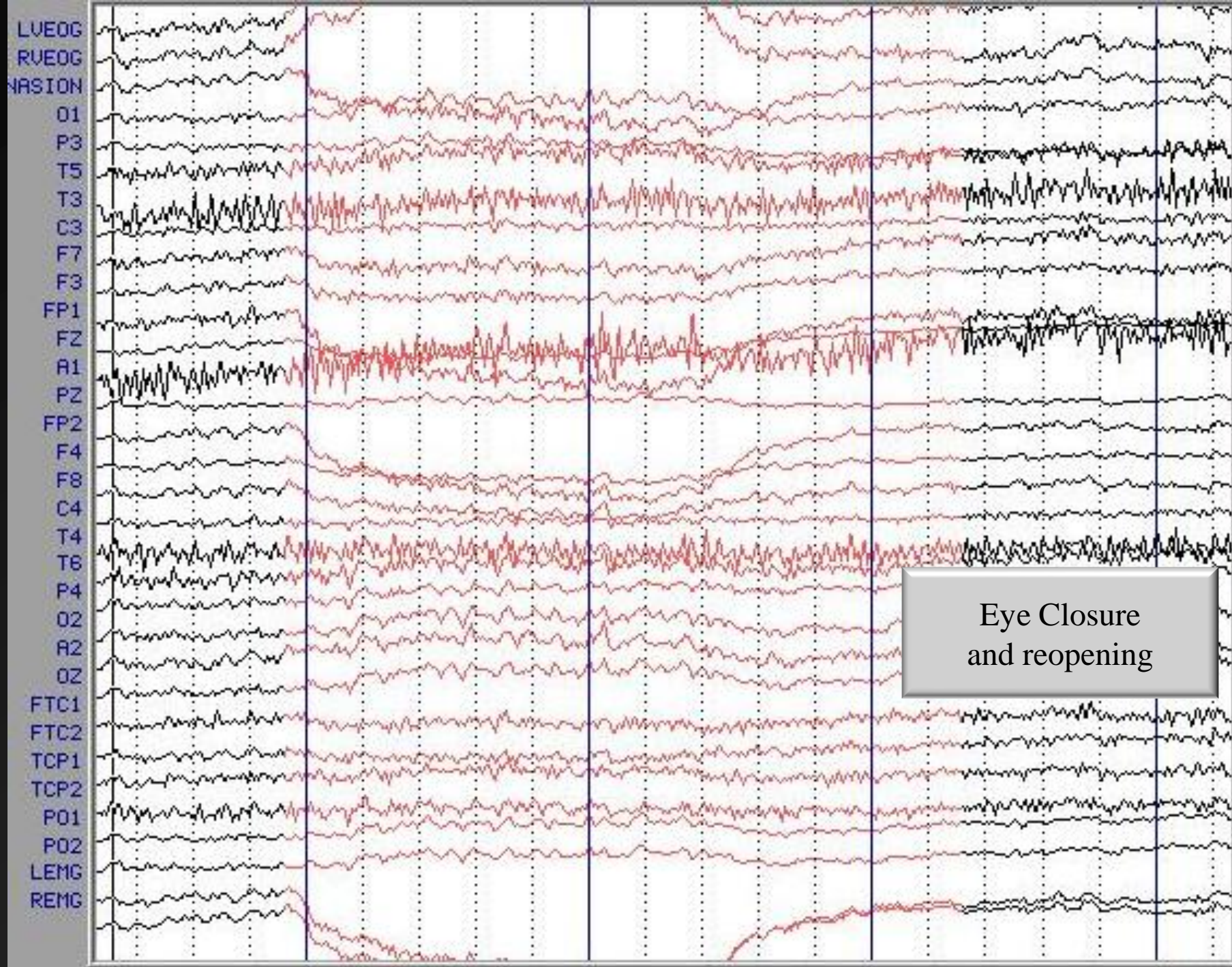




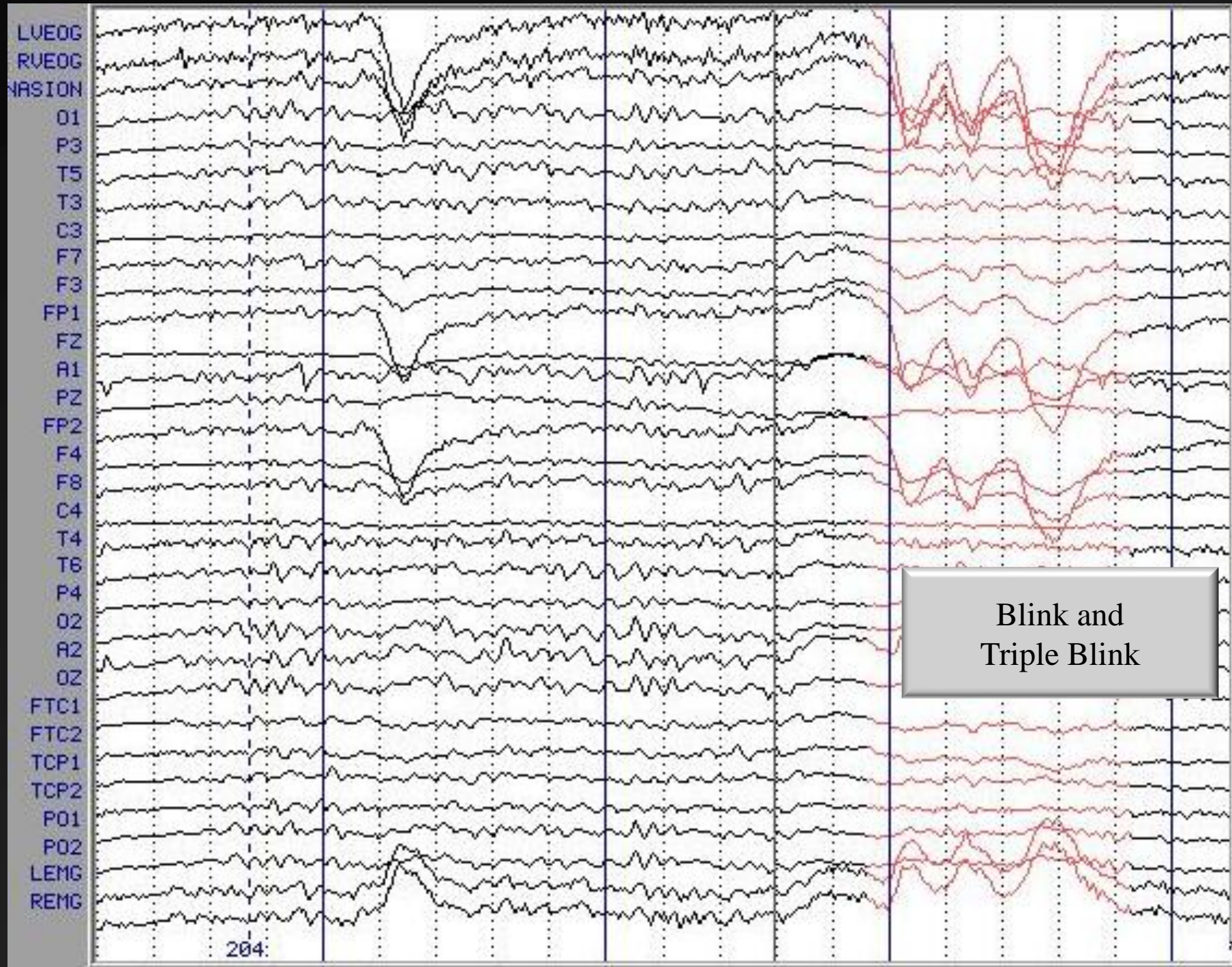
Talking and
Moving Head



Yaaaawwwwnnnn



Eye Closure
and reopening



Blink and
Triple Blink

AC Signal Recording Options

➤ Time Constant/HP filter

➤ Low frequency cutoff is related to TC by:

$$F = \frac{1}{(2\pi(TC))}$$

Where F = frequency in Hz, TC = Time Constant in Seconds

Applying formula:

Time Constant (sec)

Frequency (Hz)

10.00

.016

5.00

.032

1.00

.159

.30

.531

.10

1.592

.01

15.915



Setup

Misc Events EKG reduction Blink Reduction

Startup Amplifiers Channel Attributes Triggers Epochs Fsp Average Frequency Sorting Audio Mapping

Acquisition

A/D Rate: 1000

Number of Channels: 68

Acquisition Type: Continuous

AC/DC: AC DC

DC Auto Correction: Enable

Level: 80

Notch: Off Frequency

Amplifier Settings

Selected Channel: FZ

Gain: 30

Range: 183 mV

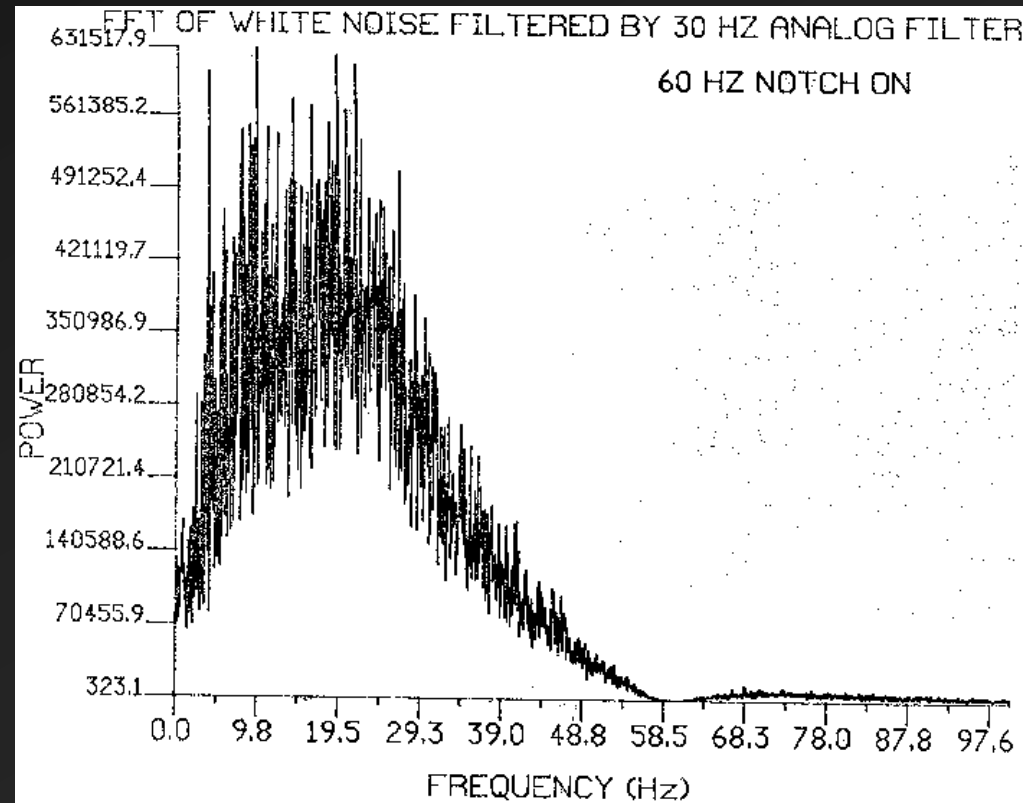
Accuracy: 2.797 uV/LSB

Low pass: 200 Hz

High pass: 0.15 Hz

Hi Frequency/LP Settings

- Do not eliminate frequencies of interest
- Analog systems have broad roll-off characteristics
- Be mindful of digitization rate (more info soon!)



Digital Signal Acquisition

➤ Analog Vs Digital Signals

➤ Analog

- Continuously varying voltage as fxn of time

➤ Discrete Time

- Discrete points on time axis, but full range in amplitude

➤ Digital

- Discrete time points on y axis represented as a limited range of values (usually 2^x , e.g $2^{12} = 4096$; $2^{16} = 65536$)
- CDs are 16-bit sampled at 44.1 kHz (as is Spotify)

Bit depth/sample rate pair from some popular music services

Music Service	Subscription Tier	Minimal bit-depth/sample rate	Maximal bit-depth/sample rate	AirPlay	Google Cast
Spotify	Spotify Free/Premium	16-bit/44.1 kHz	Same	Fixed to 16-bit/44.1 kHz	16-bit/44.1 kHz
Amazon Music	Amazon Prime Music	16-bit/44.1 kHz	Same	Fixed to 16-bit/44.1 kHz	16-bit/44.1 kHz
	Amazon Music Unlimited - HD	16-bit/44.1 kHz	Same	Fixed to 16-bit/44.1 kHz	16-bit/44.1 kHz
	Amazon Music Unlimited – Ultra HD	24-bit/44.1 kHz	24-bit/192kHz	Fixed to 16-bit/44.1 kHz	16-bit/44.1 kHz
TIDAL	HiFi	16-bit/44.1 kHz	Same	Fixed to 16-bit/44.1 kHz	Use TIDAL Connect
	HiFi Plus (Master)	24-bit/44.1 kHz	FLAC: 24-bit/48 kHz MQA core decoder: 24-bit/96 kHz MQA with external render: 24-bit/192 kHz or higher	Fixed to 16-bit/44.1 kHz	Use TIDAL Connect (up to 24-bit/96 kHz)
Qobuz	Studio/Sublime	16-bit/44.1 kHz	24-bit/192 kHz	Fixed to 16-bit/44.1 kHz	Up to 24-bit/96 kHz
Deezer	Premium/HiFi	16-bit/44.1 kHz	Same	Fixed to 16-bit/44.1 kHz	16-bit/44.1 kHz

A/D converters

- Schmidt Trigger as simple example
- The A/D converter
 - Multiplexing (several channels); A/D converter is serial processor
 - Result is a vector [1 x n samples] of digital values for each channel ($[x(t_0), x(t_1), x(t_2), \dots, x(t_{n-1})]$)
 - 12 bit converters allow $2^{12} = 4096$ values
 - 16 bit converters allow $2^{16} = 65536$ values
- 12 bit is usually adequate for EEG
 - 4096 values allow 1 value for each ~ 0.02 μ volts of scalp voltage (depending upon sensitivity of amplifier, which will amplify signal $\sim 20,000$ times before polygraph output)
 - e.g.,
 - 2.1130 μ volts \Rightarrow 2481 D.U.'s (2480.74)
 - 2.1131 μ volts \Rightarrow 2481 D.U.'s (2480.76)
 - 2.1250 μ volts \Rightarrow 2483 D.U.'s (2483.20)

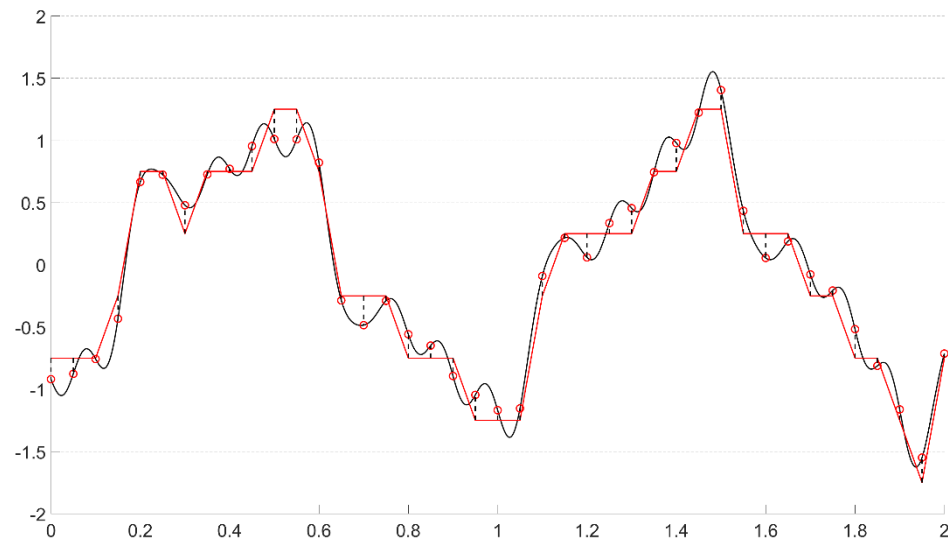
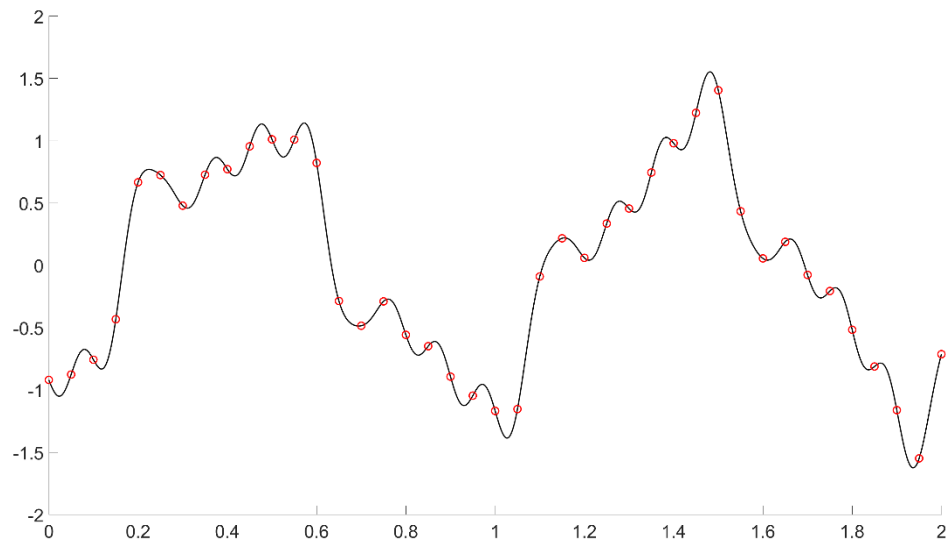


Figure 5: A signal sampled at 20 Hz. Discrete-time sampling (left panel) allows for continuous y-axis (μV) values, whereas digitally-sampled signals (right panel) must use a limited number of y-axis values. The three bit converter illustrated here (right panel) allows for $2^3=8$ distinct values, providing only a coarse approximation of the signal voltage. The right panel depicts the discrete sample value (red circle) and the 3-bit digital equivalent (red line), and the discrepancy (dashed vertical black lines).

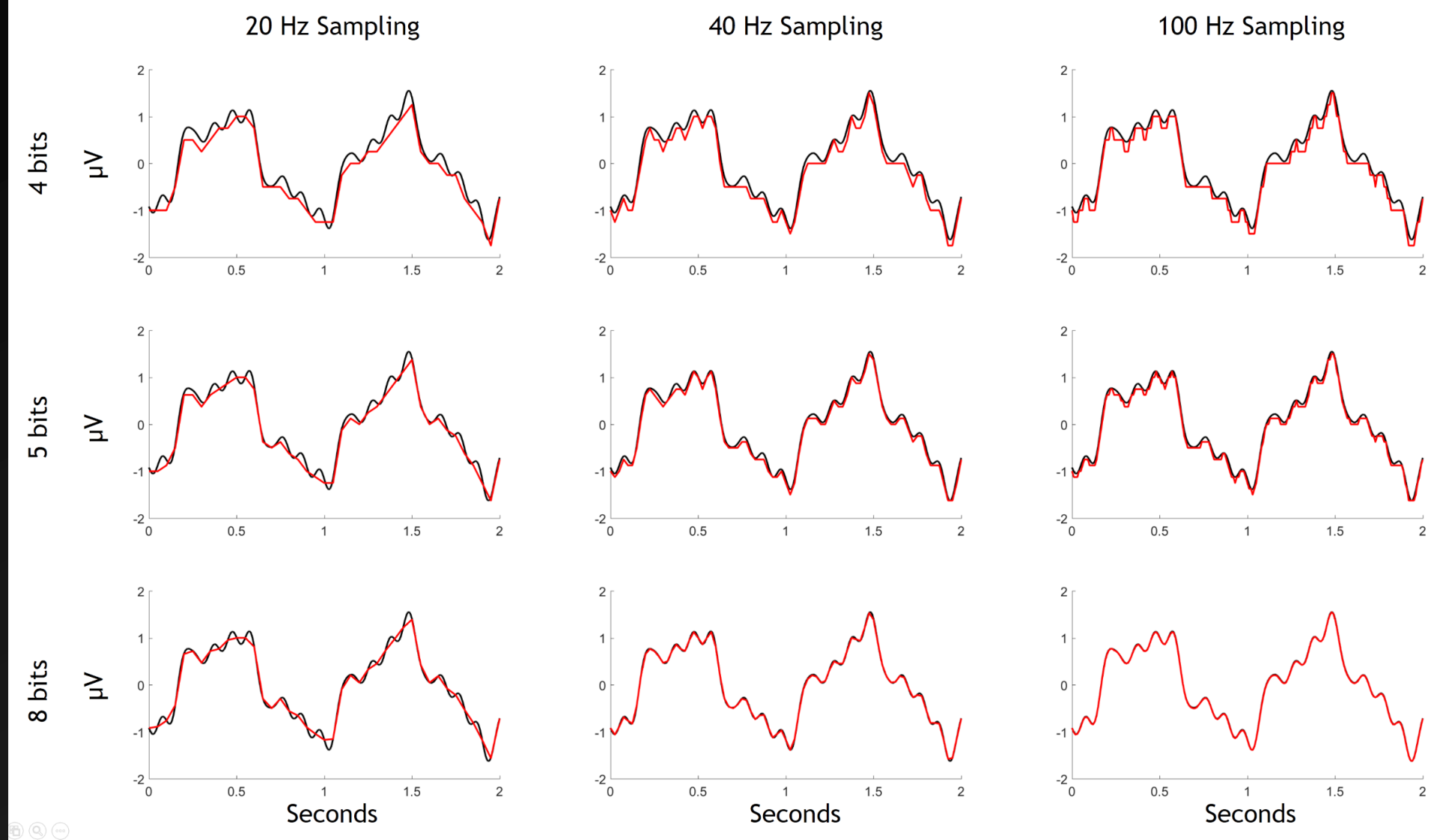


Figure 6: A comparison of a signal (black line) sampled (red line) at three sampling rates (20, 40, 100 Hz) and using three different converter resolutions (4-bit, 5-bit, and 8-bit) that allow for 16, 32, and 128 distinct μV values. Low bit-resolution was used here for illustrative purposes; commercial converters are typically 12-bit (4096 values) or 16-bit (65536 values).

From: Curham & Allen (2022)

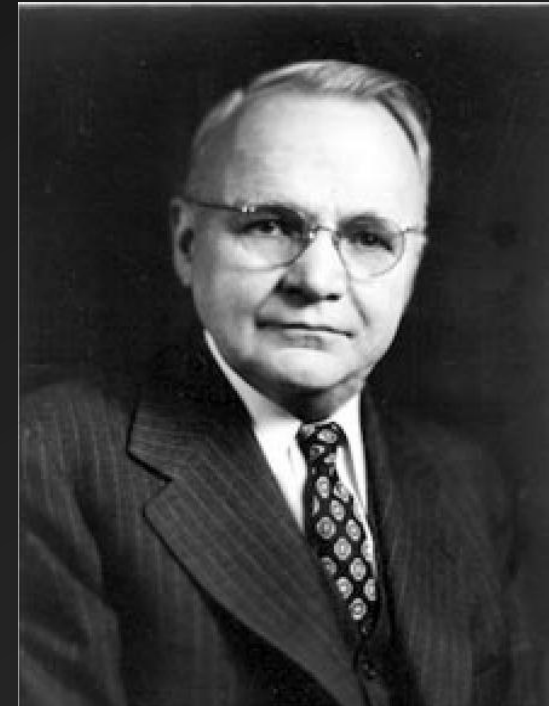
The Problem of Aliasing

➤ Definition

- To properly represent a signal, you must sample at a fast enough rate.
- Nyquist's (1928) theorem
 - a sample rate twice as fast as the highest signal frequency will capture that signal perfectly
 - Stated differently, the highest frequency which can be accurately represented is one-half of the sampling rate
 - This frequency has come to be known as the Nyquist frequency and equals $\frac{1}{2}$ the sampling rate

➤ Comments

- Wave itself looks distorted, but frequency is captured adequately.
- Frequencies faster than the Nyquist frequency will not be adequately represented
- Minimum sampling rate required for a given frequency signal is known as Nyquist sampling rate



Harry Nyquist

Aliasing and the Nyquist Frequency

- In fact, frequencies above Nyquist frequency represented as frequencies lower than Nyquist frequency
 - $F_{Ny} + x$ Hz will be seen as $F_{Ny} - x$ Hz
 - “folding back”
 - frequency $2F_{Ny}$ seen as 0,
 - frequency $3F_{Ny}$ will be seen as F_{Ny}
 - accordion-like folding of frequency axis

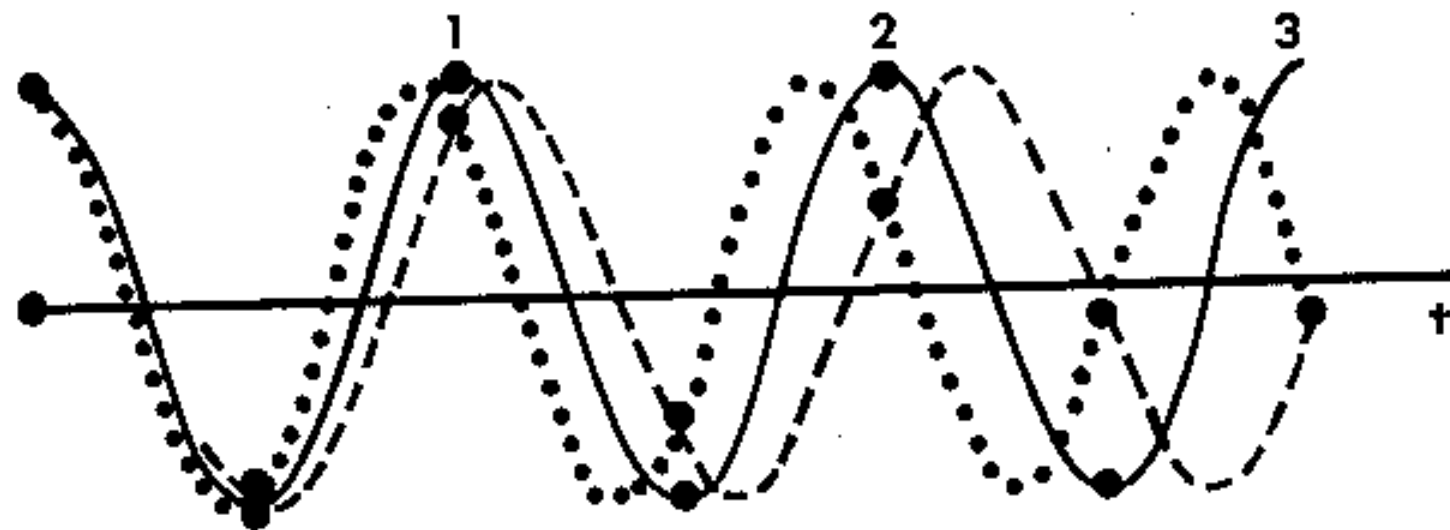


Fig. 3.1. A cosine wave of frequency F (solid line) sampled at its Nyquist rate. A higher frequency (dotted) wave, frequency $F + a$, is shown sampled at the same rate. At the sample times it is indistinguishable from a lower frequency (dashed) wave, frequency $F - a$.

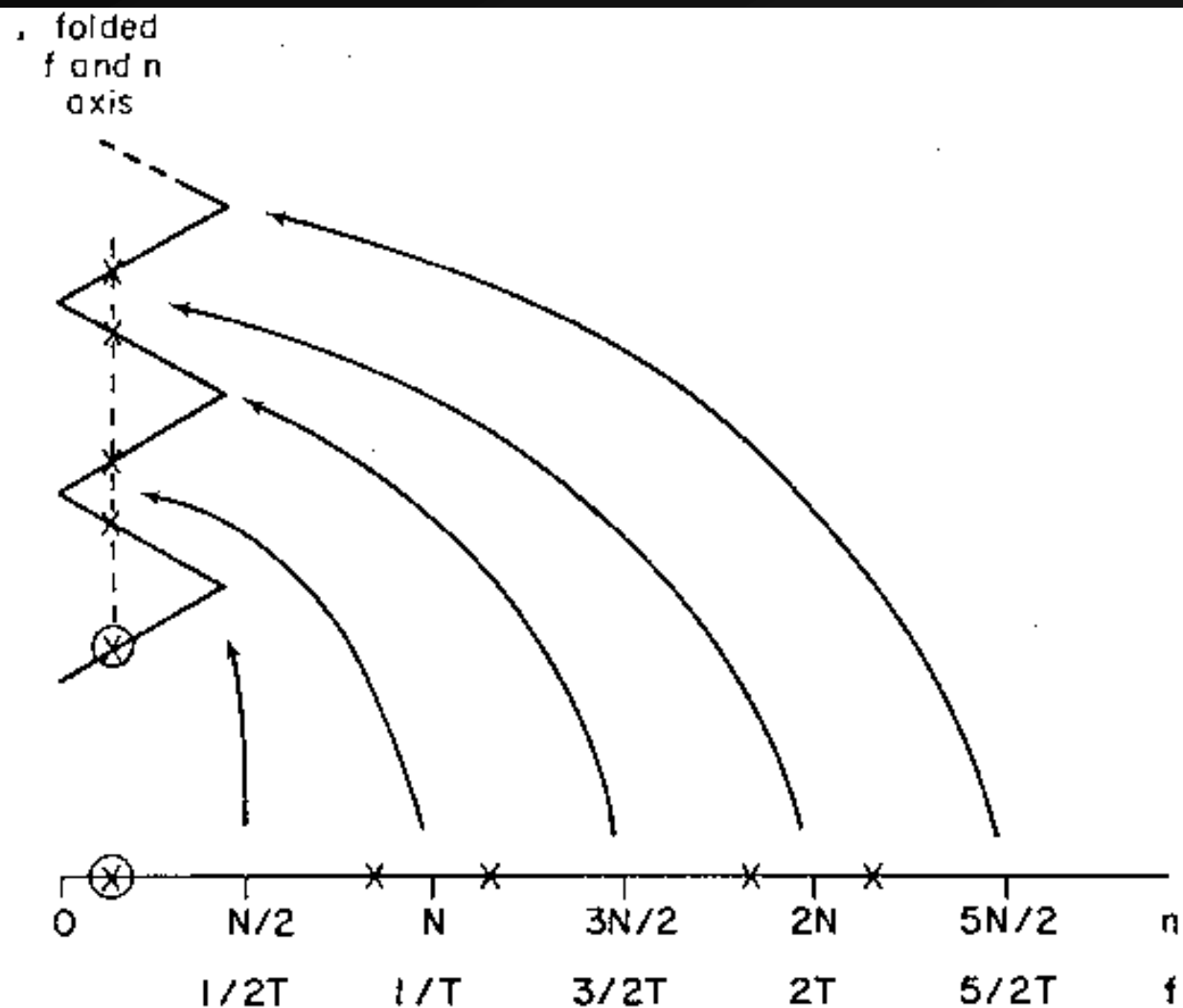
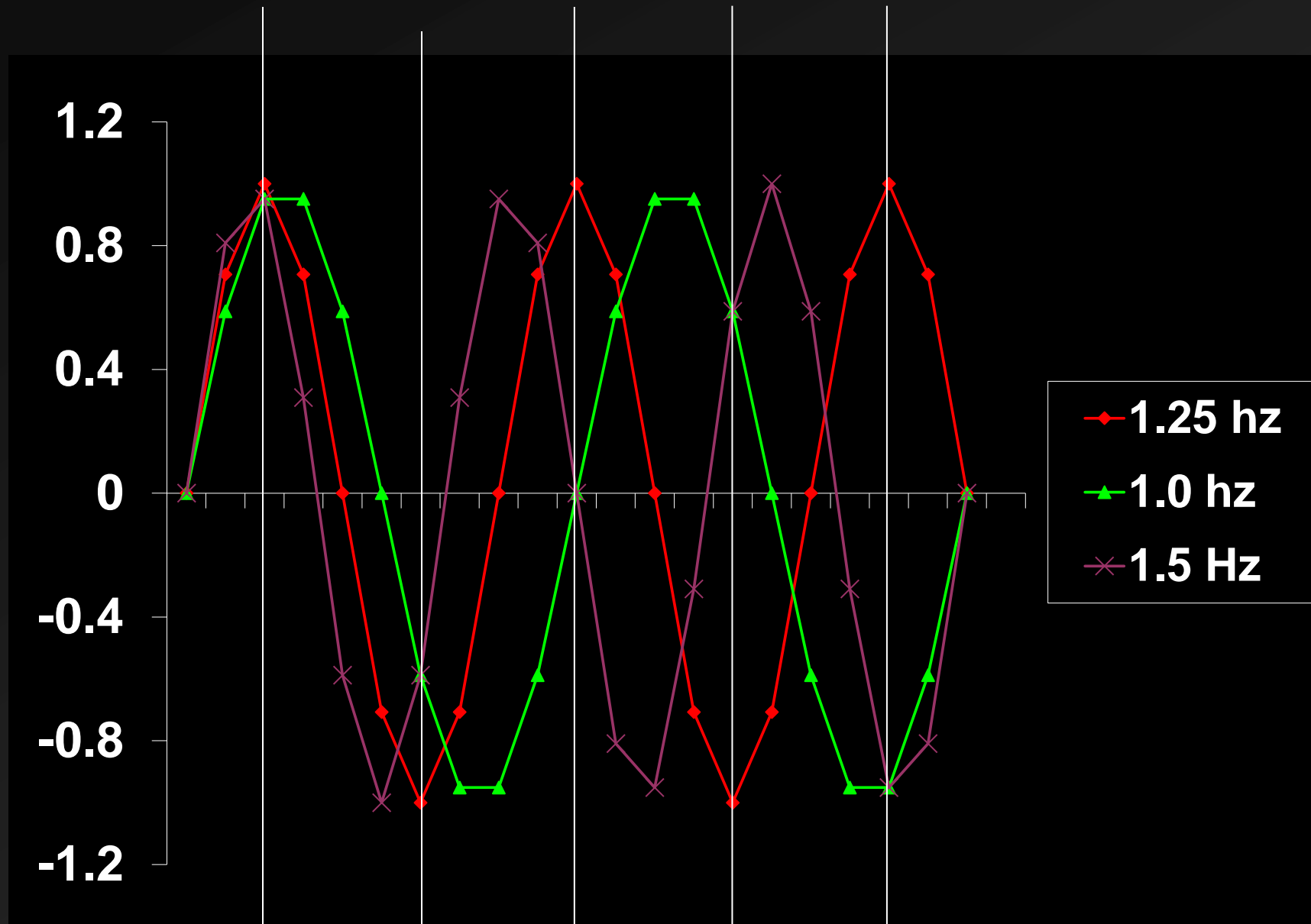
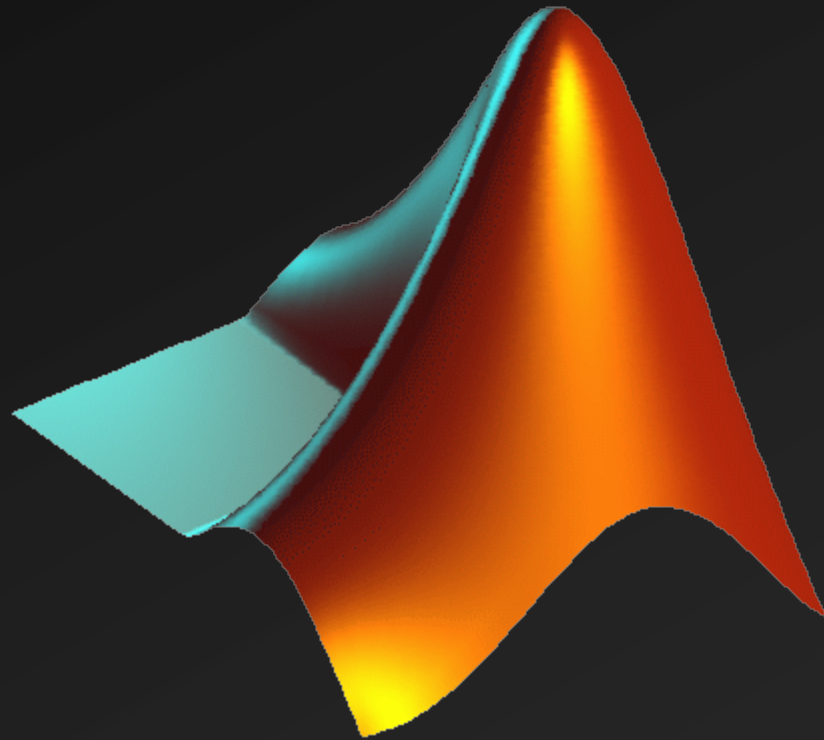


Fig. 3.2. The accordionlike folding of the frequency (or n) axis due to sampling of a continuous signal. Frequency components of the original signal marked with x 's on the f axis are interpreted in the sampled version as belonging to the lowest frequency, an encircled x .

Aliasing Demo (Part 1, 10 Hz Sampling Rate)



Matlab Demo of Aliasing



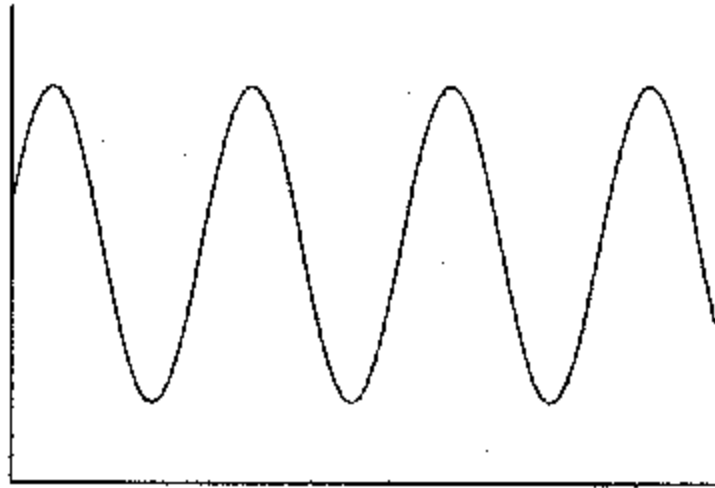
Solutions to Aliasing

- Sample very fast
- Use anti-aliasing filters
- **KNOW YOUR SIGNAL!**

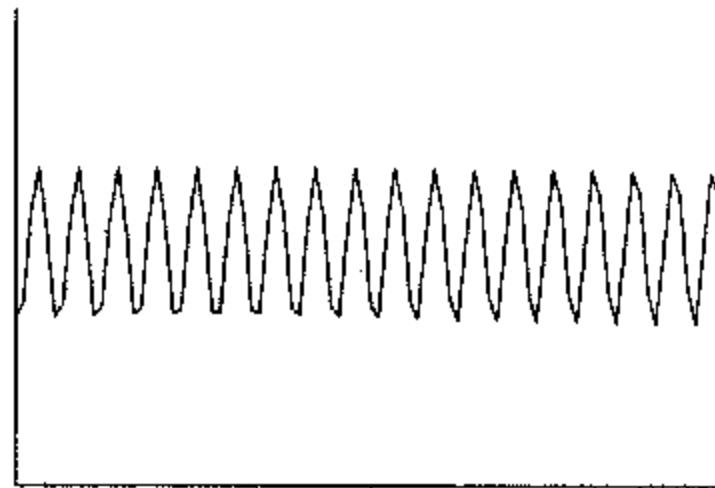
Time Domain Vs Frequency Domain Analysis

- Frequency Domain Analysis involves characterizing the signal in terms of its component frequencies
 - Assumes periodic signals
- Periodic signals (definition):
 - Repetitive
 - Repetitive
 - Repetition occurs at uniformly spaced intervals of time
- Periodic signal is assumed to persist from infinite past to infinite future

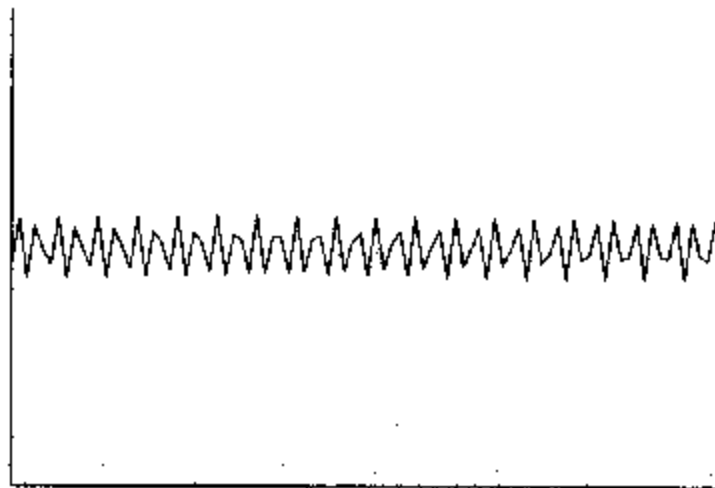
Wave 1



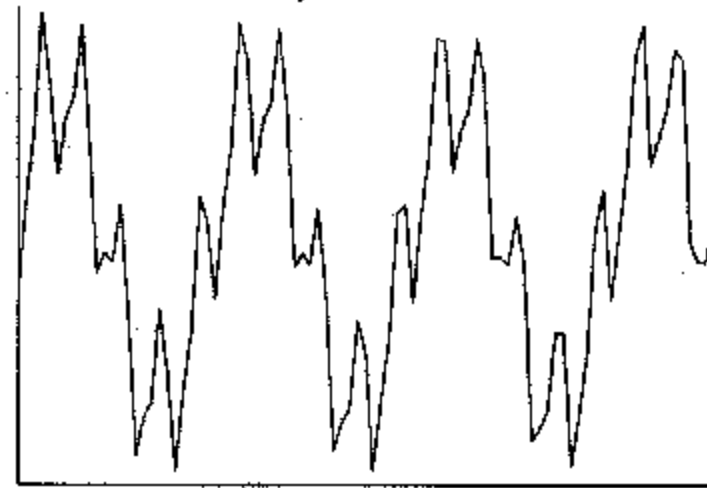
Wave 2



Wave 3

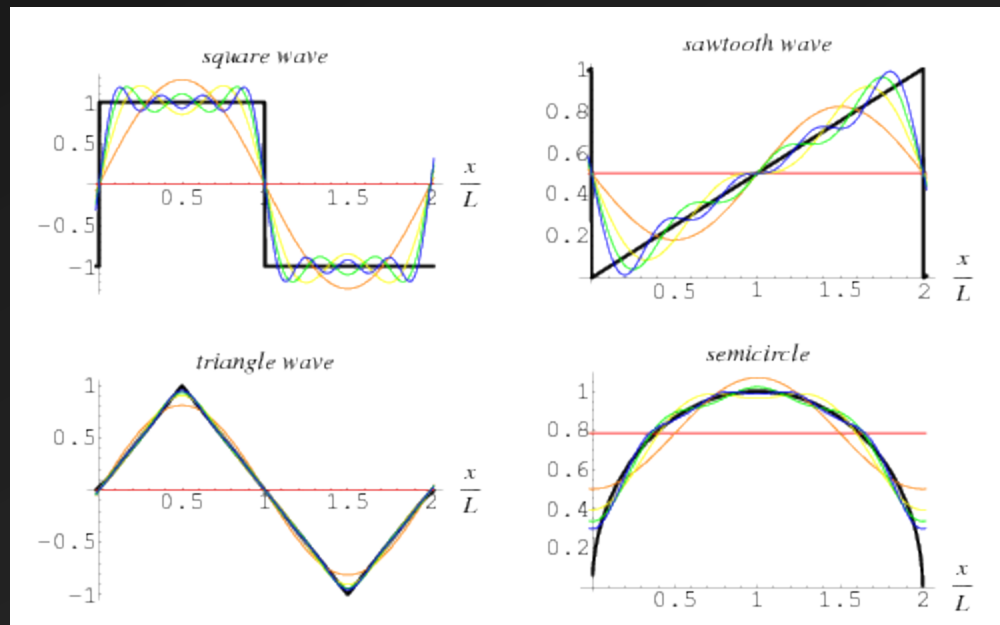


Composite Wave



Fourier Series Representation

- If a signal is periodic, the signal can be expressed as the sum of sine and cosine waves of different amplitudes and frequencies
- This is known as the Fourier Series Representation of a signal



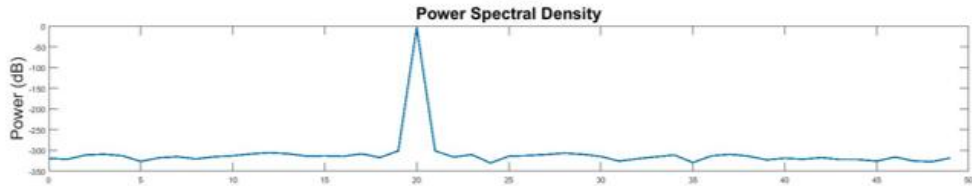
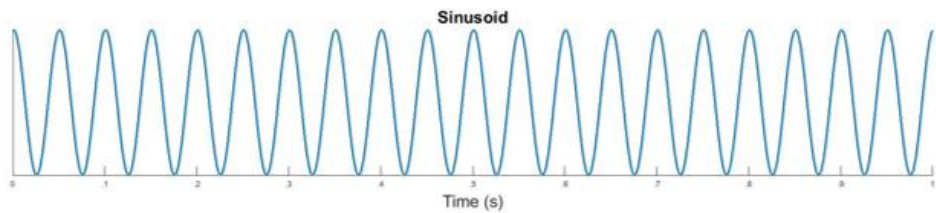
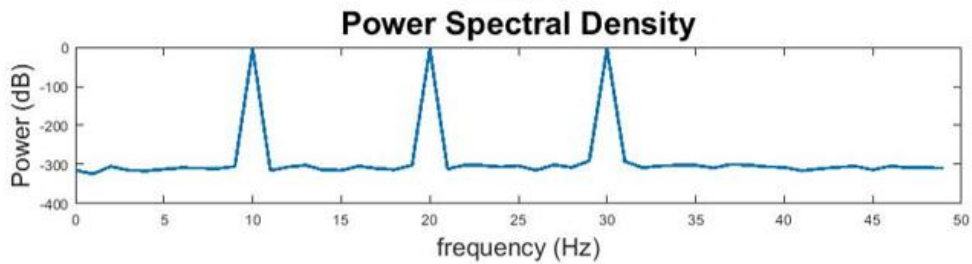
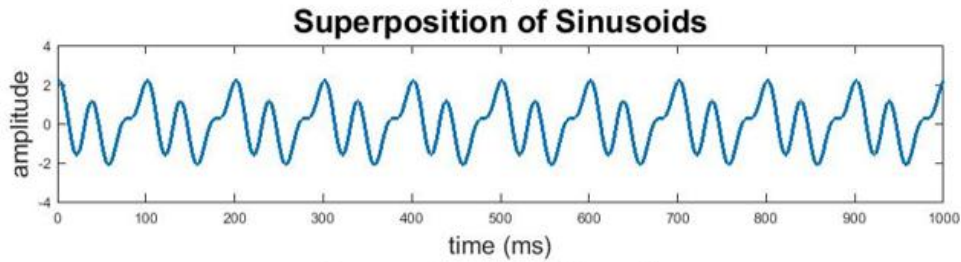
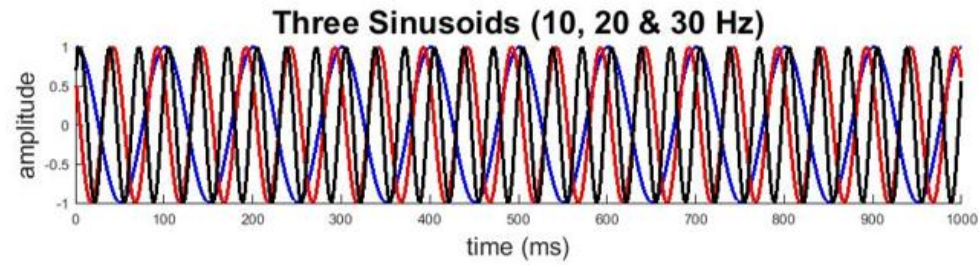


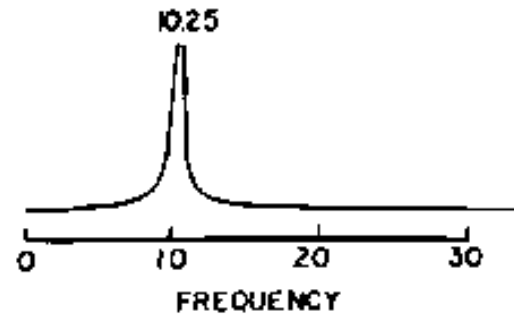
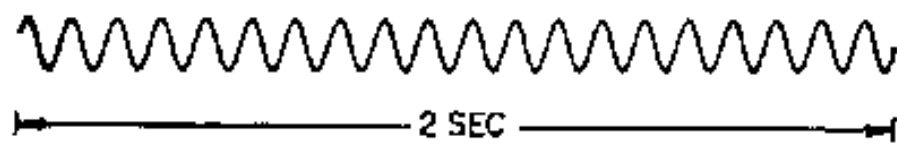
Figure 9: Constructing a complex signal from the superposition of sinusoids (top). The power spectrum of the signal show distinct peaks at the frequencies of the component sinusoids. A single sinusoid corresponds to a single peak in the power spectrum (bottom).

Interactive Fourier!

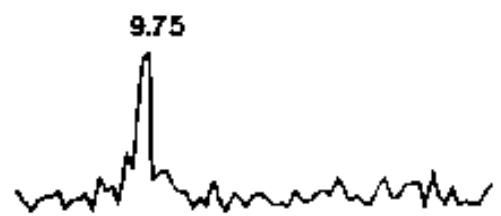
➤ Web Applet

Fourier Series Representation

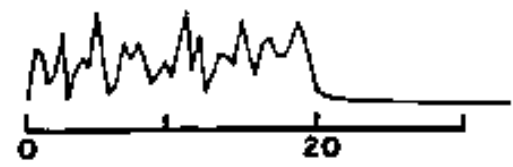
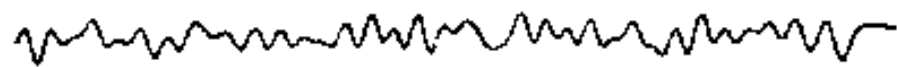
- Pragmatic Details
 - Lowest Fundamental Frequency is $1/T$
 - Resolution is $1/T$
- Phase and Power
 - There exist a phase component and an amplitude component to the Fourier series representation
 - Using both, it is possible to completely reconstruct the waveform.



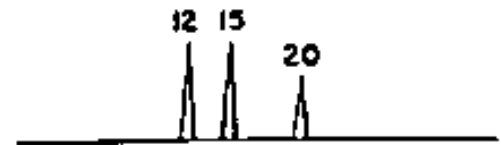
d



b



c



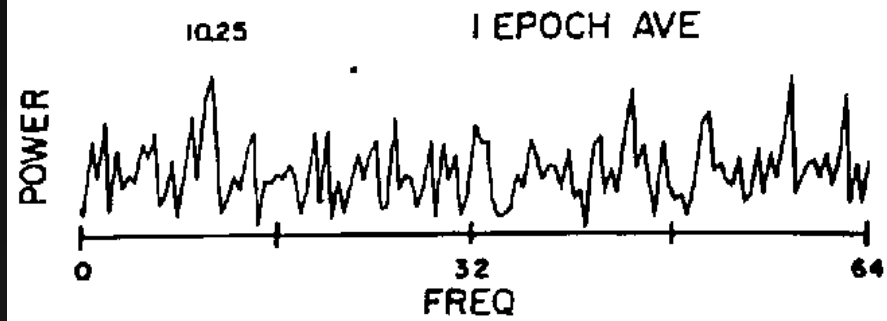
d

Time Domain

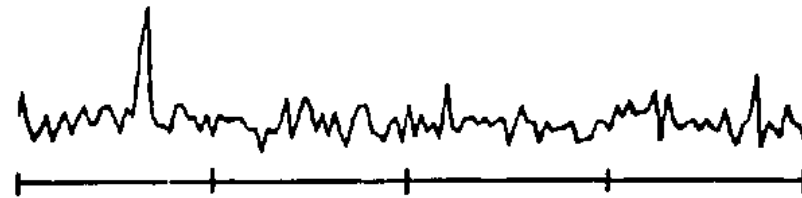
Frequency Domain

Averaging
Multiple
Epochs
improves
ability to
resolve signal

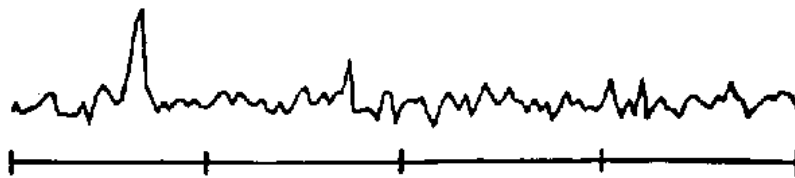
Note noise is twice
amplitude of the signal



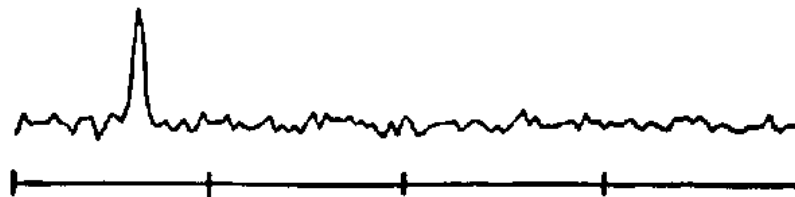
5



10



30



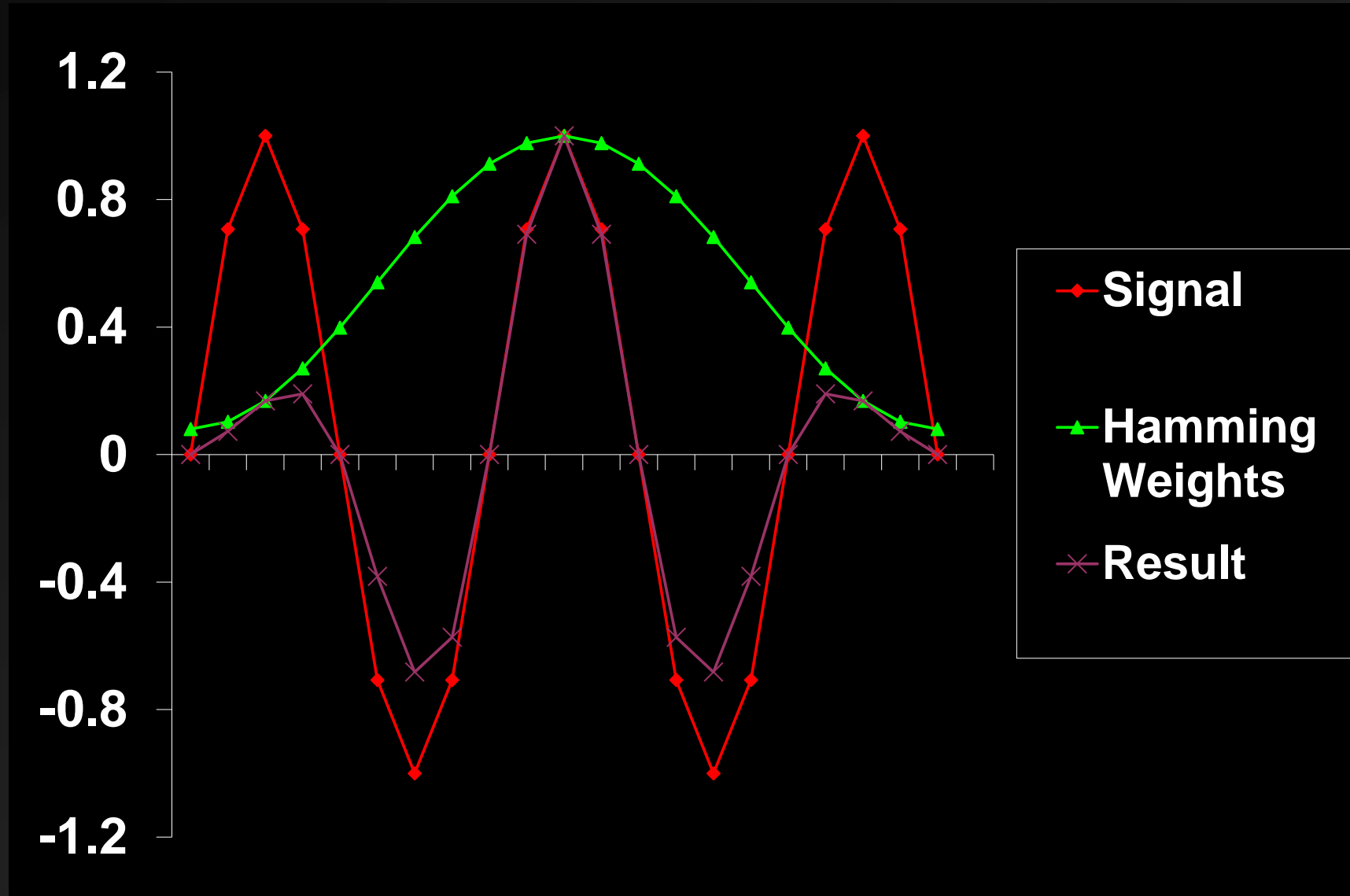
Lingering details

- In absence of phase information, it is impossible to reconstruct the original signal
 - **Infinite** number of signals that could produce the same amplitude or power spectrum
- Spectra most often derived via a **Fast Fourier transform (FFT)**; a fourier transform of a discretely sampled band-limited signal with a power of 2 samples
- Sometimes **autocovariance function** is used (a signal covaries with itself at various phase lags; greater covariation at fundamental frequencies)
- **Windowing: the Hamming Taper**

Preventing Spectral Leakage

- Use windows
 - not Micro\$oft Windows
 - Hamming
 - Hanning
 - Cosine
 - Etc.

Hamming Demo



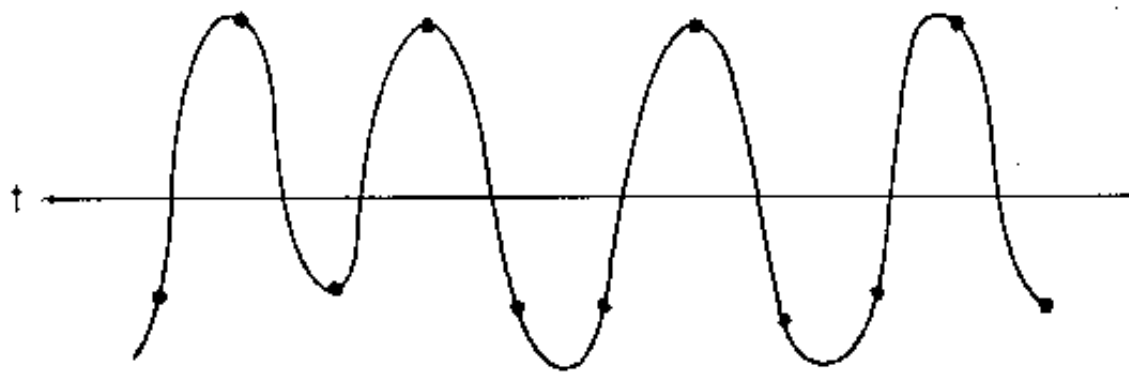
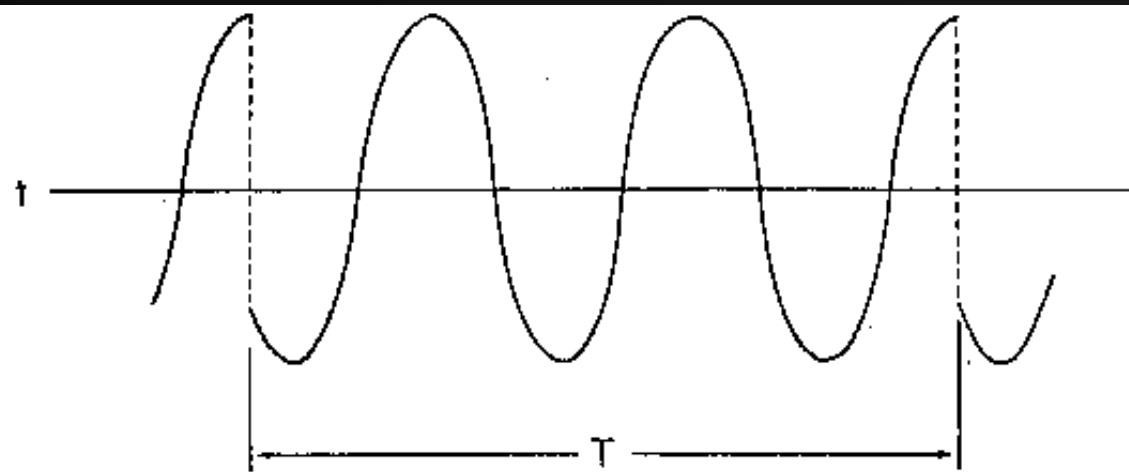
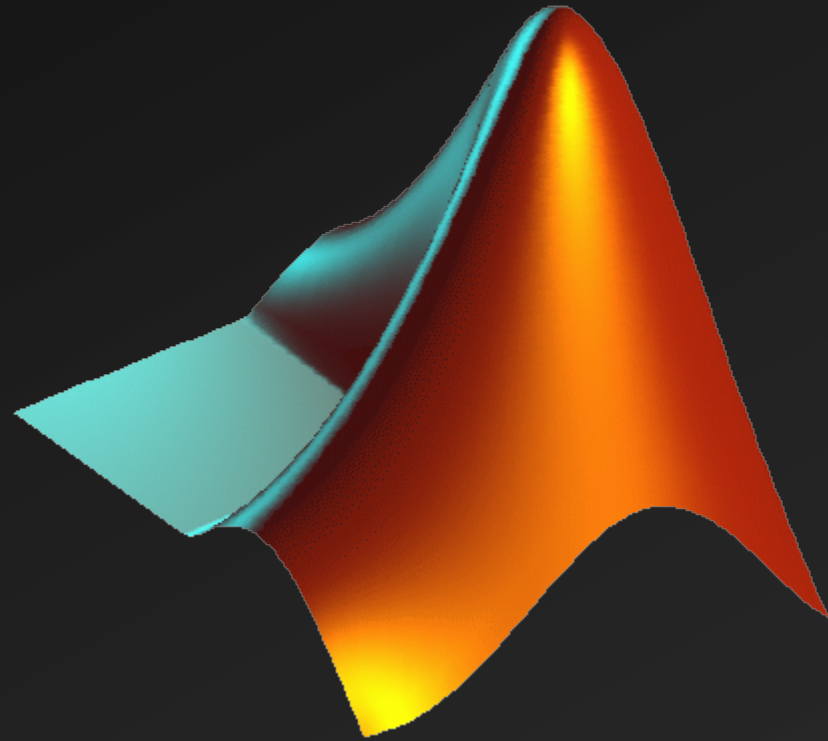


Fig. 3.3. Top, a periodicized segment of a cosine wave. T is the observation time and $3T/8$ the period of the wave. Note the discontinuities at 0 and T . Bottom, a continuous and periodic band-limited wave drawn through the sample points $\Delta = T/16$ sec apart.

Matlab Demo of Hamming Window



Pragmatic Concerns

- Sample fast enough so no frequencies exceed Nyquist
 - signal bandwidth must be limited to less than Nyquist
 - Violation = **ERROR**
- Sample a long enough epoch so that lowest frequency will go through at least one period
 - Violation = **ERROR**
- Sample a periodic signal
 - if subject engaging in task, make sure that subject is engaged during entire epoch
 - Violation = ??, probably introduce some additional frequencies to account for change

Demo of EEG Data

- CNT Data to Frequency Domain Representation

*Frequency-domain EEG applications and
methodological considerations*

Applications

- Emotion Asymmetries
 - Lesion findings
 - Catastrophic reaction (LH)
 - RH damage show a belle indifference
 - EEG studies
 - Trait (100+ studies)
 - State (oodles more studies)

Types of Studies

➤ Trait

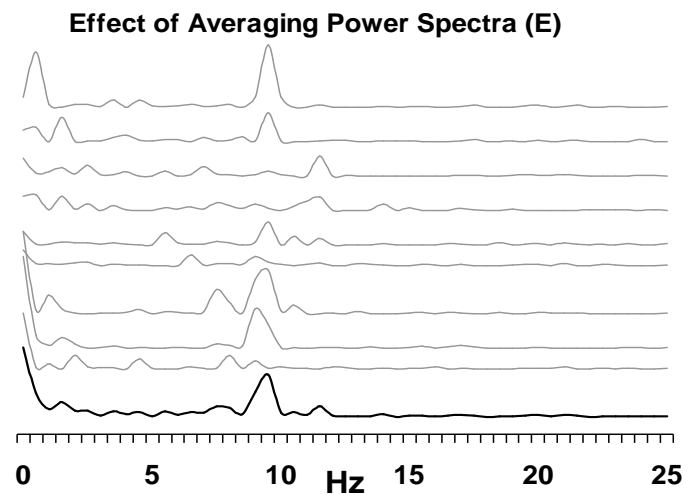
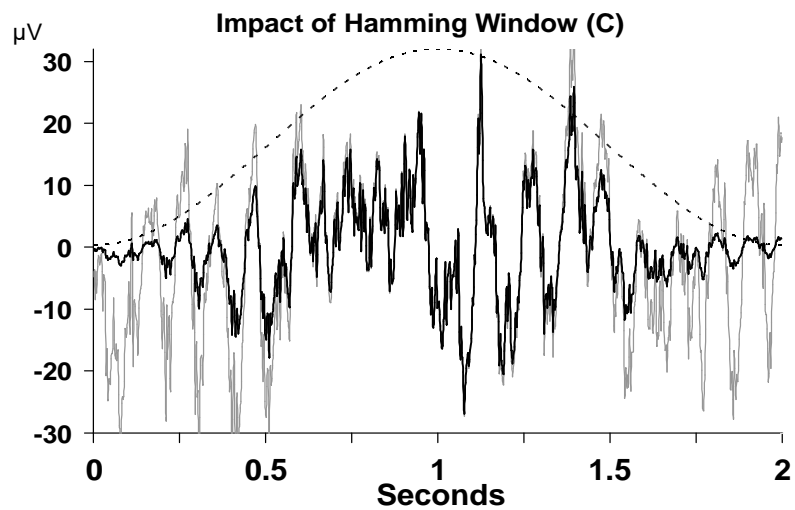
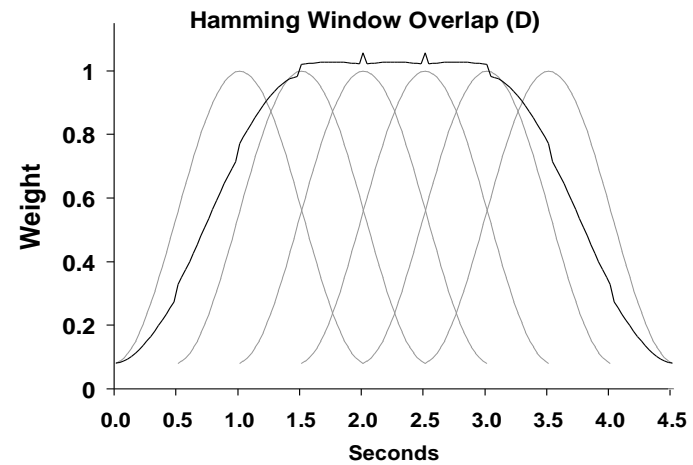
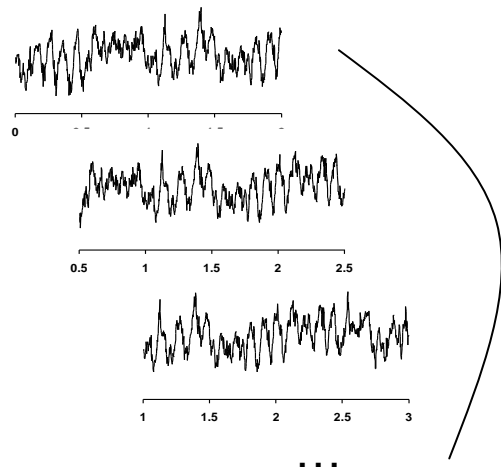
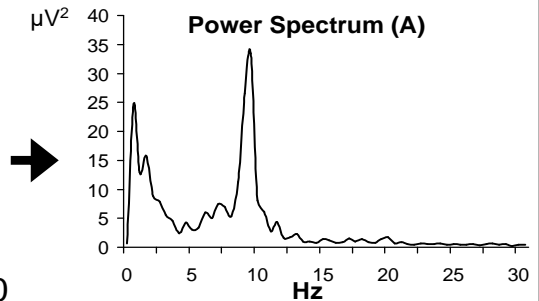
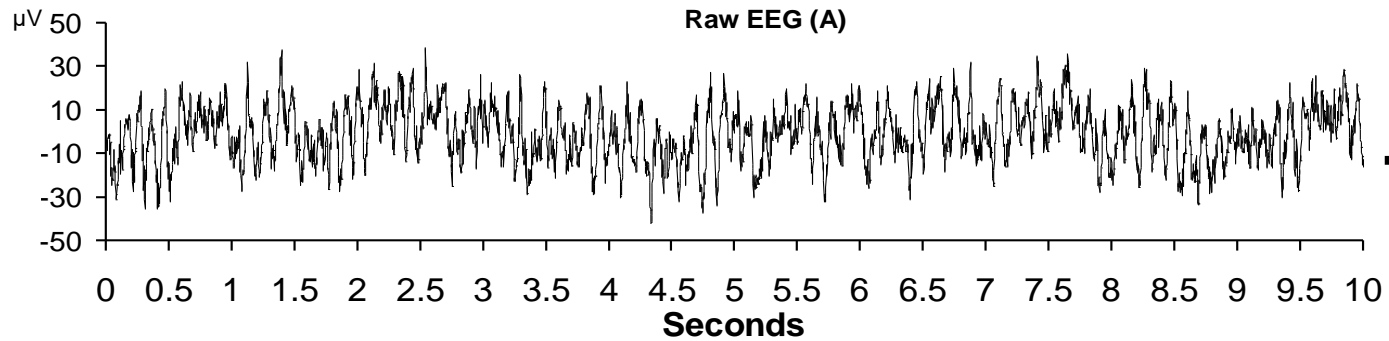
- Resting EEG asymmetry related to other traits (e.g. BAS)
- Resting EEG asymmetry related to psychopathology (e.g. depression)
- Resting EEG asymmetry predicts subsequent emotional responses (e.g. infant/mom separation)

➤ State

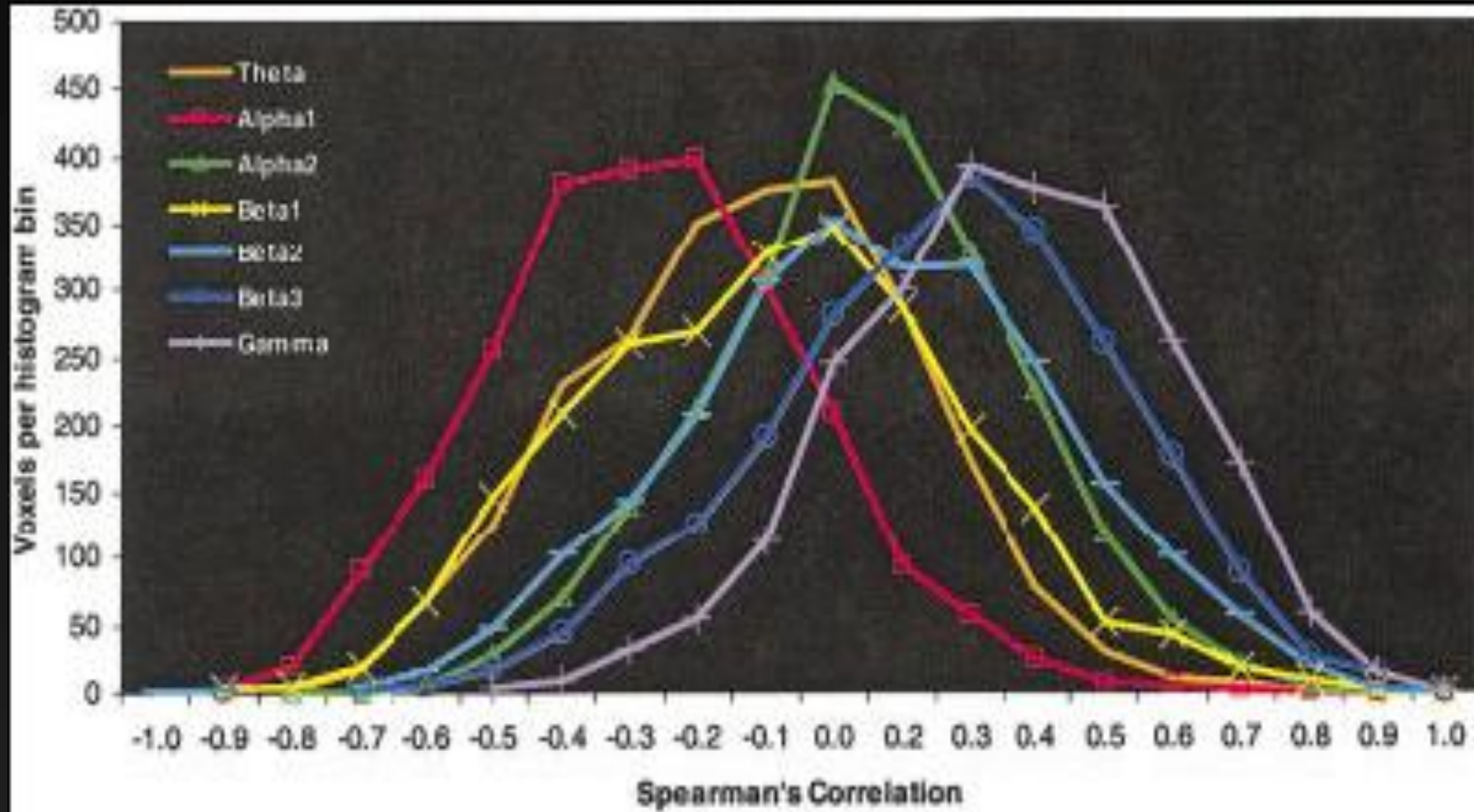
- State EEG asymmetry covaries with current emotional state (e.g., self report, spontaneous emotional expressions)

Trait, Occasion, and State variance

- Three sources of reliable variance for EEG Asymmetry
 - *Stable trait consistency* across multiple assessments
 - *Occasion-specific* variance
 - reliable variations in frontal asymmetry across multiple sessions of measurement
 - may reflect systematic but unmeasured sources such as current mood, recent life events and/or factors in the testing situation.
 - *State-specific* variance
 - changes within a single assessment that characterize
 - the difference between two experimental conditions
 - the difference between baseline resting levels and an experimental condition.
 - conceptualized as proximal effects in response to specific experimental manipulations
 - should be reversible and of relatively short duration
- Unreliability of Measurement (small)



Alpha Vs Activity Assumption (AAA)



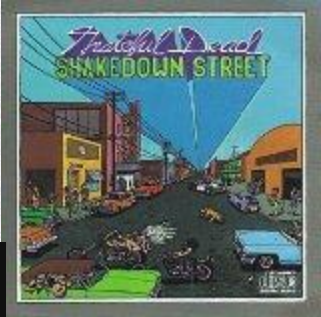
Alpha and Activity

- May be more apt to think of alpha as regulating network activity
- High alpha has inhibitory function on network activity (more in advanced topics)

EEG Asymmetry,
Emotion, and Psychopathology

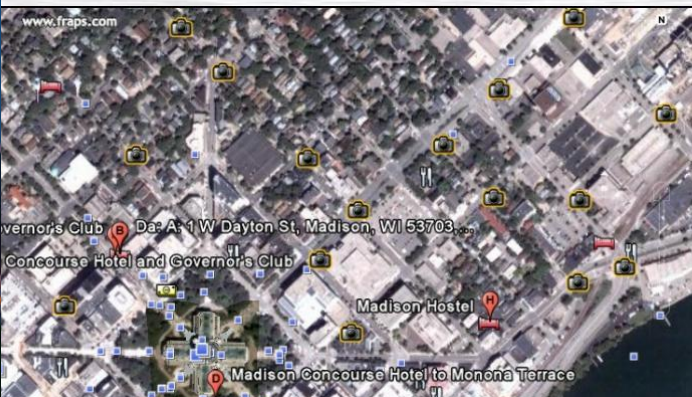
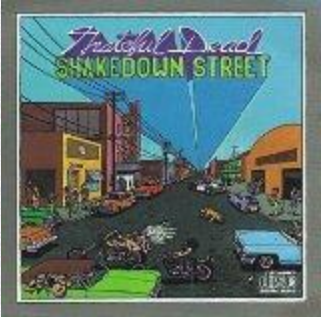


1978





1978



EIGHTEENTH ANNUAL MEETING SOCIETY FOR PSYCHOPHYSIOLOGICAL RESEARCH

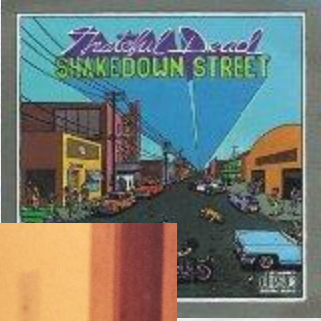
The Eighteenth Annual Meeting of The Society for Psychophysiological Research was held at The Concourse Hotel in downtown Madison, Wisconsin, September 15, 16, 17, and 18, 1978. Members of the Program Committee were: Rafael Klorman and Ted Weerts (Co-Chairmen), Michael Coles, Don Fowles, Linda Gannon, James Jean, J. Richard Jennings, Rathe Karrer, Michael Nelson, Arne Öhman, Leonard Salzman, and David Siddall.

As in recent years, the bulk of the research reports were given and discussed informally at Friday and Sunday evenings, September 15 and 17. In addition, research reports were presented in sessions on Saturday and Monday mornings, and others were included in the Display and Discussion sessions which ran in tandem with the meetings on Saturday from 8:30 to 5:00. Several symposia, workshops were also included in this year's program.

Following are the abstracts of research reports presented and discussed during the Paper Session, Display and Discussion poster session.



1978



PAPER SESSION II

“During positive affect, the frontal leads display greater relative left hemisphere activation compared with negative affect and vice versa”

202

SPR ABSTRACTS, 1978

Vol. 16, No. 2

PAPER SESSION II

I. Silverstein, L. D., & Graham, F. K. (University of Wisconsin - Madison) Selective attention effects on reflex activity. Bohlin and Graham (1977) found that reflex blinking, unlike spontaneous blinking, was facilitated in association with cardiac deceleration when subjects were required to attend to the reflex-eliciting stimulus. The enhancement of sensory processing on the attended channel was proposed as an explanation for the facilitation. If so, directing attention to a different channel should remove the facilitation. This hypothesis was tested in two experiments analogous to the Bohlin and Graham (1977) studies. The critical change was requiring subjects to attend to a stimulus in a modality orthogonal to that of the reflex-eliciting stimulus.

In each experiment, 15 college students received 60- or 120-msec, low-intensity, electrocutaneous stimuli concurrently with a 50-msec auditory startle pulse. A warning tone preceded electrocutaneous and startle stimuli by 2 sec in the experimental conditions, while in the control conditions the two stimuli were presented without warning. Subjects' task was to discriminate electrocutaneous stimulus duration.

As in earlier intramodal studies, the warning tone elicited significant cardiac deceleration during the warning intervals of both experiments. Significantly better discrimination occurred on warned than unwarned control trials (Exp. 1—73.7% vs 60.3%; Exp. 2—73.2% vs 49.5%). Reflex blink latency was also significantly facilitated in both experiments. However, unlike the intramodal studies, blink magnitude was reduced. A small reduction in Experiment 1 was not a reliable effect, but increased startle pulse intensity in Experiment 2 resulted in a larger and significant reduction.

The hypothesis that reflexive motor activity is influenced by selective sensory enhancement was closely supported. The results are interpreted with respect to a general theory of orienting and reflex control.

(Supported by the Grant Foundation, by an NSF grant BMS75-17075, and by a Research Scientist Award K3-MH21762 and a Fellowship Award MH07198-01 from NIMH)

2. Washon, A. M. (New York Medical College) Autonomic and stimulus control of conditional cardiac rate responses in rhesus monkeys. Conditional cardiac rate responses (cardiac CRs) of 6 rhesus monkeys were examined under systematic and broad manipulation of the temporal variable of CS-US interval length. A Pavlovian delay conditioning procedure was employed in which the duration of a visual conditional stimulus (CS) preceding an aversive electric-shock unconditional stimulus (US) was increased progressively from 2 to 120 sec for each animal. At each of 8 differing CS-US interval conditions, selective autonomic blocking agents were administered to assess the relative roles of the sympathetic and parasympathetic branches of the autonomic nervous system in the elaboration of observed cardiac rate CRs. Each subject was tested both in the absence of any drugs and under: 1) sympathetic blockade with propranolol, 2) parasympathetic blockade with atropine, 3) double blockade with a

combination of propranolol and atropine, and 4) ganglionic blockade with chlorisondamine.

The within-CS waveform of the cardiac rate CR was least consistent at the first 3 CS-US intervals of 2-6 sec, where instances of accelerative, decelerative, and biphasic HR patterns were observed during CS both within and among subjects, with the direction of response varying with the level of HR just prior to CS onset. By contrast, at CS-US intervals from 10 to 120 sec, a stable and consistent biphasic HR pattern of initial acceleration followed by deceleration was uniformly observed during CS despite continued wide fluctuations in pre-CS HR.

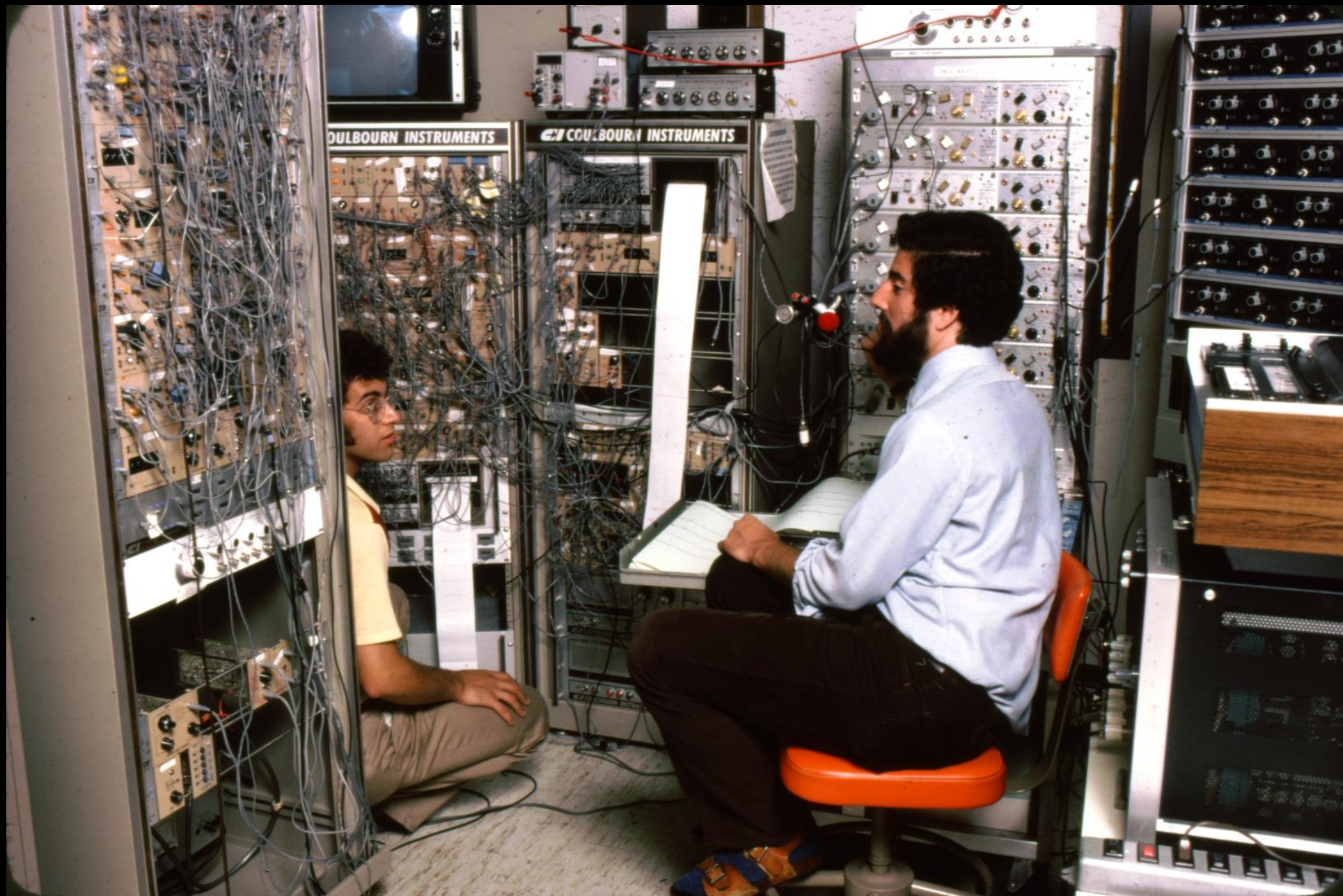
Both accelerative and decelerative HR changes within the CS-US interval were eliminated almost entirely by parasympathetic blockade alone, combined sympathetic and parasympathetic blockade, and ganglionic blockade. Sympathetic blockade alone left large HR changes within the CS-US interval, with CR deceleration often facilitated relative to pre-drug. These effects were similar across the full range of CS-US intervals employed, and whether the pre-drug form of the cardiac CR was monophasic or biphasic. The unconditional HR response (UCR) to shock was similar in form to the CR, consisting of an initial accelerative and subsequent decelerative component, and was similarly affected by the pharmacological agents, although the UCR was less suppressed by the drugs.

3. Davidson, R. J. (State University of New York at Purchase), Schwartz, G. E. (Yale University), Saron, C., Bennett, J. (State University of New York at Purchase), & Goleman, D. J. Frontal versus parietal EEG asymmetry during positive and negative affect. A variety of data suggest that positive and negative affect may be differentially lateralized in the human brain. This

report describes an experiment which explored the differential effect of positive versus negative affect on parietal and frontal brain regions. Seventeen right-handed subjects were exposed to portions of a television show judged to vary in emotional content. Subjects were asked to press down on a pressure-sensitive knob according to how much they disliked and to let up according to how much they liked the program, with hand use counterbalanced across subjects. These pressure changes, along with EEG filtered for 8-13 Hz recorded from F₄, F₃, F₂, and F₁ referenced to C_z were digitized and printed every 30 sec. Two epochs representing the most positively and most negatively judged segments were chosen for analysis on the basis of each subject's ratings and were compared on parietal and frontal asymmetry as reflected in the ratio R-L/R+L alpha. The results revealed a significant Region (Frontal vs Parietal) × Affective Valence (positive vs negative) interaction. During positive affect, the frontal leads display greater relative left hemisphere activation compared with negative affect and vice versa. Parietal asymmetry does not discriminate between these conditions, but does show right hemisphere activation during both.

A second experiment was conducted (Schwartz, Davidson, & Saron) during which self-generated positive and negative affective imagery served as the main inde-

3. Davidson, R. J. (State University of New York at Purchase), Schwartz, G. E. (Yale University), Saron, C., Bennett, J. (State University of New York at Purchase), & Goleman, D. J. Frontal versus parietal EEG asymmetry during positive and negative affect. A variety of data suggest that positive and negative affect may be differentially lateralized in the human brain. This report describes an experiment which explored the differential effect of positive versus negative affect on parietal and frontal brain regions. Seventeen right-handed subjects were exposed to portions of a television show judged to vary in emotional content. Subjects were asked to press down on a pressure-sensitive knob according to how much they disliked and to let up according to how much they liked the program, with hand use counterbalanced across subjects. These pressure changes, along with EEG filtered for 8-13 Hz recorded from F₄, F₃, P₄ and P₃ referenced to C_z were digitized and printed every 30 sec. Two epochs representing the most positively and



Left Hypofrontality in Depression

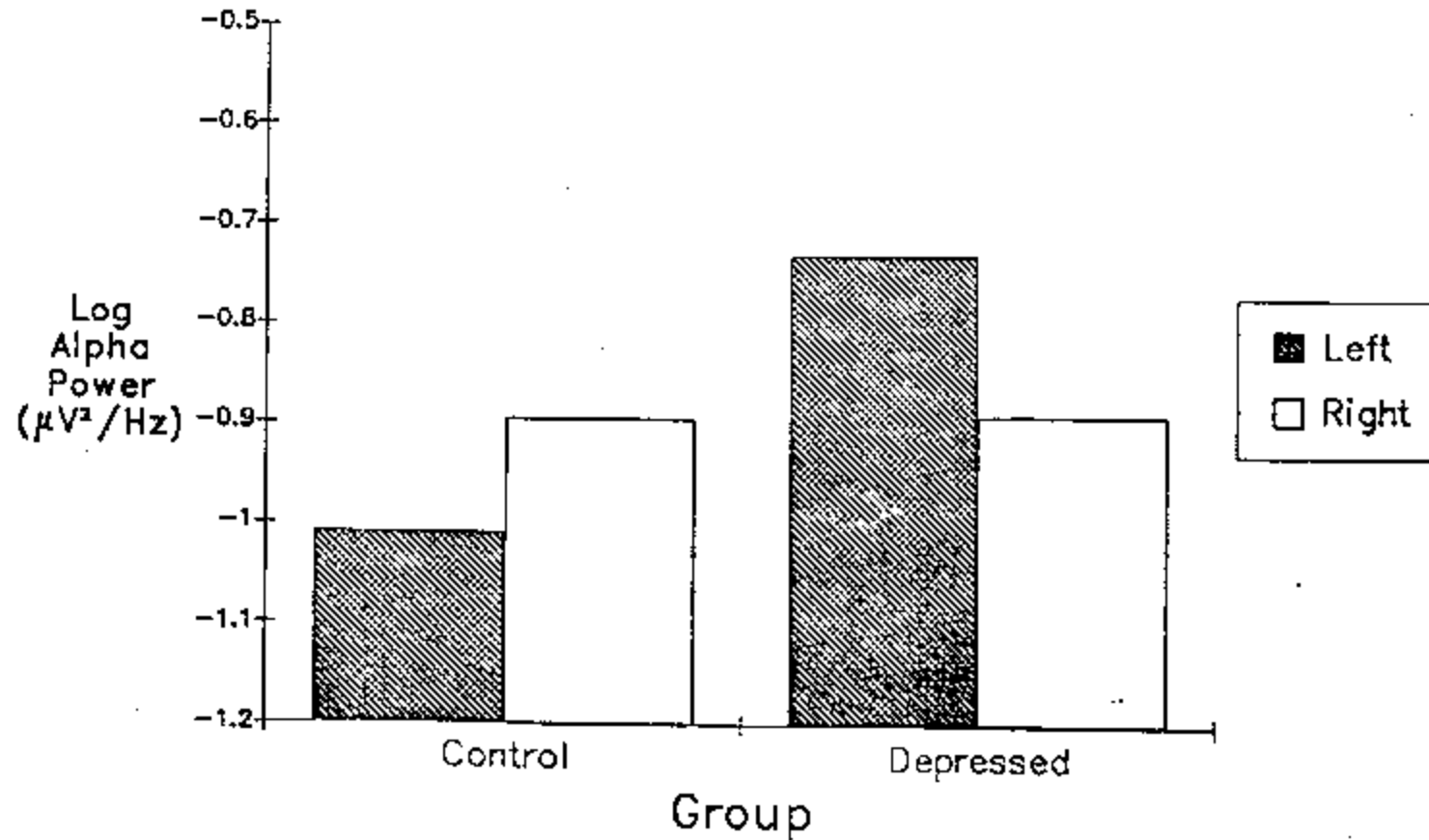
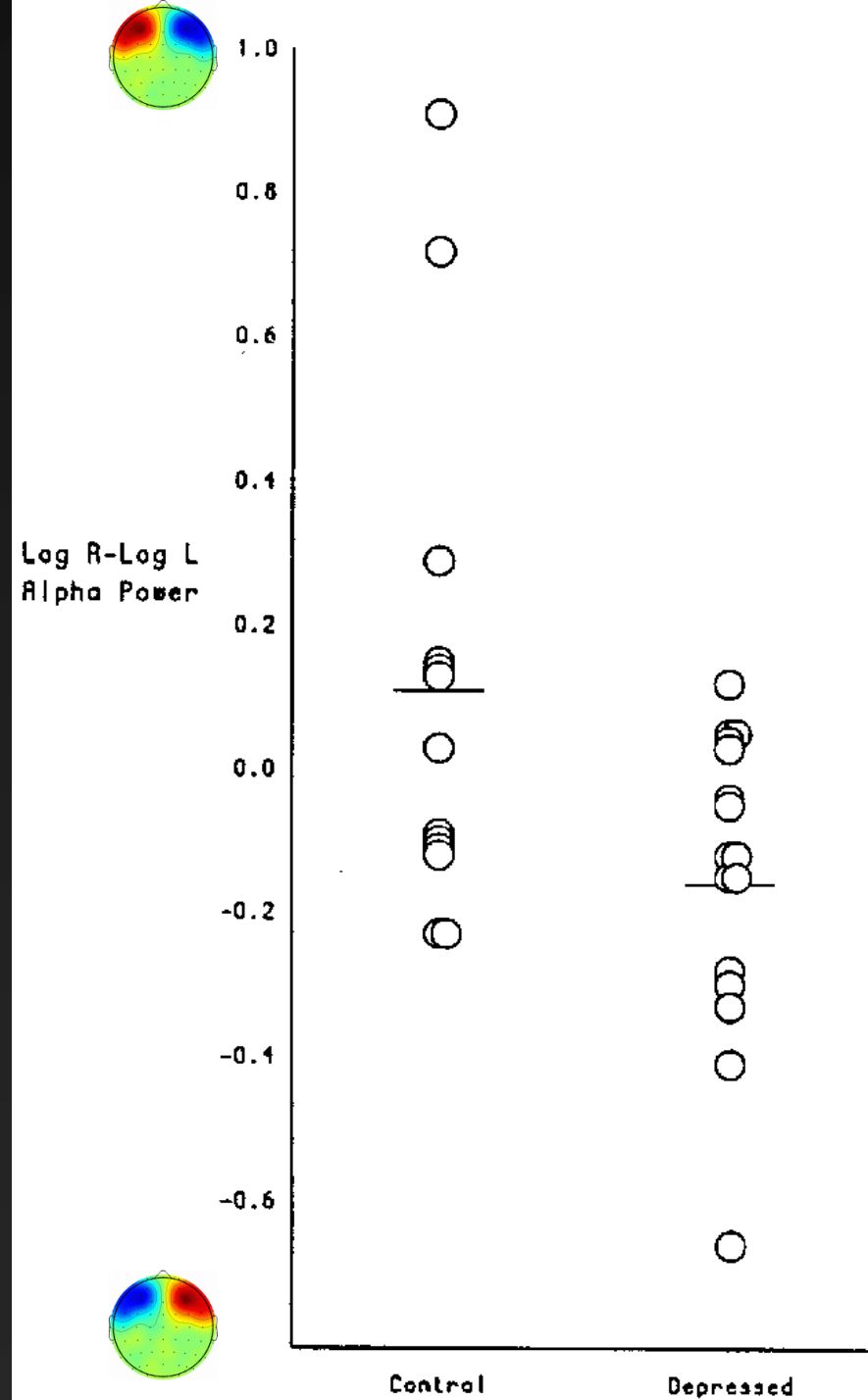


Figure 1. Mean log-transformed alpha (8–13 Hz) power (in $\mu V^2/Hz$) for Cz-referenced electroencephalograms (averaged across eyes-open and eyes-closed baselines), split by group and hemisphere, for the mid-frontal region. (Decreases in alpha power are indicative of increased activation.)

Henriques & Davidson (1991); see also, Allen et al. (1993), Gotlib et al. (1998);
Henriques & Davidson (1990); Reid Duke and Allen (1998); Shaffer et al (1983)

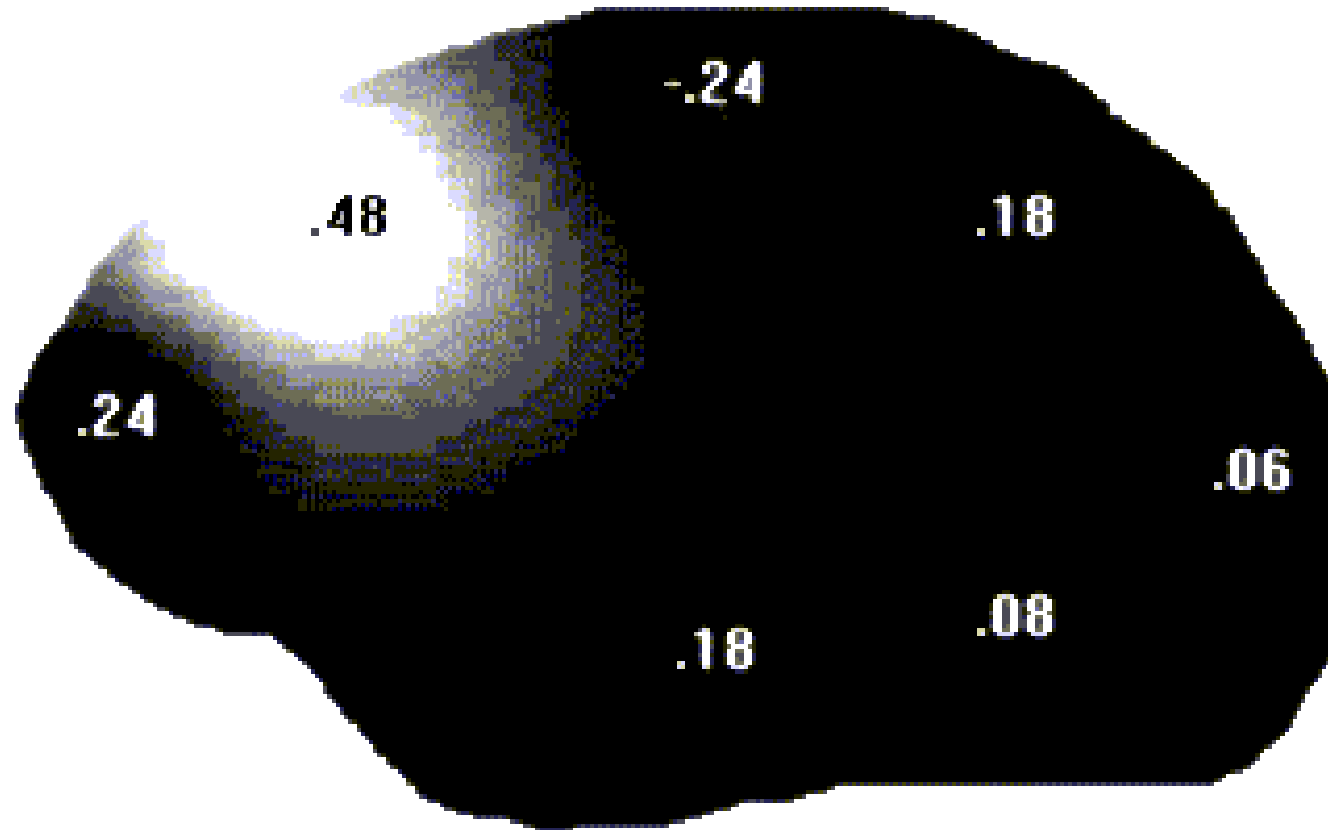
Individual Subjects' Data



Valence Vs Motivation

- Valence hypothesis
 - Left frontal is positive
 - Right frontal is negative
- Motivation hypothesis
 - Left frontal is Approach
 - Right frontal is Withdrawal
- Hypotheses are confounded
 - With possible exception of Anger





Correlation with alpha asymmetry ($\ln[\text{right}] - \ln[\text{left}]$) and trait anger. Positive correlations reflect greater left activity (less left alpha) is related to greater anger.

After Harmon-Jones and Allen (1998).

State Anger and Frontal Asymmetry

- Would situationally-induced anger relate to relative left frontal activity?

Method

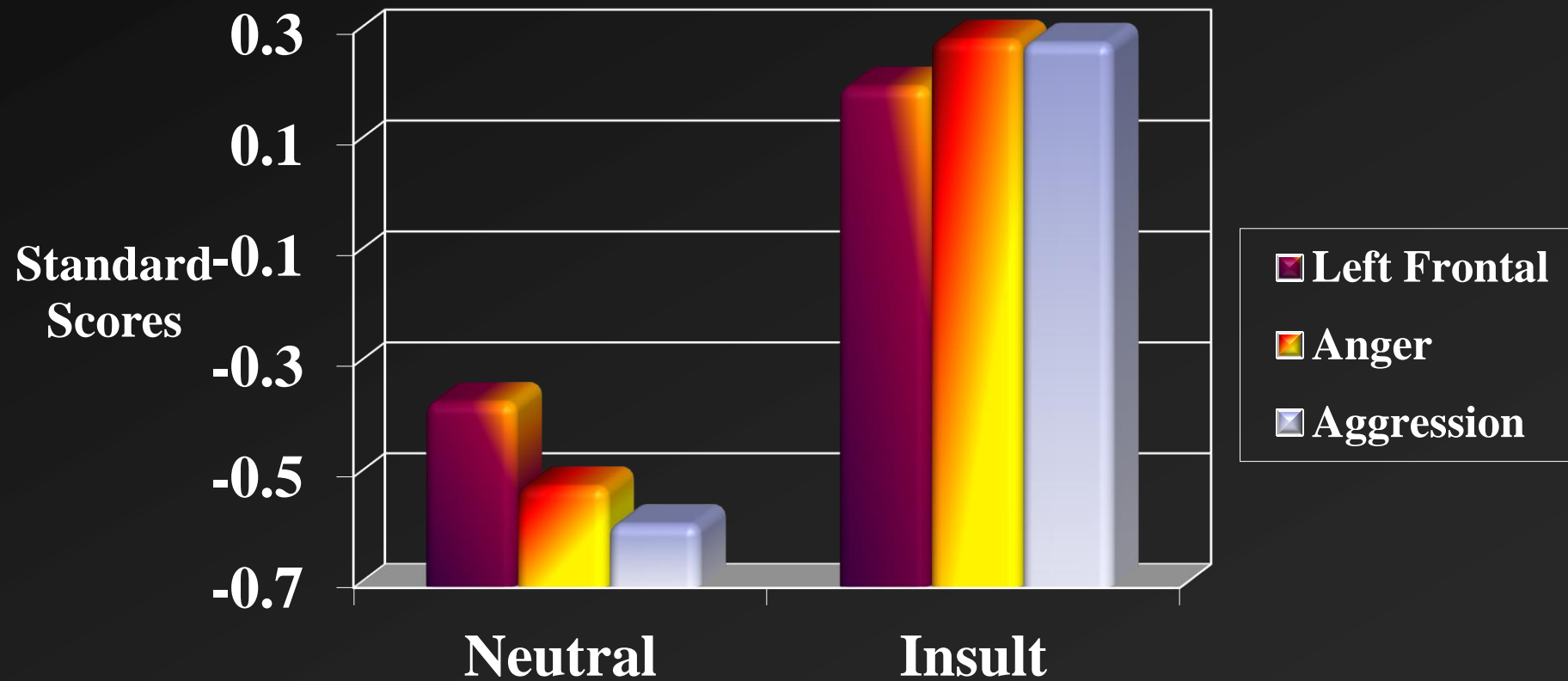
- Cover story: two perception tasks – person perception & taste perception
- Person perception task – participant writes essay on important social issue; another ostensible participant gives written feedback on essay
- Feedback is neutral or insulting
 - negative ratings + “I can’t believe an educated person would think like this. I hope this person learns something while at UW.”

- Record EEG immediately after feedback
- Then, taste perception task, where participant selects beverage for other participant, “so that experimenter can remain blind to type of beverage.”
- 6 beverages; range from pleasant-tasting (sweetened water) to unpleasant-tasting (water with hot sauce)
 - Aggression measure



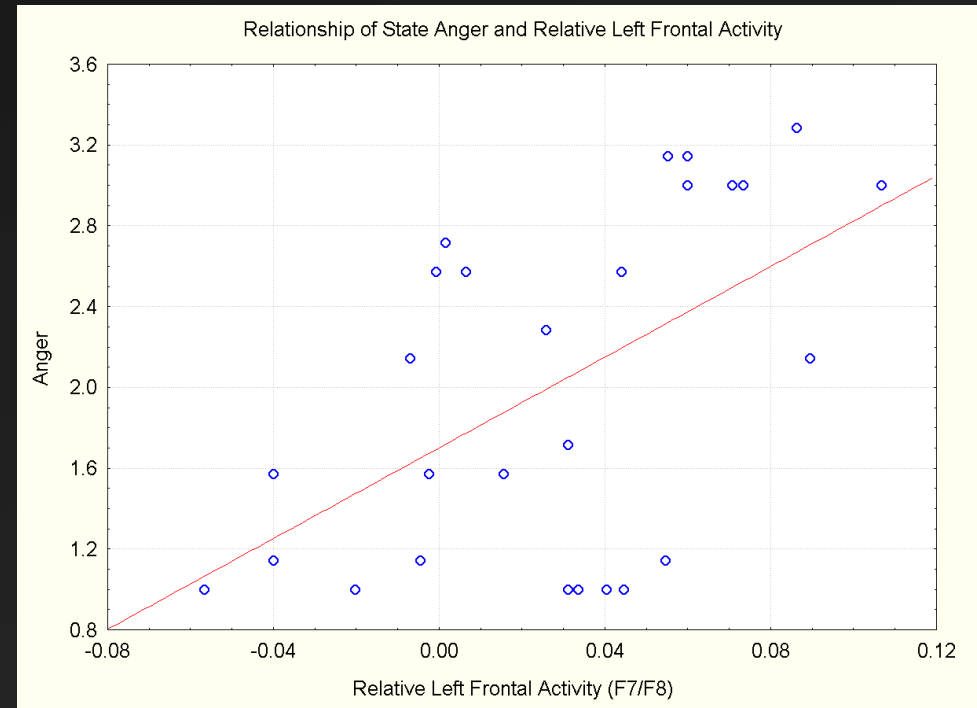
Harmon-Jones & Sigelman, *JSPS*, 2001

Relative Left Frontal, Anger, & Aggression as a Function of Condition



Frontal EEG asymmetry predicts Anger and Aggression

- Not in Neutral condition ... no relationship
- Strongly in Insult condition
 - $r = .57$ for anger
 - $r = .60$ for aggression
 - Note: partial r adjusting for baseline indiv diffs in asymmetry and affect



Manipulation of EEG

Peterson, Shackman, Harmon-Jones (2008)

- Hand contractions to activate contralateral premotor cortex
- Insult about essay (similar to Harmon-Jones & Sigelman, *JPSA*, 2001) followed by chance to give aversive noise blasts to the person who insulted them
- Hand contractions:
 - altered frontal asymmetry as predicted
 - Altered subsequent aggression (noise blasts)
- Asymmetry during hand contractions predicted aggression

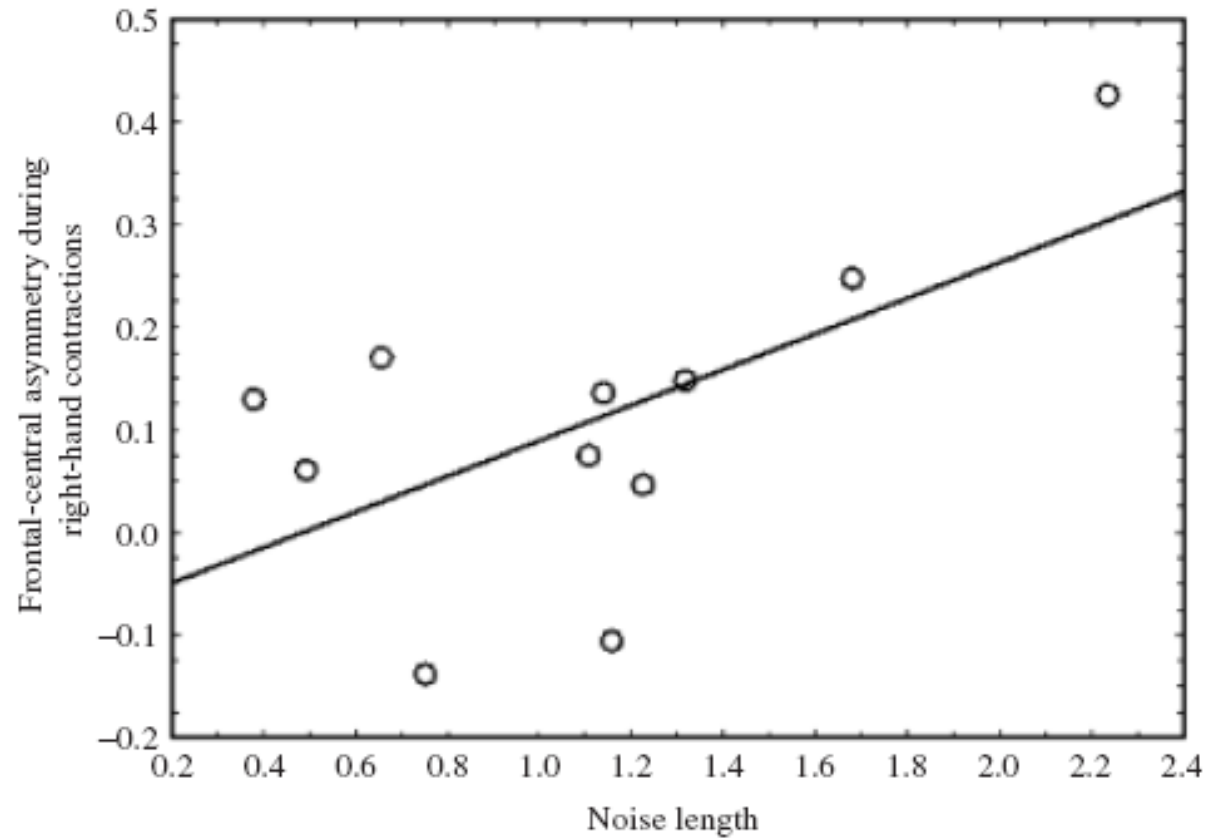


Figure 1. Relation between noise length and frontal-central asymmetry during right-hand contractions. Higher asymmetry scores indicate greater relative left than right activation.